

**SEGREGATION, CAPTURE AND RECOVERY OF TUMOR CELLS IN
HUMAN BODY FLUIDS FOR MICROFLUIDIC ASSAY & RAT
EXPERIMENTS WITH A CTC-DIALYSIS ANIMAL MODEL**

A Dissertation
Presented to
The Academic Faculty

by

Tang Zhewen

In Partial Fulfillment
of the Requirements for the Degree
Doctor of Philosophy in
Materials Science and Engineering

Georgia Institute of Technology
May 2017

Copyright © 2017 by Tang Zhewen

Segregation, Capture and Recovery of Tumor Cells in Human Body Fluids for
Microfluidic Assay & Rat Experiments with A CTC-Dialysis Animal Model

Approved by:

Dr. Ching Ping Wong, Advisor
School of Materials Science and
Engineering
Georgia Institute of Engineering

Dr. Ray P.S. Han, Co-Advisor
School of Materials Science and
Engineering
Peking University

Dr. Meilin Liu
School of Materials Science and
Engineering
Georgia Institute of Engineering

Dr. Shuxiang Dong
School of Materials Science and
Engineering
Peking University

Dr. Ruqiang Zou
School of Materials Science and
Engineering
Peking University

Dr. Haifeng Yu
School of Materials Science and
Engineering
Peking University

Date Approved: June 05, 2016

Tomorrow we will discover what our

God in heaven has in store.

ACKNOWLEDGEMENTS

Upon the completion of my PhD dissertation, I pay sincerest respect and appreciation to my advisor, Prof. Han Pingchou, for his long-term guidance and care on me. During our nine years' cooperation, he has been a teacher, a friend and a father to me. Our agreements, disagreements, insists and struggles have been the power to drive the whole project. I would also like to thank Prof. C.P. Wong, who has been helping me since I joined the GT-PKU joint PhD program, and Prof. V.V. Tsukruk, Prof. ZL. Wang for their guidance and help on me when I was studying in Georgia Tech. It was not the best period of my life, but I will keep learning from my experience and underachievement there. I would also like to pay respect and appreciation to Prof. Liang Xingjie of NCNST, Prof. R. Kamm of SMART and Prof. CT Lim of NUS, as well as all their lab members. It is during my study in their labs that I started to learn everything about biomedical and microfluidics research, that a mechanics student started to put his hands on cancer research, and a undergraduate student started to know what research is like.

The works in the dissertation can never been completed without the cooperation and help from clinical and laboratory animal institutes: Prof. Guo Mingzhou of 301 Hospital, Prof. Zhu Desheng and Prof. Li Jun of LAC, PKU, Prof. Dai Menghua of PUMCH, Prof. Zhang Yu of HSC, PKU, Prof. Cui Heng, Prof. Chang Xiaohong and Dr. Zhu Honglan of PKU People's Hospital. They brought me into the world of clinical research. Prof. Xu Kaifeng of PUMCH and Prof. Jin Baiye of No. 1 Affiliated Hospital of Zhejiang Univ. also has helped a lot in my study, though their projects are not presented in the dissertation. The works in the dissertation involves a wide range

of knowledge. I would like to thank all Professors and students who have taught me and helped to acquire those knowledge during my 12-year of study at PKU. I will treasure all those moments and knowledge, and keep learning throughout my life.

My research cannot be accomplished without the cooperation of my fellow students: Lv Peitao and Li Ying, who started the project with me from the first day; Sun Yukun, Chen Anqi, Chen Shuiyu and Tony Ouyang, who joined and expanded the research on CTC/DTCs to a wide aspects of topics; Neoh Kuang Hong, who has been working very hard in his first year not only in lab, but also in helping with the revision of the dissertation; students at NCNST, NUS, Georgia Tech, PKU LAC, PUMCH, PKU HSC and PKU People's Hospital, who have helped me to become a qualified clinical and experimental animal researcher.

I would also like to thank my parents and family, who have been supporting me without any condition and requirements throughout my study in Beijing. And my friends in College of Engineering, Loveheart Society, BDWM BBS and Musical Club of PKU. They have made my life at PKU much more than study and research.

Looking back on the boy who entered PKU at 18, I am aware and grateful that my soul and character have been changed much, most of which must be attributed to my Professors and friends.

Last but far beyond least, I want to pay appreciation and respect to those patients who participated in our research with consent, and those animals who sacrificed without consent. Their contribution and devotion has shed light to the future of cancer research and clinical management with knowledge.

TABLE OF CONTENTS

ACKNOWLEDGEMENTS.....	IV
LIST OF TABLES	X
LIST OF FIGURES.....	XII
NOMENCLATURE	XIV
SUMMARY.....	XVII
CHAPTER ONE INTRODUCTION.....	1
1.1 Body fluids and tumor cells	2
1.1.1 Body fluids and their role in cancer	2
1.1.2 Circulating Tumor Cells and Disseminated Tumor Cells	5
1.2 Current harvesting methods of CTC/DTCs.....	7
1.2.1 Biomarker based capture methods	8
1.2.2 Motion based capture methods	10
1.2.3 Size-based capture methods	10
1.3 Thesis layout	11
CHAPTER TWO DEVELOPMENT OF THE MICROFLUIDIC ASSAY	12
2.1 Development of a size-based microfluidic assay for CTC/DTC capture and recovery.....	12
2.1.1 Principle of size-based CTC/DTC segregation.....	12
2.1.2 Development of the microfluidic chip	13
2.1.3 Protocol of the microfluidic assay	17
2.1.4 Chip characterization study.....	18
2.2 Challenges and difficulties encountered	21

2.2.1 Blood coagulation	21
2.2.2 Limited throughput and capacity	23
2.2.3 Contamination by background cells.....	24
2.3 Identification of CTC/DTCs	24
CHAPTER THREE APPLICATIONS OF THE MICROFLUIDIC ASSAY IN CANCER RESEARCH	28
3.1 CTC Enumeration and Staging of Pancreatic Cancer	28
3.1.1 CTC Enumeration Methodology and Its Clinical Importance	28
3.1.2 Pancreatic Cancer and Its Staging.....	30
3.1.3 Pancreatic Cancer Staging Prediction Based on CTC Enumeration.....	31
3.2 CTC Characterization and Mitochondrial Autophagy of NSCLC CTCs.....	35
3.2.1 Image-based Characterization Methodology	35
3.2.2 Mitochondrial Autophagy	36
3.2.3 Putative Mitochondrial Autophagy of NSCLC CTCs	37
3.3 Detection of CEC/PECs and Their Role in Pathogenesis and Clinical Management of Endometriosis	40
3.3.1 Endometriosis and Its Pathogenesis Pathways	40
3.3.2 Detection of CEC/PECs in Endometriosis Patients	43
3.3.3 CEC – a Potential Biomarker for Endometriosis Diagnosis.....	45
3.3.4 The Role of CEC/PECs in Endometriosis Pathogenesis and Clinical Management.....	50
CHAPTER FOUR CTC-DIALYSIS ANIMAL MODEL ON RATS	52
4.1 Concept and Prototype of CTC-Dialysis.....	52
4.2 Development of the CTC-Dialysis Protocol	53
4.2.1 Selection of the Hematogeneous Metastatic Animal Model.....	56

4.2.2 Microsurgery to Divert the Rat’s Blood through the Extracorporeal Circuit	58
4.2.3 Circulation Pump System	62
4.2.4 Protocol of the experiment	63
4.2.5 Restrictions of the System	64
4.3 Effects of the CTC-Dialysis System	65
4.3.1 Capture of Seeded Tumor Cells	65
4.3.2 Minimal Effects on the Operated Rat	66
4.3.3 Potential Applications of the System	67
CHAPTER FIVE SUMMARY AND PROSPECTS FOR FUTURE WORK...	70
APPENDIX A PROTOCOL: SIZE-BASED MICROFLUIDIC ASSAY FOR CTC/DTC CAPTURE AND RECOVERY	72
A.1 Materials	72
A.1.1 Reagents	72
A.1.2 Equipments	73
A.1.3 Reagent Setup	75
A.1.4 Equipment Setup	76
A.2 Procedure	76
A.2.1 Chip design and mold preparation	76
A.2.2 Chip fabrication	76
A.2.3 Chip assembly	80
A.2.5 Chip priming	82
A.2.6 Sample preparation	83
A.2.7 Pre-capture immunofluorescence staining	85
A.2.8 Sample processing	87

A.2.9 Post-capture immunofluorescence staining	88
A.2.10 Recovery of captured cells	90
A.2.11 Imaging of stained cells.....	90
A.2.12 Data Interpretation	90
A.2.13 Troubleshooting	90
A.2.14 Timing	91
APPENDIX B PROTOCOL: CTC-DIALYSIS ANIMAL MODEL ON A RAT	
.....	93
B.1 Materials.....	93
B.1.1 Reagents	93
B.1.2 Equipments.....	93
B.1.3 Medicine (subjected to approved use).....	94
B.2 Procedure.....	94
B.2.1 Preparation of tubing pipelines	94
B.2.2 Preparation of pumps	95
B.2.3 Preparation of animals.....	96
B.2.4 Surgery	97
B.2.5 Tubings fixation.....	99
B.2.6 Dialysis.....	100
B.2.7 Closure of surgical wounds	101
B.2.8 Imaging and Data Analysis	102
REFERENCES	103

LIST OF TABLES

Table 1.1	List of Extracellular Body Fluids	3
Table 1.2	Unspecific and Specific Biomarkers in CTC/DTC segregation	10
Table 2.1	Physical Properties of RBCs, WBCs and CTCs	13
Table 2.2	Cell lines Tested in Mock Experiments	19
Table 2.3	Misidentification of Tumor Cells in Different Strategies	27
Table 3.1	Identification of Pancreatic CTCs	33
Table 3.2	Records of Participants of Pancreatic Cancer Research	33
Table 3.3	CTC Enumeration Records of Pancreatic Cancer Research	34
Table 3.4	NSCLC CTCs with Putative Autophagy Signal	39
Table 3.5	Participant Data of Endometriosis Research	44
Table 3.6	Captured CECs in Peripheral Blood and PECs in PW of EM Patients	45
Table 3.7	Comparison of CEC Detection Rate and CA125 Abnormal Rate	48
Table 4.1	Extracorporeal Circulation Connection Port Recommendations	59
Table 4.2	Tail-Vein-Seeded Tumor Cells Captured in CTC-Assay	65
Table 4.3	Expected Control Experiment for the Verification of the Effect of CTC- Dialysis on Cancer Metastasis	69
Table A.1	Parameters for Plasma Treatment	88
Table A.2	Items Needed per Piece of Capture Chip and Recovery Chip	90
Table A.3	Syringe Pump Parameters	93
Table A.4	Troubleshooting Table	101
Table A.5	Timing Information for Capture Chip and Recovery Chip	102

Table B.1	Recommended Ports for Extraction and Infusion of Blood	108
-----------	--	-----

LIST OF FIGURES

Figure 1.1	Typical Body Fluids in a Human Body	2
Figure 1.2	CTCs and DTCs	6
Figure 2.1	Size-Based Rare Cell Segregation and Recovery System	15
Figure 2.2	Schematic Illustration of the Tumor Cell Capture Process	16
Figure 2.3	Protocol Flowchart and Estimated Timing of Each Step	18
Figure 2.4	Clinical Application of the Microfluidic Assay	20
Figure 2.5	Optimized Chip Design to Reduce Shear Rate	22
Figure 2.6	A Typical Combined Identification Flow Chart	26
Figure 3.1	Enumeration of Rare Cells	29
Figure 3.2	Staging of Pancreatic Cancer	32
Figure 3.3	ANOVA Plot of CTC Enumeration Versus Pancreatic Cancer Staging	34
Figure 3.4	Mitochondrial Autophagy of T-Cells	37
Figure 3.5	Occurrence of Endometriosis, and its Pathogenesis Pathways	42
Figure 3.6	Flowchart Applied to Identify CEC/PECs	44
Figure 3.7	CEC Detection Rate in EM Patients and Control Groups	46
Figure 3.8	CEC Detection Rate in EM Patients and Healthy Volunteers	46
Figure 3.9	Detection Rate of CECs in EM Patients and Other Gynecology Disease Patients	47
Figure 3.10	Detection Rate of CEC and Abnormal Rate of Serum CA125 Level in EM Patients and other Gynecology Disease Patients	49
Figure 3.11	ROC Curve of CEC Detectability, CA125 Level and Joint Test	49

Figure 3.12	Pie Chart of CEC Detectability and CA125 Abnormality	49
Figure 4.1	The Prototype of CTC-Dialysis System	53
Figure 4.2	Hematogeneous Metastatic Animal Models and Potential CTC-Dialysis Sites	56
Figure 4.3	Post Cava Sites for the CTC-Dialysis System Hookup	59
Figure 4.4	Illustration of the Microsurgery	61
Figure 4.5	Circulation Pump System Based on Plunger Pump	62
Figure 4.6	Flow Chart for the Procedures of the CTC-Dialysis Experiment	63
Figure 4.7	B-Ultrasound Images of Post Cava before Experiment and One Week after Experiment	66
Figure 4.8	Doppler-Ultrasound Measurement of Flowrate in Post Cava before Experiment and One Week after Experiment	67
Figure A.1	Illustration of the Experimental Setup of Recovery Chip	92
Figure A.2	Illustration of Chip Priming, Sample Processing and Cell Recovery in Recovery Chip	95
Figure B.1	Recommended Ports for Extraction and Infusion of Blood	108
Figure B.2	Illustration of the Microsurgery	109

NOMENCLATURE

AA	Abdominal Aorta
AF	Alexa Fluor
ANOVA	Analysis of Variance
AUC	Area Under the Curve
BGCs	Background Cells
BSA	Bovine Serum Albumin
CECs	Circulating Endometrial Cells
cfDNA	Cell-Free DNA
CK	Cytokeratin
CTCs	Circulating Tumor Cells
DALYs	Disability-Adjusted Life Years
DEP	Dielectrophoresis
DIE	Deep Infiltrating Endometriosis
DTCs	Disseminated Tumor Cells
EAOC	Endometriosis Associated Ovarian Carcinomas
EDTA	Ethylenediaminetetraacetic Acid
EM	Endometriosis
EMT	Epithelial-Mesenchymal Transition
EpCAM	Epithelial Cell Adhesion Molecule
ER	Estrogen Receptor
FRI	Fluorescence Reflectance Images
IF	Immunofluorescence

IID	Integrated Identification
IV	Iliac Vein
LRV	Left Renal Vein
MCU	Micro-Control Unit
NECs	Normal Exfoliated Cells
NPC	Not Pancreatic Cancer
NSCLC	Non-Small Cell Lung Cancer
ODE	Oxygen-Deficient Environment
OEE	Oxygen-Enriched Environment
OEM	Ovarian Endometriosis
OS	Overall Survival
OtEM	Other Endometriosis
PBS	Phosphate Buffer Saline
PC	Pancreatic Cancer
PDAC	Pancreatic Ductal Adenocarcinoma
PDMS	Polydimethylsiloxane
PE	Phycoerythrin
PECs	Peritoneal Endometrial Cells
PEM	Peritoneal Endometriosis
PFA	Paraformaldehyde
PFS	Progression Free Survival
PR	Progesterin Receptor
PSMA	Prostate Specific Membrane Antigen
PUMCH	Peking Union Medical College Hospital
PW	Peritoneal Wash

RBCs	Red Blood Cells
ROS	Reactive Oxygen Species
ULN	Upper Limit of Normal
Vim	Vimentin
WBCs	White Blood Cells
WHO	World Health Organization

SUMMARY

In a cancerous human body, tumor cells rapidly proliferate and metastasize in body fluids and it is this liquid manifestation that provides us with an opportunity for their segregation, capture and recovery. The liquid biopsy approach is now recognized as one of the most important tools for understanding the etiopathogenesis of neoplastic diseases such as cancers by studying not only the physical appearance and response of the cell but also, its molecular information contained inside it. Tumor cells in the peripheral blood are termed as Circulating Tumor Cells (CTCs) and in a pseudostatic collection of body fluid such ascitic fluid, peritoneal fluid, thoracic fluid, urine, sputum, etc. are generally termed as Disseminated Tumor Cells (DTCs). To segregate and capture tumor cells in a body fluid is most challenging because of the vast order of magnitude difference among the constituents of the fluid; take for example, in 1 ml of blood, the ratio is like 100 CTCs compared to over 10 million white blood cells (WBCs) and half a trillion red blood cells (RBCs) and these rare tumor cells are also, highly heterogeneous with diameters in the micron scale. It is because of their small size, that the harvesting process is painstakingly slow for the macro volume of fluid environment that is typically encountered. Various capture methodologies have been developed; biomarker-specific (mostly EpCAM) based approach for CTC adhesion, magnetic and electric field for deflection of the rare cells, centrifugation and Deaggn force techniques for steering the rare cells in a preset trajectory, cellular size-based methods for the physical separation, etc. After harvesting, these rare cells need to be properly processed in order to accurately identify them as tumor cells. Immunofluorescence staining is most popular but a well-tested algorithm with specific antibodies to their

antigen by targeting the fluorescent dyes to a specific biomolecule needs to be in place to correctly distinguish the tumor cells from normal cells, WBCs and other cellular constituents that are inadvertently captured.

The cell capture technology adopted in my thesis research is based on the strong difference in the physical size and stiffness of tumor cells to separate them from background cells in the body fluid. This size-based method allows for the harvesting of intact CTCs and DTCs. Further, by optimizing the flow pattern and modifying the surface property of the capture chamber to reduce the adverse effects of the high shear flow environment, it is possible to attain close to 90% capture efficiency and capture purity. A comprehensive set of protocols for a stable and reliable capture and recovery of tumor cells in peripheral blood and peritoneal fluid is presented in the thesis. The results of the microfluidic assay applied in cancer research have the following outcomes: 1) the assay enumerates CTCs and their capture magnitude constitutes a measure of the severity of the pancreatic cancer in patients; 2) the assay yields high resolution images for the characterization of non-small cell lung cancer CTCs to reveal their mitochondrial autophagy; 3) the assay harvests circulating and peritoneal endometrial cells for use as a biomarker for the diagnosis of endometriosis and 4) the assay yields intact endometrial cells to provide an insight into the pathogenesis of endometriosis.

The thesis concludes by carrying out some pioneering rat experiments using a proposed CTC-dialysis animal model. Just like the hemodialysis system for the removal of body wastes in peripheral blood, the objective of the experiments is to demonstrate that a microfluidic chip can be used to remove CTCs in the peripheral blood of a rat in an attempt to inhibit cancer metastasis. The limited experiments clearly showed that a chip

attached to the rat via a post cava microsurgery protocol is able to capture cancer cells that are tail-vein injected into the live animal.

CHAPTER ONE

INTRODUCTION

Cancer is not only a major threat to human lives but it also, significantly affects the quality of life for a patient. In 2015, 4.3 million new cancer cases and 2.8 million cancer mortalities were recorded in China^[1]. Cancer ranks as the 4th leading contributor to the higher Disability-Adjusted Life Years (DALYs)^[2-6], which provides a measure of the overall disease burden^[7, 8]. In the light of ever increasing threat posed by cancers, the World Health Organization (WHO) has identified prevention, treatment and palliative care as the most effective ways to control and manage cancer^[9, 10]. Nevertheless, a cancer can behave differently from one person to another. Therefore, the “one-size-fits-all” approach has rendered some treatment methods marginally effective to totally ineffective for a certain class of cancer patients. In early 2015, the Precision Medicine Initiative initiated by the White House encompasses precise diagnosis and treatment of cancer^[11]. In view of the rising demand for precision diagnosis and treatment of cancer, a cell-based liquid biopsy methodology is developed in this dissertation. As a tool, the chip could potentially lead to an early stage detection by facilitating a more precise microfluidic assay of the disease. Further, by incorporating the chip into the extracorporeal circulation, it could potentially inhibit cancer metastasis in a procedure termed as *CTC-dialysis*.

1.1 Body fluids and tumor cells

1.1.1 Body fluids and their role in cancer

Body fluids (or biofluids) are simply fluids found inside a *living* organism or body and in a human body, there are all kinds of body fluids (Figure 1.1) that can be

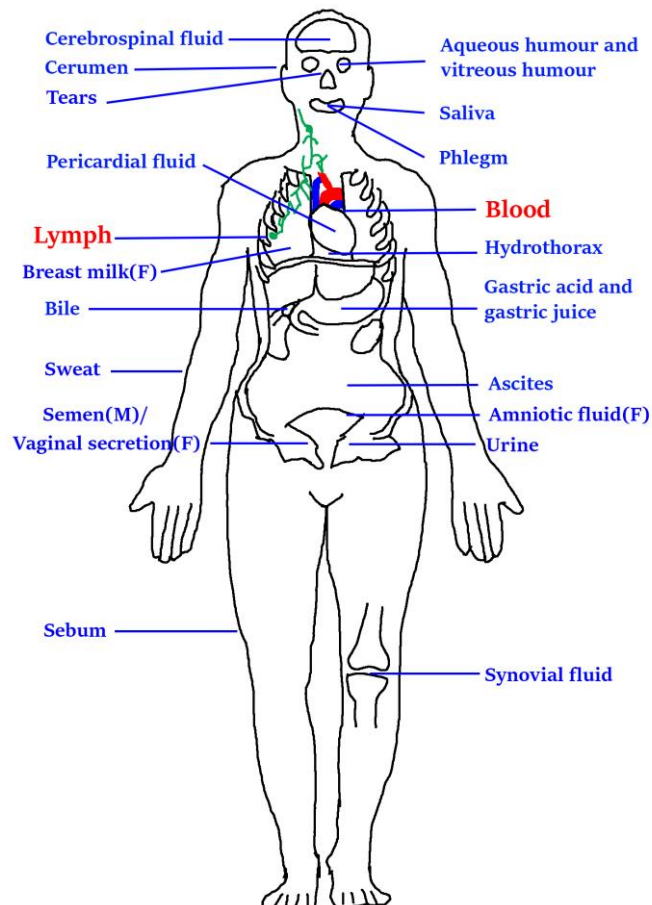


Figure 1.1 Typical body fluids in a human body, female body (F) or male body (M).

classified as 60-65% intracellular and 35-40% extracellular, depending on where the fluid resides. Under the latter category, it can be further sub-divided as 6-10 liters of interstitial (fluid between cells), 6-10 liters of lymph (fluid in the lymphatic system) and 3-6 liters of intravascular fluid (blood plasma) and 5-12 liters of transcellular fluid (Table 1.1). Interstitial and transcellular fluids are confined to certain tissue, organ or

Table 1.1 List of extracellular body fluids, including **pathological body fluids**.

Interstitial	Dermal	Cerumen, Sebum, Sweat
	Motor	Synovial fluid, ears
	Respiratory	Saliva, Sputum, Rheum
	Digestive	Bile, Chyme, Feces, Gastric acid, Gastric juice, Vomit
	Urinary	Urine
	Reproductive (Female)	Amniotic fluid, Breast milk, Female ejaculate, Vaginal secretion
	Reproductive (Male)	Semen, Smegma
	Endocrine	Hormone
	Immune	Chyle, Endolymph and perilymph
	Uncertain	Exudates, Mucus, Pus, Serous fluid
Transcellular	Pleural fluid (Hydrothorax), Peritoneal fluid (Ascites), Pericardial fluid, Cerebrospinal fluid, Aqueous humour and vitreous humour	
Intravascular	Blood serum	
Lymphatic	Lymph	

system in the body, whereas, blood and lymph circulates the entire body, with or without the aid of a “pump” (for blood, there is the heart but for the lymphatic system, there is no “pump” to circulate the lymph). The human body fluid is predominantly water and the sum of all its body fluids comprises about 70% of the total body weight. Tumor cells rapidly proliferate and metastasize in a body fluid and it is this liquid manifestation that provides us with an opportunity for their segregation, capture and recovery.

Cells interact with body fluids in several ways: their physical conditions are regulated by fluid environment, they exchange molecules to and from body fluids during feeding and waste excretion and when they apoptose they shed their DNAs (cell-free DNAs) in body fluids. Often, they get detached from solid tissue and become suspended in a body fluid. When a pathological change occurs, the body reacts via a body fluid by sending compensative molecules to revert the pathological condition or immune cells to kill the invading pathological cells.

Liquid biopsy is a general term for investigating the condition (physical, chemical or molecular) of pathological cells (especially tumor cells), through an assay of a body fluid; the term is conceptually similar to a tissue biopsy except that it is not necessary to physically reach or come into contact with the lesion site. It is now widely applied in the diagnosis of diseases as the liquid biopsy is minimally to non-invasive. In contrast to traditional diagnosis tools, liquid biopsy is particularly valuable in the diagnosis of cancer for 2 crucial reasons: it is often less harmful and/or painful to patients and it gives a status evaluation of the metastatic loci compared to a sole assessment of the

primary tumor ^[12-15]. The latter is particularly important because the vast majority of cancer patients succumb to cancer metastasis rather than the primary tumor. ^[16]

1.1.2 Circulating Tumor Cells and Disseminated Tumor Cells

Circulating tumor cells (CTCs) are cancer cells found in the peripheral blood and disseminated tumor cells (DTCs) are found in pseudostatic body of fluids such as the transcellular and interstitial fluids (Figure 1.2). CTCs ^[17] and DTCs ^[18, 19] are highly capable of forming metastatic foci. Their importance was recognized when CTCs were discovered in early-stage cancer patients ^[20]. Since they are the vectors for the spread of cancer, their capture provides information for the early detection, progress and prognosis of the disease and the associated treatment feedback ^[21, 22]. Further, they are believed to be carriers of mutation information for a more precise diagnosis ^[23]. When a cell apoptotizes in a body fluid, it sheds its DNA into the fluid and this cell-free DNA (cfDNA) is an important source for the molecular characterization of the tumor. The cfDNA is often highly fragmented and available in a trace amount (measured in picogram), in contrast to the high quality but just as minute amount of DNA harvested from an intact tumor cell and this DNA is termed as CTC-DNA or DTC-DNA, depending on where it taken from. The technology to extract, amplify and purify DNA and RNA from single tumor cells is highly challenging due to their low molecular content, exciting results have been obtained ^[24-29].

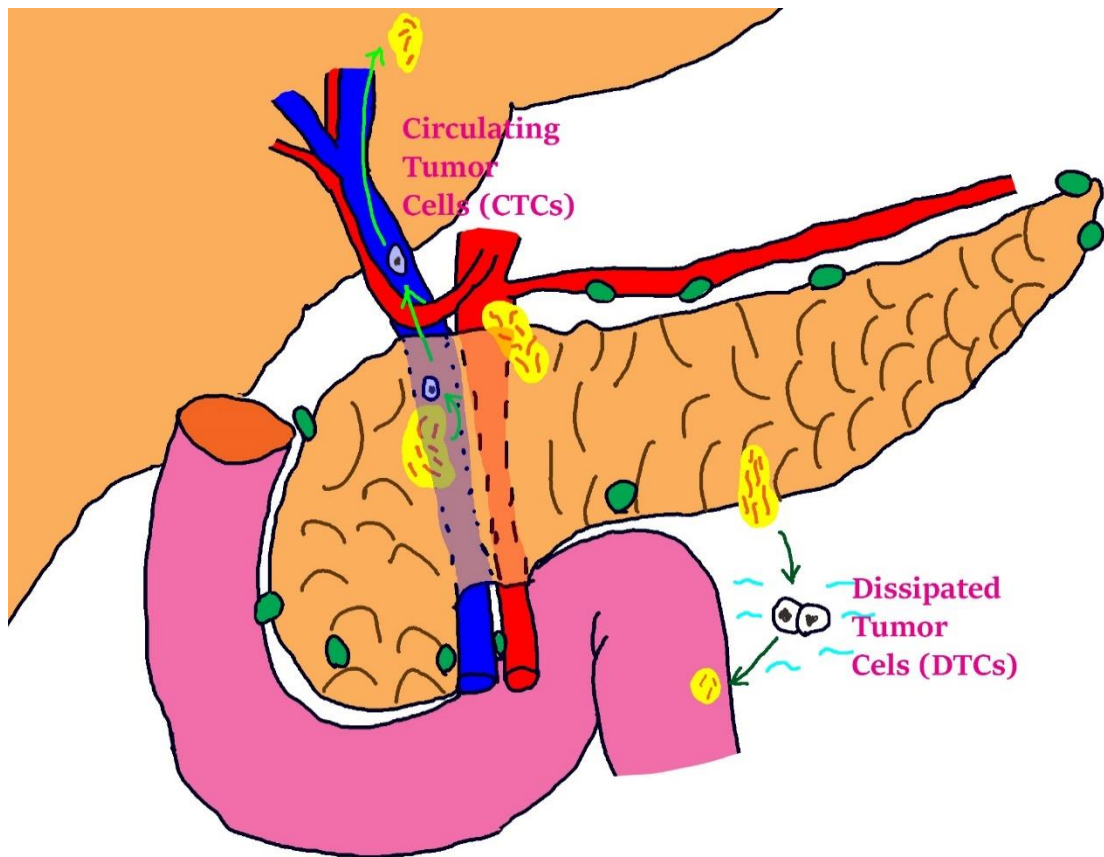


Figure 1.2 CTCs and DTCs: CTCs are tumor cells in circulation system, they enter blood vessel (intravasation) from original tumor (which is not necessarily the primary tumor), travel along blood flow and invade other tissue, where they may form metastatic tumor. DTCs are tumor cells in body fluids other than blood, they shed from tumors, attach to other tissue and form metastatic tumor.

Molecular mutations can be detected through both tumor cells and cfDNA in body fluids and they are different but they complement each other in many respects ^[30, 31]. Further, cell free molecules are available mostly from the solid tumor through exosomes, dead primary tumor cells and dead CTCs ^[32], and the molecular information they yield is not the same as harvested from intact and live CTCs and DTCs. With the advancement of CTC/DTC identification and characterization technologies, oncologists may further distinguish aggressive CTCs and DTCs that are able to survive in the body fluids to form metastatic foci at distal sites ^[33]. This metastatic route is the leading cause of cancer deaths.

The capture and recovery of CTC/DTCs in body fluids is highly challenging for 2 reasons: they are extremely rare compared to the other constituents of the body fluid and they could be highly heterogeneous, which reflects the heterogeneity of mutations in tumor cells ^[34]. The number of CTCs in one ml of blood ranges from several to hundreds compared to half a billion of Red Blood Cells (RBCs) and several millions of White Blood Cells (WBCs) ^[35, 36]. In transcellular fluids like ascites and urine, there is a huge population of Normal Exfoliated Cells (NECs) in addition to the DTCs. The heterogeneity of the tumor cells can be characterized in terms of size, type, protein expression, etc.

1.2 Current harvesting methods of CTC/DTCs

To overcome the challenges of rarity and heterogeneity of tumor cells, various assaying methods have been developed. To qualify as a good CTC/DTC segregation assay, the following criteria should be met:

1. High efficiency: efficiency refers to the effectiveness (expressed in percentage term) in capturing the tumor cells. It is characterized by the ratio of number of tumor cells captured to total number of tumor cells in the system. The simplest method to perform this measurement is to use spiked blood where a known number of tumor cells taken from a cell-line is first deposited in the system and the number of captured cells are then enumerated. The drawback of using cell-lines is the cultivated cells are generally size-homogeneous and therefore, measurements using spiked blood err on the high side as they do not accurately reflect the actual situation of using a patient's blood, where the tumor cells come in all sizes.

2. High accuracy: accuracy refers the ability of the method to focus only on the capture of tumor cell without being contaminated by background cells. It is usually expressed by the ratio of number of captured *tumor* cells to total number of cells captured.

3. High viability and intactness of the captured cell: the capture and recovery of viable and intact tumor cells constitute an important outcome of the microfluidic assay, as it enables cellular and molecular analyses on tumor cells to be carried out. Further, viable and intact cells allow them to be proliferated in a laboratory environment.

4. High flow throughput: the flow throughput represents the speed of the microfluidic assay. If the flow is too slow, the capture process may be limited in application and if the flow is too fast, the ensuing high shear stress may damage or destroy the captured cells, an optimum speed is not only required for practical assaying but is also ensures that the blood does not clog during the flow process.

Currently, three types of CTC/DTC assays: methods based on biomarker, cell motion and cell size are widely applied in harvesting the tumor cells for clinical research. Although their performance criteria vary, scientists and oncologists have obtained profound understanding of cancer through these methodologies.

1.2.1 Biomarker based capture methods

Several biomarker-based capture methods have been reported (Table 1.1), including the first FDA-approved CTC assay method named CellSearch^[36]. The CellSearch technique captures and identifies tumor cells by a surface adhesion technique of the specially coated magnet beads. Later, some innovative approaches attempt to remove the background cells, which in blood are mostly WBCs using CD45

or a combination of leukocyte identifiers. However, considering the several orders magnitude difference between the CTC and WBC concentrations, a 99.99% removal efficiency would still leave behind several hundreds to thousands of WBCs with each captured CTC.

For captured cell identification, most methods employ the Epithelial Cell Adhesion Molecule (EpCAM) approach, which is a surface biomarker for epithelial cells. Epithelial cells are the predominant constituent of solid tumors, and are generally not detected in the blood of healthy people. However, the majority of CTCs are mesenchyme (or are undergoing the Epithelial-Mesenchymal Transition (EMT) to mesenchyme) and therefore, are not detectable by EpCAM ^[37] (and other epithelial markers).

Unspecific biomarker-based capture methods discussed so far generally have low efficiency in harvesting the heterogeneous tumor cells. There is another group of biomarker-based methods that are target specific markers for certain tumors. As depicted in Table 1.2, the Prostate Specific Membrane Antigen (PSMA) for prostate cancer CTCs has a very high capture accuracy but it is not for general cancers. One of the biggest disadvantage of biomarker based capture method is the captured cells are generally not amenable to the subsequent molecular analysis.

Table 1.2 Unspecific and Specific Biomarkers in CTC/DTC segregation.

Biomarker	Type	Applicability	Reference
CD45	Negative selection	All solid tumors	[38, 39]
EpCAM	Unspecific (Epithelial)	Breast Cancer, Colorectal Cancer, Prostate Cancer	[6, 36, 40-42]
PSMA	Specific	Prostate Cancer	[43-45]

1.2.2 Motion based capture methods

Motion based capture methods work on the principle of deflecting CTCs from RBCs and WBCs during a continuous flow. Two motion-based assays are dielectrophoresis (DEP), which deflects cells by harnessing their dissimilar dielectric properties^[46-48] and circular channel flows that deflects cells by balancing the Dean and centrifugal forces^[49-52]. The big advantage of motion-based capture methods is that they generally have high flow throughputs without compromising the heterogeneity efficiency. Their big drawback is the poor capture accuracy. Although the motion properties of RBCs and eukaryotic cells are distinctly different, the difference between WBCs and CTCs are not that distinct and this inevitably introduces inaccuracies into these methods.

1.2.3 Size-based capture methods

Size-based capture methods differentiate CTCs from RBCs through their highly distinctive physical size difference and cell deformability. Filters made with polymer membrane^[53, 54], silicon^[55], and PDMS microfluidic devices^[56, 57] have been applied in the segregation of CTCs. However, this “brute-force” approach is generally not good

due to the poor capture efficiency and accuracy arising from the debris conglomeration at the membrane level. Since the CTC capture and recovery method employed in this work is completely size-based, it would be prudent to defer a full discussion of size-based capture methods to *Chapter Two* of the thesis.

1.3 Thesis layout

The dissertation begins with *Chapter One* that depicts an introduction of the main ideas of the doctoral research. The development of a size-based microfluidic assay for the capture and recovery of CTCs is presented in *Chapter Two*. It includes a detailed protocol for obtaining stable and reliable results, as well as, methods for interpreting the outcomes. In *Chapter Three*, the following four distinct cancer applications of the assay technique will be discussed with clinical results: enumeration of CTCs for staging pancreatic cancer detection, image-based characterization and discovery of mitochondrial autophagy in non-small cell lung cancer (NSCLC) CTCs, detection of circulating endometrial cells (CECs) as a biomarker for the diagnosis of endometriosis (EM), and the detection and recovery of CECs and peritoneal endometrial cells (PECs) for the pathogenesis research and clinical management of EM. In *Chapter Four*, the chip is incorporated into the extracorporeal circulation of a rat and using a rat model to study the potential for CTC-Dialysis. The approach includes the extracorporeal circulation setup and the microsurgery required for enjoining the filtering system with the circulation system of the animal. The dissertation concludes in *Chapter Five* with a presentation of the overall summary and future prospects. In the *Appendix*, step-by-step protocols and detailed materials lists of the microfluidic assay, as well as the CTC-dialysis experiment are provided.

CHAPTER TWO

DEVELOPMENT OF THE MICROFLUIDIC ASSAY

To achieve a satisfactory capture and recovery of CTCs from peripheral blood and DTCs from non-blood body fluids of cancer patients, several microfluidic chips have been developed. These chips are evaluated for their ability to capture the heterogeneous population of CTCs/DTCs with a high efficiency, high purity, reasonable flowrates and good viability and intactness of the recovered cells. This chapter explains the design and fabrication of the microfluidic chips, the challenges and difficulties encountered and how they are resolved and ends with a presentation of the full protocol for the microfluidic assays.

Our equipment setup consists of a microfluidic chip, connections and tubing, pumps and an imaging system (microscopy) for visual examination. The protocol includes a proper procedure to collect and store body fluids for best results and a comprehensive flowchart for the interpretation of the results via an immune-fluorescent imaging scheme.

2.1 Development of a size-based microfluidic assay for CTC/DTC capture and recovery

2.1.1 Principle of size-based CTC/DTC segregation

The size-based segregation of tumor cells in body fluids is premised on the simple observation that background cells (BGCs) have very distinct size and stiffness from

tumor cells. The tumor cells originated from solid tissues and are generally larger and stiffer than many BGCs. In blood, RBCs are much smaller than CTCs, whereas, WBCs could be comparable in size but are generally more deformable than CTCs. Table 2.1 shows the typical size and stiffness of RBCs, WBCs and tumor cells^[58-65].

Table 2.1 Physical properties of RBCs, WBCs and CTCs

	Size	Stiffness
RBCs	Diameter: 6-8 μm , Thickness: 2-2.5 μm	N/A (not blocked by pillars)
WBCs	Diameter: 6-8 μm (Most) 15-30 μm (macrophage)	20-50 Pa (Normal), 75-200 Pa (Leukemia)
CTCs	Diameter: 6-30 μm	500-2000 Pa

In body fluids such as urine and peritoneal fluid, the observed size difference is not so obvious as CTCs could be comparable in size to the normal exfoliated cells (NECs)^[60], which originate as epithelial cells in solid tissues. Therefore, a systematic technique for identifying CTCs from NECs is developed to clearly distinguish the captured cells.

2.1.2 Development of the microfluidic chip

Patterned micro-pillars are erected in the size-based microfluidic chips to block large and stiff cells from flowing through. The gap between pillars ranges from 25 microns, which allows most RBCs and WBCs to flow through down to 6 microns to trap single tumor cells to clusters of tumor cells. The spatial gradation of pillars with the decreasing gap size (in the flow direction) have in the first row the largest gap width

and the last row with the smallest gap size. This arrangement is designed in such a way so that large cell clusters can be blocked in the first few rows while ensuring a smooth flow of other smaller cells to pass through. The pillars can either fill the entire flow section in a matrix formation to provide sufficient checks of each cell going through, or occupy a certain section of the flow in a cluster formation with in-between empty spaces to reduce the shear stress magnitudes. The design of the pillar pattern will be further discussed in details in *section 2.2.1*.

Two types of chips are designed to serve two different functions: a Capture Chip, which traps the passing CTCs/DTCs for rapid imaging, identification, enumeration and image-based characterization; and a Recovery Chip, which allows the captured CTCs/DTCs to be retrieve undamaged for the downstream cellular and molecular characterization and analyses. The schematic layout of the microfluidic chips is shown in Figure 2.1, and their processing workflow is illustrated in Figure 2.2.

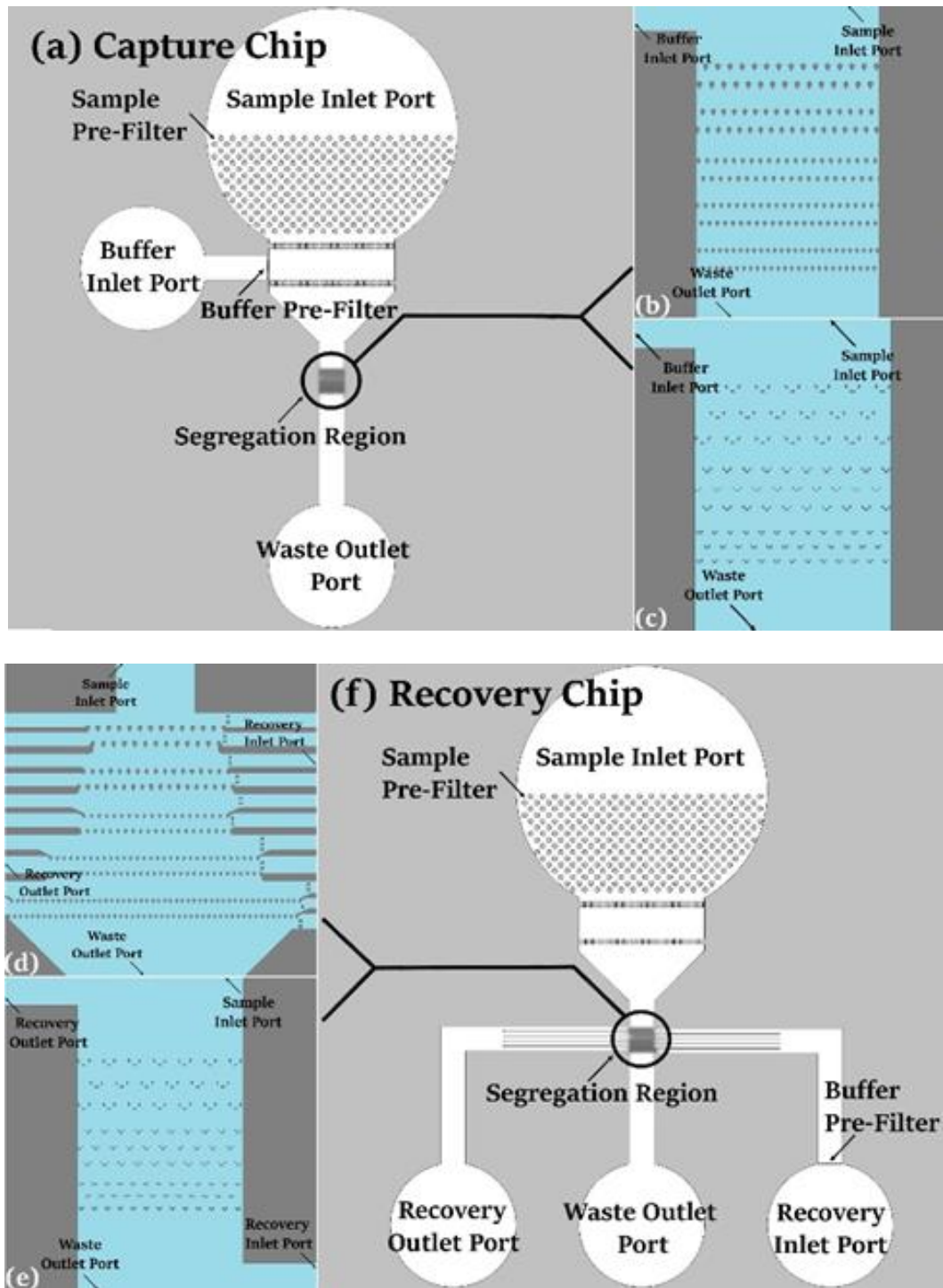


Figure 2.1 Size-based rare cell segregation and recovery system: schematic Capture Chip (a) and Recovery Chip (f) layout, in which the cell segregation region is schematically enlarged in (b) for continuous Capture Chip, in (c) for discrete Capture Chip, in (d) for continuous Recovery Chip and in (e) for discrete Recovery Chip.

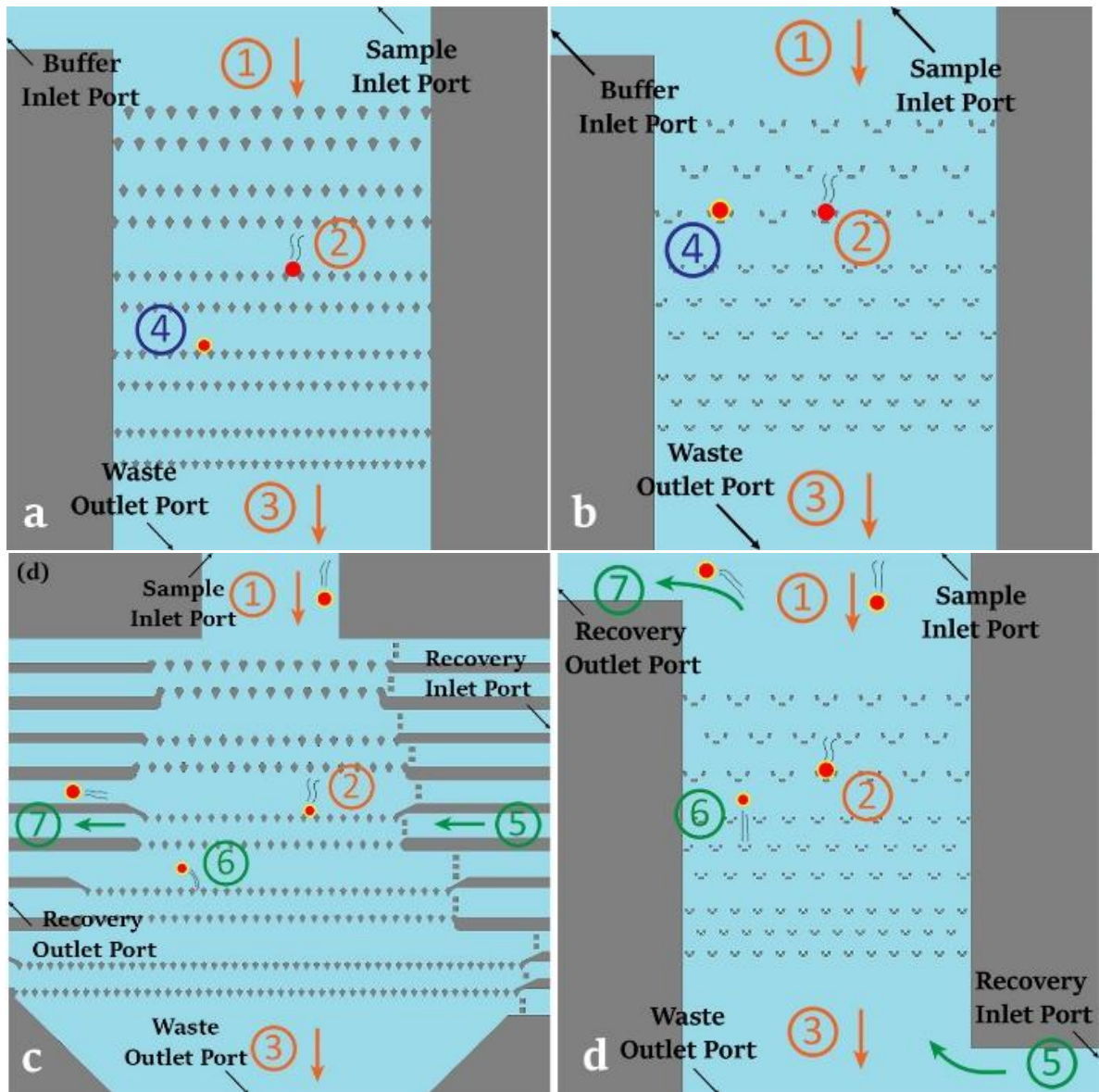


Figure 2.2 Schematic illustration of the tumor cell capture process in continuous Capture Chip (a) and discrete Capture Chip (b): ① tumor cell flow into the segregation region in the sample solution, ② tumor cell captured between the pillars, ③ the rest of the sample flow out of the waste outlet, and ④ cells captured are stained with fluorescent labels. Schematic illustration of the tumor cell recovery process in continuous Recovery Chip (c) and discrete Recovery Chip (d): ① tumor cell flow into the segregation region in the sample solution, ② tumor cell captured between the pillars, ③ the rest of the sample flow out of the waste outlet, and ⑤ recovery buffer enters the recovery inlet, ⑥ releases the cells captured from the pillars, ⑦ carry them out of the chip through the recovery outlet.

2.1.3 Protocol of the microfluidic assay

The procedure of tumor cell capture/recovery starts with the design of the microfluidic chip, which has been discussed in *Section 2.1.2*. Upon the completion of mold preparation, chip fabrication and assembly, the chip is ready for use. The actual experiment starts with sample collection and preparation, with different procedures for blood and peritoneal wash and alternative sample size reduction methods for blood.

With primed chip and processed sample, researchers need to capture tumor cells through flowing the sample through the chip, and in most cases carry out immunofluorescence staining to label the cells for identification and further applications; in a Recovery Chip there is an extra recovery step to harvest the captured cells. The experiment concludes with imaging and interpretation of the images.

To achieve the best performance, the Capture Chip and the Recovery Chip execute two different sample processing pathways.

To stabilize the tumor cells in the Capture Chip, the protocol schedules the whole staining process in-chip, after the tumor cells have been captured. The process of fixing, permeabilization, blocking, staining and incubation will collectively stabilize the trapped tumor cells in the chip. On the other hand, to activate the tumor cells in the Recovery Chip, the protocol schedules the staining process in-tube prior to the capture, and suspends the sample in a surfactant to minimize the adhesion between tumor cells and the chip. If viable tumor cells are required for downstream analyses, the process of

fixing and permeabilization can be skipped, and the buffer solution can be applied for the recovery. The protocol flowchart is illustrated in Figure 2.3, and the detailed procedure of the protocol is presented in *Appendix A*.

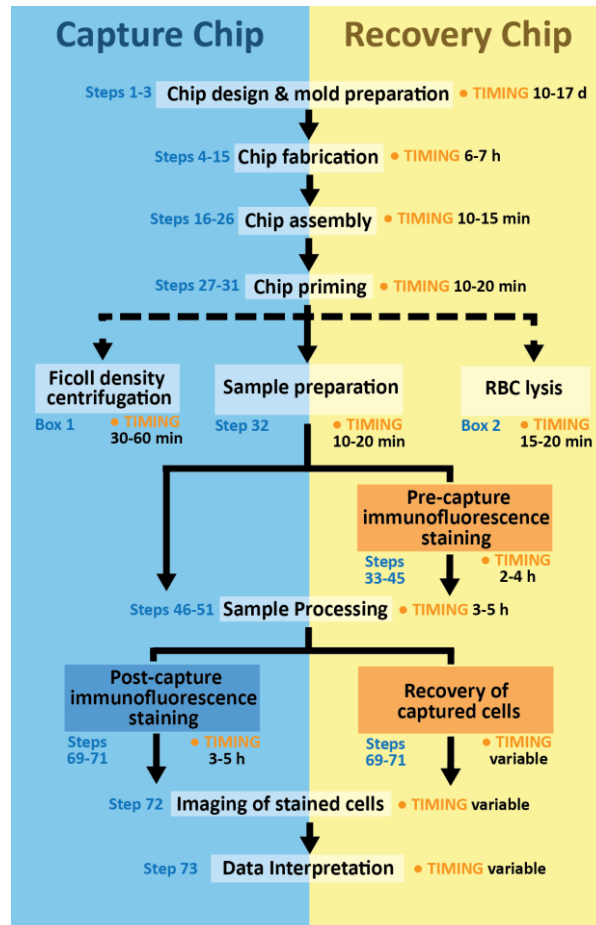


Fig 2.3 Protocol flowchart and estimated timing of each step, detailed in *Appendix A*.

2.1.4 Chip characterization study

To characterize the microfluidic chip for its effectiveness in the capture and recovery of CTCs and DTCs, we conducted several mock experiments with cancer cell lines (listed in Table 2.2) suspended in blood and saline. Often mock experiments can

Table 2.2 Cell lines Tested in Mock Experiments

Cell-line Tested	Origin of the Cell Line	Chips Tested	Results
HeLa	Cervical Cancer	Capture/Recovery	Recovered cells proliferate.
MCF-7	Breast Cancer	Capture	Captured.
A549	Lung Cancer	Capture/Recovery	Recovered cells proliferate.
MDA-MB-231S	Breast Cancer	Capture	Captured.
4T1	Breast Cancer	Capture	Captured.
SKOV3	Ovarian Cancer	Capture	Captured.
S18	Sarcoma	Capture	Captured.
HEm15A	Endometriosis	Capture	Captured.

troubleshoot potential issues, as well as, to obtain optimum flow rates and parameters for a particular body fluid type. This information will help us to design better chips for good efficiency and purity. Besides, the harvested cell line cells remain intact and viable to proliferate in a proper culture environment. According to the results of our mock experiments, the optimized flowrate for our cell capture and recovery is 0.5 mL/hr, which yields an efficiency over 90% and purity of around 90% in our Capture and Recovery Chips, and the A549 and HeLa cells recovered from the Recovery Chip can proliferate in standard culture environment. These results have been reported in our previous publication ^[66].

After the characterization study, we then conducted several clinical trials using body

fluid samples taken from cancer patients. We collected 12 blood samples (10 from Hepatocellular Carcinoma patients and 2 from Gastric Carcinoma patients at the General Hospital of PLA or “301 Hospital” in Beijing), and CTCs were found in all of them (Figure 2.4.a). After clinical verification of the effectiveness of our system, the system has now been applied to blood and urine samples from cancer patients of other Beijing and Zhejiang hospitals (Figure 2.4.b). We will provide a more detailed description of some of these cases in *Chapter Three*.

All clinical experiments carried out are approved by IRB, and are with consent of the participant.

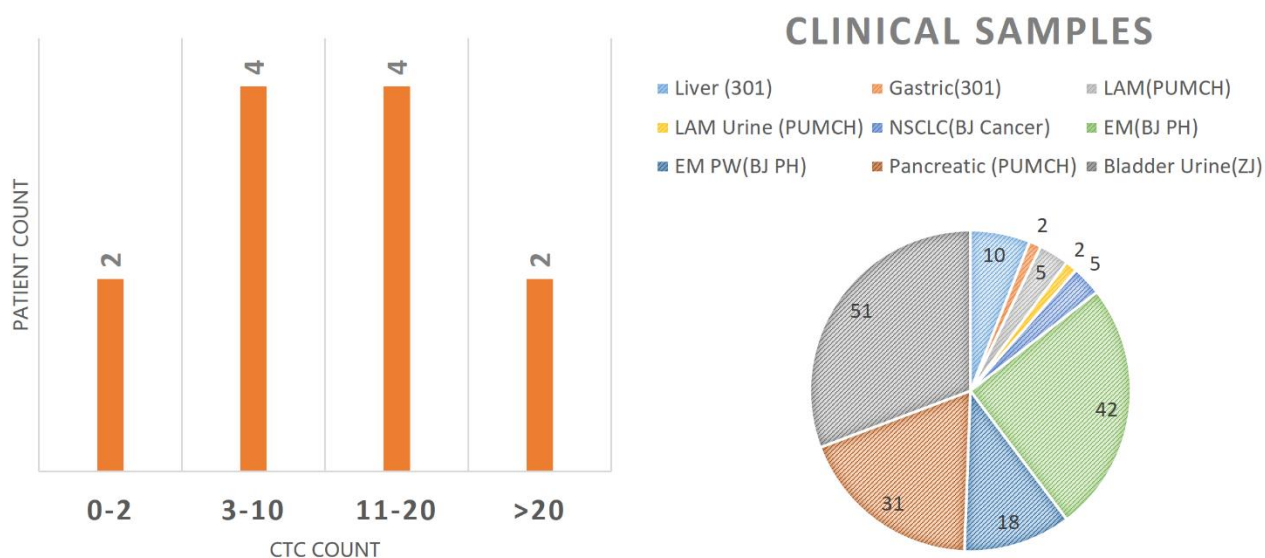


Fig 2.4 Clinical application of the microfluidic assay. (a) CTC enumeration in 12 cancer patients (10 HCC, 2 GC) in 301 Hospital, Beijing. (b) Clinical sample size up to date, the results of Pancreatic Cancer, Non-small Cell Lung Cancer (NSCLC) and Endometriosis (EM) will be discussed in *Chapter Three*. Hospital abbreviations: 301 – General Hospital of People’s Liberation Army, Beijing; PUMCH – Peking Union Medical College Hospital; BJ Cancer – Peking University Cancer Hospital; BJ PH – Peking University People’s Hospital; ZJ – 1st Affiliated Hospital of Zhejiang University.

2.2 Challenges and difficulties encountered

2.2.1 Blood coagulation

A major difficulty with size-based capture systems is blood coagulation. This difficulty can be attributed to high shear rates^[67, 68] arising from the high shear flows around bluff bodies (the numerous pillars) with wakes and mixing layers that can lead to the formation of blood coagulation in those regions. The occurrence of blood coagulation can adversely affect the flowrates by changing the flow field pattern inside the capture chamber of the chip.

To minimize the possibility of blood coagulation, flow separations in the capture region should be kept to a minimum by reducing the shear rates. To address this issue, we considered two aspects. Firstly, the shear rate is dependent not only on the flow velocity but also, on the geometry of the flow field. A normal segregation region with fixed width and fixed duty ratio (ratio between the total width of pillars to total width of gaps) results in uniform average flow velocity in gaps of different sizes, and inevitably small gaps will encounter larger shear rate. Thus we place of pillars in a trapezoidal segregation region, which lowers the average flow velocity between small gaps to reduce shear rate there.

Secondly, coagulation generally occurs in areas of high flow separations (singular points in the flow field). Thus, the shape of the bluff body to the incident flow is crucial – it should be such that it does not encourage flow separations behind the pillars. To minimize this possibility, we attempt to reduce shear velocities in the affected areas to lower values by employing spindle-shaped pillars and having larger separation gaps behind the pillars. An optimized design of the capture chamber with our patented pillar

distribution is shown in Figure 2.5.

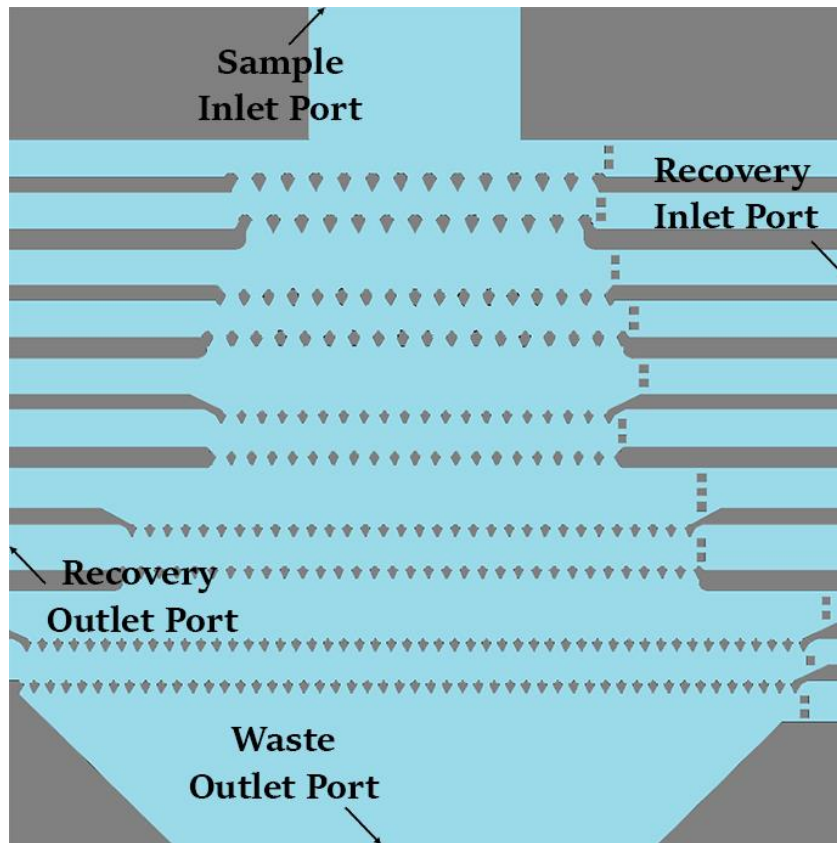


Figure 2.5 An optimized Recovery Chip design with spindle-shaped pillar to reduce the shear rate of singular point, as well as to provide stable support to tumor cells to avoid damage of cells. The trapezoid distribution of pillars evens the shear rate among different rows.

Anti-coagulation treatment of the surface of the pillar can also help to suppress the formation of coagulation. The following reagents are used to generate different effects: anticoagulants such as ethylenediaminetetraacetic acid (EDTA) and heparin: EDTA chelates Ca^{2+} to prevent blood from clotting^[69, 70] and heparin activates the antithrombin to block the thrombin from the clotting^[71]. We also used surfactants such as pluronic, which is a poloxamer to alter the non-slip boundary condition of the flow field to generate a smoother flow and less adhesion of RBCs on the pillars.

Last but not least, it is most important to observe a proper handling of blood samples to minimize the risk of coagulation. Fresh blood that is stored and transported under approved conditions and processed with proper instruments and reagents described in the Protocol can significantly help in this regard.

2.2.2 Limited throughput and capacity

Due to the technical constraint of the material and photolithography process used to fabricate the chip, the aspect ratio of the capture chamber should not exceed 5. This implies that the height of the chamber, which is defined by the smallest gap between pillars and the aspect ratio limit should not exceed 30 μm . Obviously, the height limitation affects the cross sectional area of the chip and by extension, the flow volume. Further, to keep the shear stress in the capture chamber within allowable limits, the flow velocity needs to be restrained. Therefore, with the cross sectional area and flow velocities constrained, the flow throughput will be limited. To reduce the processing time of the reduced flow throughput, the blood sample volume can be overwhelmingly reduced apriori by centrifugating out the blood serum together with most of the RBCs via the blood lysis process. For a non-blood sample, which is mostly water centrifugation will greatly help to reduce the sample volume. We have also incorporated multi-channels (up to 32) in our chip design to speed up the flow throughput. Additionally, with the advent of advanced molding technology, we have experimented with stiffer plastic materials to fabricate chips with much higher heights to significantly enhance the flow throughput.

High capacity assay requires a lot more work for the identification, enumeration, characterization and analysis of the captured tumor cells and this is not an issue with

automated machines but for human researchers, they will need to balance between reasonable workload and the high capacity processing.

2.2.3 Contamination by background cells

BGCs share many similar physical characteristics with tumor cells especially, cells harvested from a non-blood medium such as the peritoneal fluid. In blood, NECs may inadvertently be brought in during the blood-drawing process. As NECs are mostly epithelial in origin, they often form clusters due to their strong adhesion for one another and we employ a pre-filter to remove most of the clusters and other large debris prior to the flow entering the capture chamber. However, some BGCs inevitably get through and to handle them, a comprehensive identification technique needs to be implemented to unambiguously distinguish between the BGCs and tumor cells. This will be described next.

2.3 Identification of CTC/DTCs

It is imperative that the captured CTCs and DTCs be accurately identified via a systematic and thorough approach. We employ the Immunofluorescence (IF) staining technique to biomark and differentiate the tumor cells from the BGCs. A flowchart of our Integrated ID (IID) scheme is shown in Fig. 2.6 and it begins with a simple question: is the captured cell a cell? We used DAPI to answer that question. Next, we employ CD45 to identify the WBCs. Then, we use a specific biomarker to identify NECs and other cells to get to the tumor cells. The details are described below.

- (i) Negative identification: CD45⁺ cells are WBCs. CD45⁻ cells are considered as putative CTC/DTCs.

(ii) Nonspecific positive identification: Cells expressing nonspecific markers are considered as putative CTC/DTCs. Examples of nonspecific markers are mesenchymal markers, e.g. anti-Vimentin (Vim) and epithelial markers, e.g. anti-Pan-Cytokeratin (pan-CK) and anti-Epithelial Cell Adhesion Molecule (EpCAM).

(iii) Specific positive identification: Cells expressing specific tumor-related markers are considered as putative CECs/PECs. These markers are also widely applied in immuno-histochemical tests in pathology departments, like TTF-1 for adenocarcinomas, PSA/PSMA for Prostate Cancer, ER/PR for gynecology-related cancers and diseases.

(iv) Combined identification: A combination of two or three strategies above to increase accuracy and efficiency. For instance, Vimentin is widely used in the identification of mesenchymal CTCs. However, as it is also expressed in some of WBCs^[72, 73], it is necessary to exclude those cells through negative identification to avoid false positive.

A typical identification flowchart is illustrated in Figure 2.6. False positives and false negatives are discussed in detail in Table 2.3.

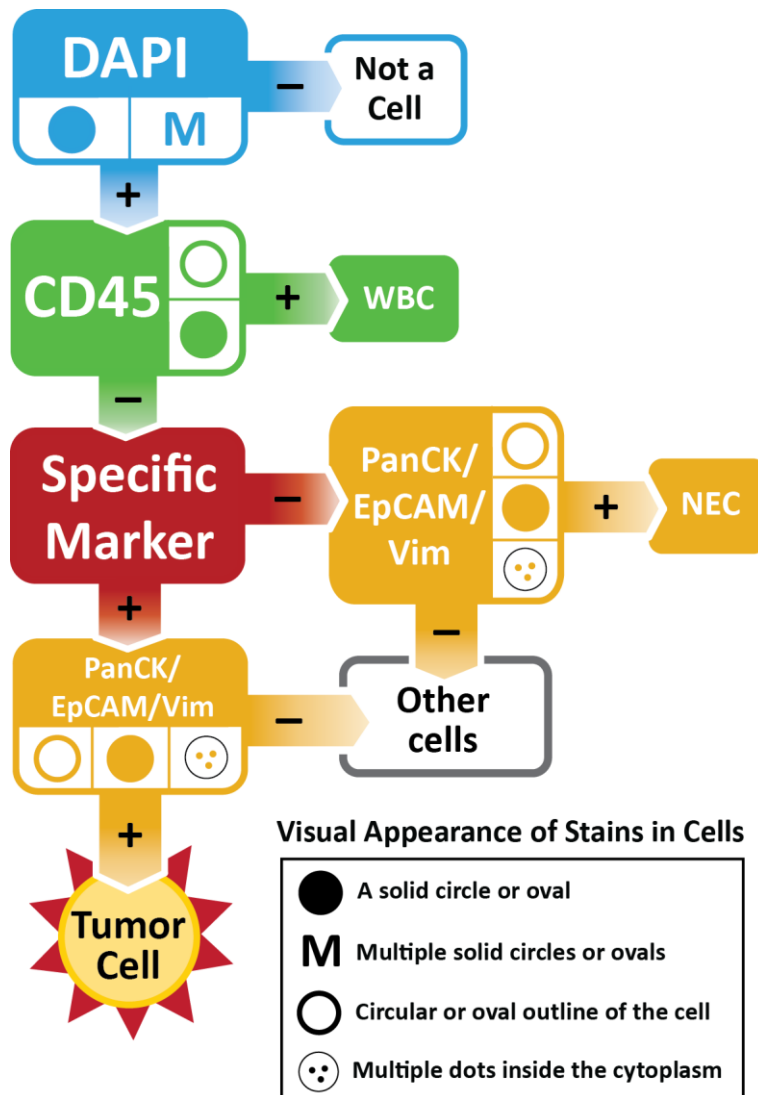


Figure 2.6 A typical combined identification flow chart. IF image can be identified as positive only when it shows proper morphology of corresponding staining. The standard appearance of specific markers is dependent on antibody used.

Table 2.3 Misidentification of tumor cells in different strategies.

Strategy		False Positive		False Negative	
Description	Example	Description	Example	Description	Example
Negative Identification	All CD45- Cells are Tumor Cells	ALL BG cells except CD45+ WBCs	CD45- WBCs, exfoliated epithelial cells, etc.	CD45+ tumor cells	Tumor Cells with CD45 unspecific staining
	All Pan-CK/EpCAM+ cells are tumor cells		Exfoliated epithelial cells, BG cells with unspecific staining		Mesenchymal tumor cells, epithelial tumor cells without staining
Non-specific Positive Identification	All Vim+ cells are tumor cells	BG cells with non-specific marker staining	Exfoliated stromal / mesenchymal cells, Vim+ WBCs, BG cells with unspecific staining	Tumor cells without unspecific staining	Epithelial tumor cells, stromal tumor cells without staining
Specific Positive Identification	All ER/PR+ Cells are tumor cells	BG cells with specific marker staining, usually unspecific staining	ER/PR unspecific stained BG cells	Tumor cells without specific marker staining	Tumor cells without ER/PR expression or staining
Combined Identification	All CD45-, Pan-CK/EpCAM/ Vim+, ER/PR+ cells are tumor cells	BG cells fallen in the criteria	Unspecific stained BG cells	Tumor cells fallen out of the criteria	Tumor cells with CD45 unspecific staining, tumor cells without unspecific or specific staining

CHAPTER THREE

APPLICATIONS OF THE MICROFLUIDIC ASSAY IN CANCER RESEARCH

In this chapter, applications of our size-based microfluidic assay developed in Chapter Two are discussed and presented. The work includes the following topics.

1. CTC enumeration and the staging of the pancreatic cancer.
2. CTCs from non-small cell lung cancer (NSCLC) patients are characterized with advanced imaging technology that reveals putative mitophagy in CTCs.
3. In blood and peritoneal fluid of patients with endometriosis (EM) the endometrial cells are detected and recovered. Their role in pathogenesis and clinical management of EM and the potential of Circulating Endometrial Cells (CECs) as a screening and differential diagnosis tool is discussed.

3.1 CTC Enumeration and Staging of Pancreatic Cancer

3.1.1 CTC Enumeration Methodology and Its Clinical Importance

Enumeration of tumor cells is conveniently performed in-chip in the capture chamber of our Capture Chip (Figure 3.1). This simple counting of the number of captured tumor cells constitutes the first and up to now, the only FDA-approved clinical application of the CTC technology. CellSearch commercialized the method by developing an EpCAM-based technique to capture and enumerate the CTCs in 7.5 mL

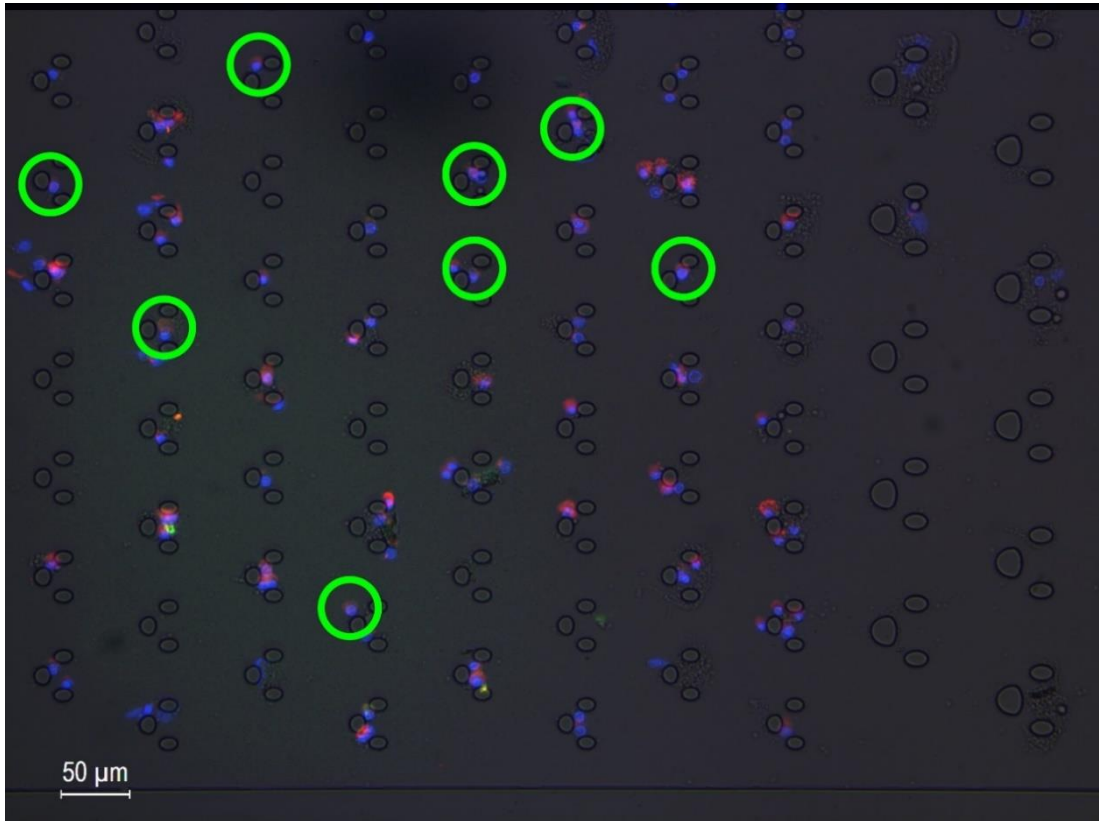


Figure 3.1 Enumeration of rare cells (marked in circles) in a merged converted microscope image.

of cancer patient's blood. The method was applied to predict the prognosis, including the Overall Survival (OS) and Progression Free Survival (PFS) of 3 types of cancer: breast ^[36, 74, 75], prostate ^[76] and colorectal ^[77, 78]. Besides, the enumeration of CTCs has been reported to be relevant to the prognosis of non-small cell lung cancer (NSCLC)^[79], small cell lung cell ^[80-82], metastatic breast cancer patients undergoing chemotherapy^[83], hepatocellular carcinoma ^[84], and has been tested as prediction biomarker in several clinical trials ^[85-87] and to predict the cancer drug sensitivity ^[88].

To yield accurate and consistent enumeration, several issues should be addressed.

1. The chip has a limited cell-capturing capacity as defined by the characteristics of the capture chamber. Further, the number of tumor cells that can be captured is determined by the collection location and volume amount of the body fluid sample. To avoid systematic errors in the enumeration data where some of the results refers to the maximum number of tumor cells (saturation capacity) a chip can capture and others are not, it is important that the chip is properly and adequately quantified. This is usually done using an aliquot of an evenly spiked sample to mimic the tumor cell concentration of an expected body fluid sample and test multiplicative volumes of it to accurately enumerate the spiked tumor cells. From the plot of the collected data, it is not difficult to see that the final enumerated sample capacity is smaller than the saturation capacity because there will not be further increase in the tumor cell enumeration with the sample volume.

2. Not only is the in-chip counting of the captured tumor cells more convenient but it is also more accurate. The classical approach of retrieving captured cells for subsequent counting in a dish can introduce errors due to incomplete retrieval and inaccurate counting when cells are stacked in a dish. In our design, the Capture Chip instead of the Recovery Chip is used for enumeration.

3. To guarantee the consistency of the experimental conditions, it is suggested that the standards referred to in Section 2.3 for tumor cell identification in a fixed volume of sample and the protocol in *Section 2.1.3* be strictly adhered to.

3.1.2 Pancreatic Cancer and Its Staging

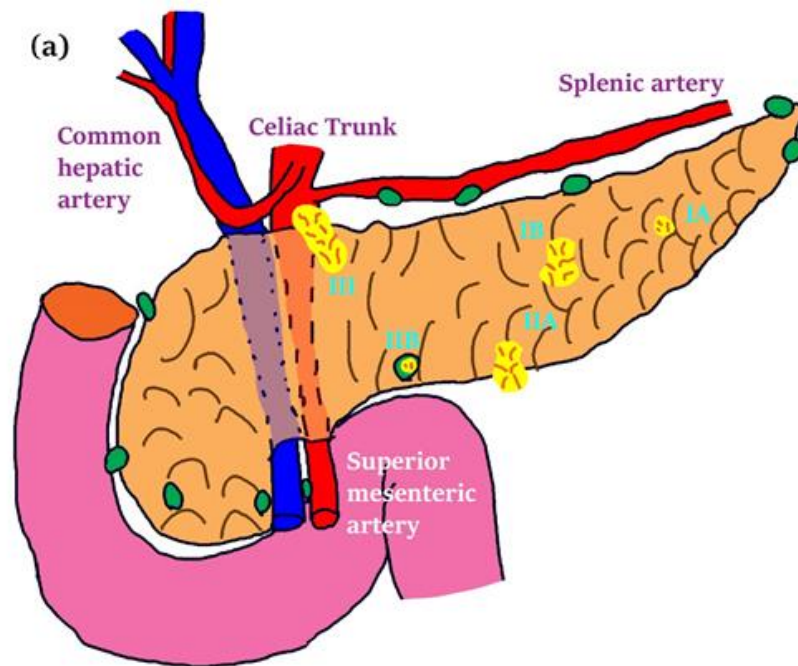
Pancreatic cancer is caused by the presence of highly malignant gastrointestinal tumors in the pancreas and the pancreatic ductal adenocarcinoma (PDAC) is the most

common. In China, this cancer is responsible for 79,400 deaths in 2015^[1]. World-wide, it is ranked as the 7th highest cancer mortality in both males and females and in developed countries, it is the 5th highest mortality in males and the 4th highest mortality in females ^[89].

Due to its aggressiveness and lack of early stage symptom or screening tools, pancreatic cancer patients have a low survival expectation (Figure 3.2 b). Complete resection of the tumor is the key to enhancing the survival rates, but surgery is not beneficial for Stage IV cancer patients.

3.1.3 Pancreatic Cancer Staging Prediction Based on CTC Enumeration

Our pancreatic cancer research is a collaboration with Peking Union Medical College Hospital (PUMCH) or XieHe in Chinese. Pancreatic CTCs are segregated from 2 mL of peripheral blood taken from 15 patients diagnosed with pancreatic cancer and 2 patients diagnosed with other pancreatic diseases (not pancreatic cancer, NPC). CTCs are identified with an integrated ID algorithm: a cell with proper shape and DAPI staining, with CD45 negative, E-Cadherin or Vimentin positive is identified as a CTC, as shown in Table 3.1.



(b) 5 Year Survival Rate of Pancreatic Cancer

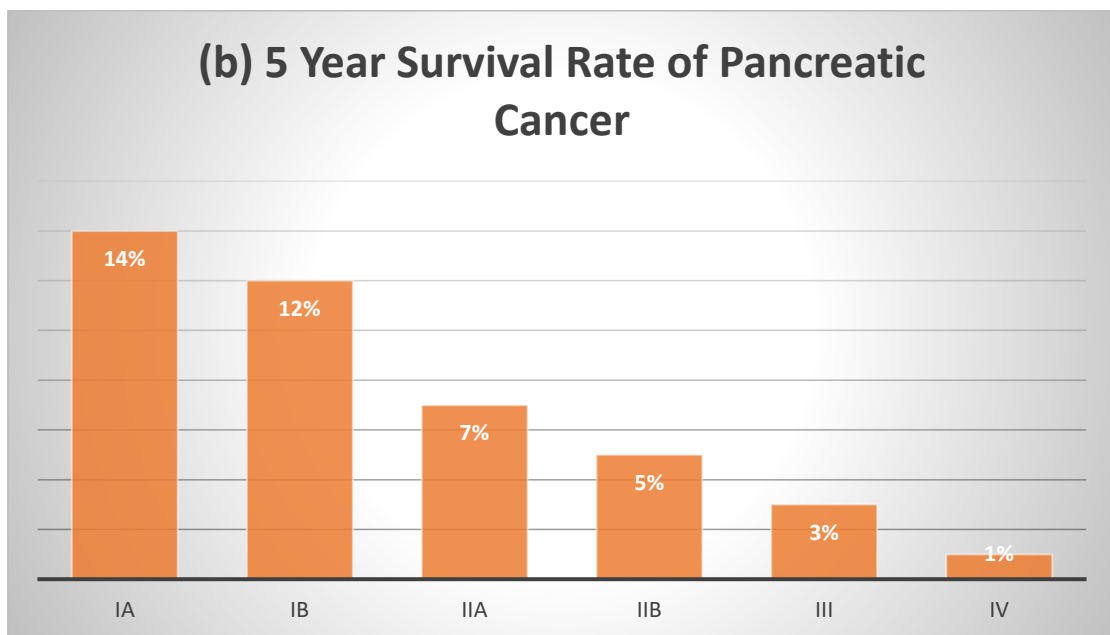


Figure 3.2 a) Staging of pancreatic cancer and b) its relevance with prognosis of patients. Stage IA and IB are tumors confined in pancreas, Stage IIA tumor intrudes out of pancreas but does not invade celiac trunk or superior mesenteric artery, which is indication of Stage IB. Invasion to lymph nodes results in Stage IIB and distant metastasis (not shown in image) indicates Stage IV.

Table 3.1 Identification of Pancreatic CTCs

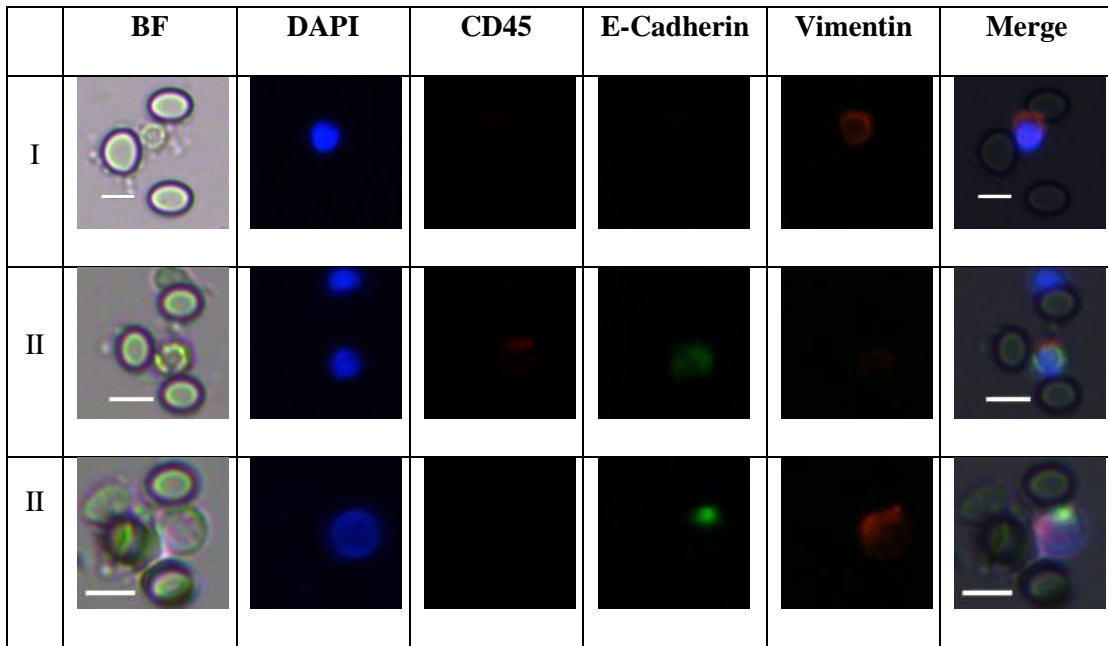


Table 3.2 Records of Participants

Patient ID	Gender	Age	Diagnosis Date	Diagnosis	Staging
2070416	M	58	2015/10/14	Acinar Cell Carcinoma of Pancreas	IIA
2070599	F	58	2015/10/20	PDAC	IIA
2071580	M	54	2015/11/04	PDAC	IIA
26263992	F	58	2015/11/17	PDAC	IIA
2075319	M	79	2015/11/30	PDAC	IIA
2075210	F	74	2015/12/01	IPMN Malignant Transformation	NPC
2075386	F	60	2015/12/01	PDAC	IIB
2072539	M	59	2015/12/03	PDAC with Hepatic Metastasis	IV
2075396	M	57	2015/12/03	PDAC	IIA
2072595	M	41	2015/12/08	Non-Cancer	NPC
2075783	M	47	2015/12/09	PDAC	IIA
2135346	M	69	2015/12/09	PDAC Invading Aorta	IV

Table 3.3 CTC Enumeration records.

Group	NC	Stage IIA	Stage IIB	Stage IV
Enumeration Records	21, 25	17, 32, 33, 34, 86, 126, 146, 158	51, 102	141, 143, 221

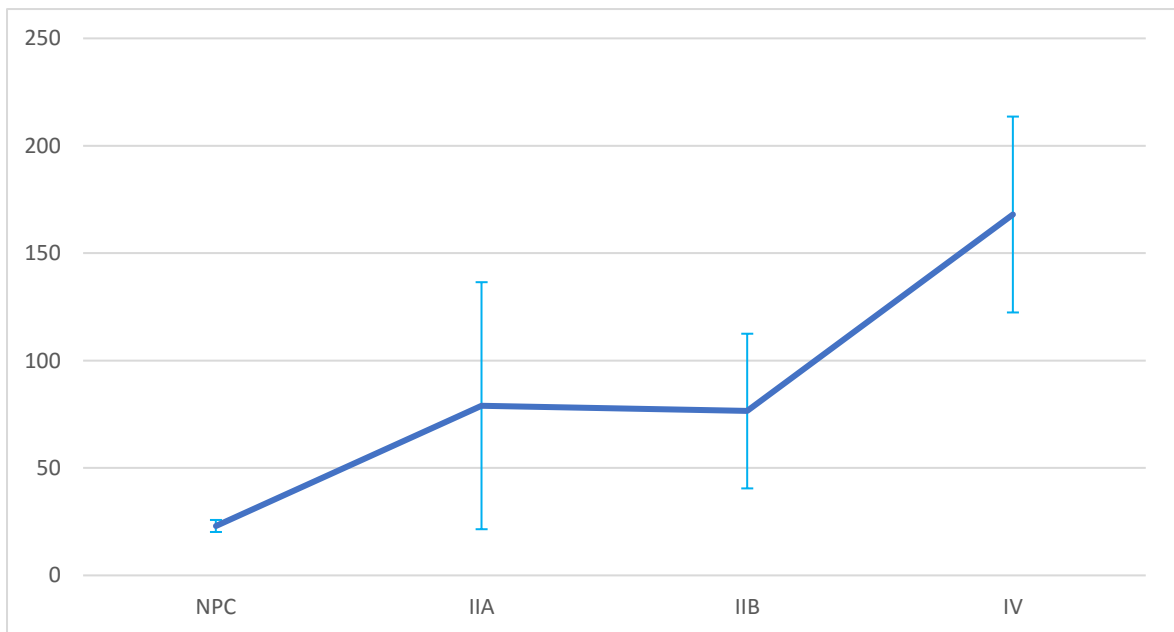


Figure 3.3 ANOVA plot of CTC enumeration versus cancer staging.

The participants of the research and their *discharge* diagnosis are summarized in Table 3.2. The enumeration results are summarized in Table 3.3 and Figure 3.3.

Through an analysis of variance (ANOVA) for a single factor, there is a significant difference in mean values of CTC enumeration at different stages of the pancreatic cancer ($p = 0.047$). Our CTC assay results showed that if the captured CTCs > 130 , it indicates a high probability of the disease being a Stage IV pancreatic cancer ($p = 0.010$).

The above results suggest that the enumeration of CTCs can serve as a biomarker for evaluating the severity of the disease. It also serves as an indirect indicator for the surgery option to remove the tumor in pancreatic cancer patients. It is also pointed out that CellSearch is unable to capture pancreatic cancer CTCs as they do not express EpCAM positive and our success in capturing these CTCs is a clear testimony of the superiority of the size-based method over the CellSearch technique.

3.2 CTC Characterization and Mitochondrial Autophagy of NSCLC CTCs

3.2.1 Image-based Characterization Methodology

In addition to simple counting of the number of CTCs and DTCs, their visual characterization can also yield important information ^[90-92]. The cell morphology (via Pep staining or HE staining), chromosome morphology (via FISH) ^[93], specific protein expression (via IF) can provide valuable molecular information about the nature of the tumor cells. These features have been adopted in the analyses on pathological sections of primary tumors guide the chemotherapy treatment after surgery in cancer patients^[94]. Potential mutation of CTCs may bring about conflict between the results of primary

tumor and CTCs, which may question the effectiveness of primary-tumor-based chemotherapy.

These characterizations are suitable for in-chip assessment, which allows for an immediate observation, and in-plate, which grants the researcher freedom to apply complicated methodologies. To facilitate in-chip imaging-based characterization of tumor cells, it is suggested that the PDMS-side of the chip be fixed on a thin cover slide, in order to yield high-quality images or with advanced imaging techniques using confocal and bi-photon imaging techniques.

3.2.2 Mitochondrial Autophagy

A mitochondrion is an organelle that generates energy (in the form of ATP) in eukaryotic cells. Excessive amount of mitochondria in a cell generates excessive Reactive Oxygen Species (ROS), which is life-threatening to the cell^[95]. An autophagy pathway, regulated by Atg7 gene and mTOR pathway, can be activated to disassemble redundant mitochondria^[96, 97].

The activation of mitochondrial autophagy (also called mitophagy) is vital to the survival of cells migrating from oxygen-deficient environment (ODE) to oxygen-enriched environment (OEE). Our collaborator has proven it with a well-studied example of the exit of mature T Lymphocytes (T-Cells) from thymus in unpublished research. Autophagy is essential in the clearance of high mitochondrial content within the mature T-Cells, which is threatened by oxygen stress in OEE (blood) when they exit ODE (thymus).

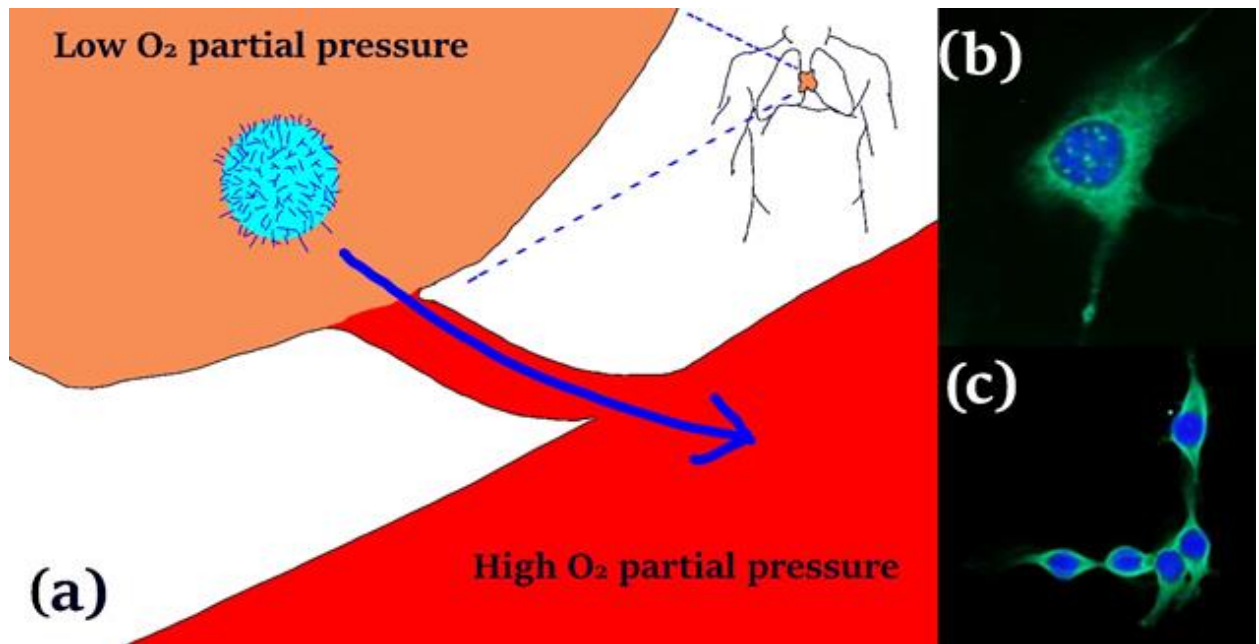


Figure 3.4 (a) Schematic illustration of the transition of T-Cell from ODE (thymus) to OEE (blood). (b) Cells undergoing induced mitochondrial autophagy can be characterized by punctuate LC3 (Green) signal, while (c) cells free from induced mitochondrial autophagy shows diffuse LC3 (Green) signal.

Autophagy can be characterized with LC3 fluorescent staining. When autophagy occurs, the diffuse cytoplasm signal aggregates and forms punctuate cytoplasm signal (Figure 3.4) [98, 99].

3.3.3 Putative Mitochondrial Autophagy of NSCLC CTCs

The extravasation process of CTCs increases the oxygen stress on the cell, as solid tumor is ODE and blood is OEE. Thus it is reasonable to expect occurrence of mitochondrial autophagy in CTCs. The mitochondrial autophagy in tumor cells can regulate both the growth and death of tumor cells, thus has been recognized as a potential mechanism to control the development of cancer [100, 101].

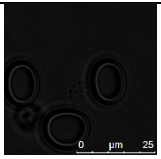
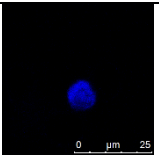
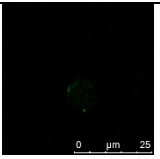
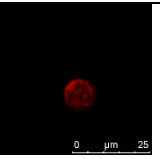
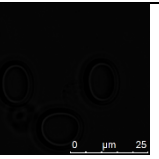
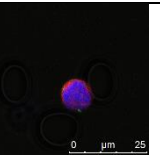
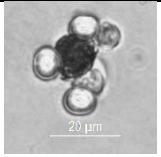
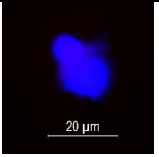
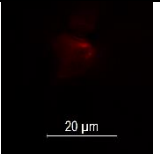
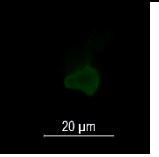
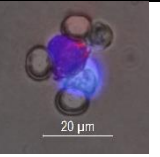
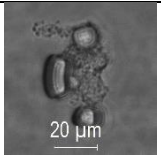
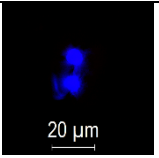
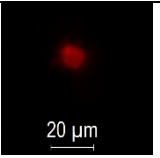
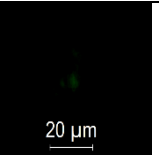
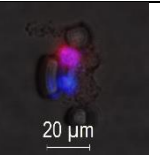
Non-small Cell Lung Carcinoma (NSCLC) accounts for 85% of lung cancer occurrences. As the lung is the organ that supplements blood with oxygen, the blood in pulmonary vein bears the highest oxygen partial pressure in the whole circulation

system. Thus it is reasonable to expect the occurrence of mitochondrial autophagy in NSCLC CTCs harvested from the pulmonary veins of NSCLC patients.

Our NSCLC research is a collaboration with Prof. Zhang Yu of Peking University Health Sciences Center, and clinical samples are provided by Peking University Cancer Hospital. Blood samples are collected from pulmonary veins and cephalic veins of NSCLC patients undergoing tumor resection surgery. CTCs segregated are characterized with DAPI, CD45, pan-CK, EpCAM, Vimentin and LC3. A cell with DAPI positive, CD45 negative, pan-CK or EpCAM or Vimentin positive is identified as a CTC, and the formation of LC3 signal indicates whether autophagy has occurred.

CTCs have been identified in all five pulmonary samples from NSCLC patients, and two cases of putative autophagy have been observed by inverted microscopy and confocal microscopy in pulmonary samples of two patients. Considering that the CTCs have gone through a change of oxygen pressure, we identify the phenomena as putative mitophagy cases. On the other hand, no putative autophagy has been observed in CTCs in peripheral samples (Table 3.4).

Table 3.4 CTCs with putative autophagy signal.

Lung	BF	DAPI	LC3	CK/Vim	CD45	Merge
(a) Confocal						
(b) 100x				N/A		
Peripheral	BF	DAPI	LC3	CK/Vim	CD45	Merge
(c) 100x				N/A		

Considering the fact that CTCs can withstand high oxygen pressure in pulmonary vein upon their exit from primary tumor, it is reasonable to speculate that the LC3 punctuate observed in CTCs reflects the occurrence of mitochondrial autophagy. Its rarity (2 cells in 5 patients) suggests a low efficiency of characterization methodology – most CTCs probably have already gone through the mitochondrial autophagy process at the point of characterization. Thus, an improvement in the methodology is required to increase the efficiency of characterization. Nevertheless, the putative occurrence of mitochondrial autophagy during CTC extravasation suggests the blockage of its mitochondrial autophagy pathway a potential therapy for the inhibition of cancer metastasis.

3.3 Detection of CEC/PECs and Their Role in Pathogenesis and Clinical Management of Endometriosis

3.3.1 Endometriosis and Its Pathogenesis Pathways

Endometriosis (EM) is a common disease in women of reproductive age. It is defined as the condition that endometrial gland or stromal appears outside the uterus, to pelvic cavity, abdominal wall, and the surface of organs like uterus, or even distant tissues like lung, pleural, brain (Figure 3.5.a-c). According to clinic pathology characteristics, endometriosis is categorized into peritoneal endometriosis (PEM), ovarian endometriosis (OEM), deep infiltrating endometriosis (DIE) and other endometriosis (OtEM) that influences distant organs like lung, brain ^[102]. EM often brings about pelvic mass, pain and infertility. Due to the lack of typical clinical symptom in some patients and the lack of reliable biomarker ^[103], the confirmation of diagnosis relies on invasive laparoscopy ^[104]. The diagnosis delay of EM reaches up to 7 to 11 years.

EM is not a cancer, and does not cause fatality. However, the biological behavior of EM, which is a benign disease, is very similar to that of malignant tumor, including invasion, angiogenesis, distant foci growth, etc. Thus it is called “A cancer without fatality”. EM patients are exposed to the risk of 50% recurrence rate and 1% malignant transformation rate.

There have been various theories to explain the pathogenesis of endometriosis (Figure 3.5.d), among which Sampson’s Retrograde Menstruation Theory is widely recognized. It ascribes the formation of endometriosis in pelvic cavity to the endometrium debris that retrograde with menstruation into the fallopian tube, then enter the pelvic cavity

through the fimbriated extremity of fallopian and end up forming endometriosis ^[105]. However, the theory cannot explain the fact that retrograde menstruation occurs to 90% women at childbearing age, while only 10% of them are diagnosed with endometriosis^[106].

An alternative hypothesis, the hematogeneous theory, proposes that active endometrial cells in the circulation are responsible for the formation of ectopic foci. It explains the occurrence of EM at distant organs. Other theories are coelomic metaplasia theory and induction theory which propose that mesothelial cells in ovary, pelvic cavity and abdominal wall can differentiate or be induced to differentiate to endometrial-like cells. They can explain not only abdominal endometriosis and ovary endometriosis, but also EM in thoracic cavity and EM of pre-puberty, adolescent and women who has not ever had period. However, the metaplasia/induction mechanism is not clear yet.

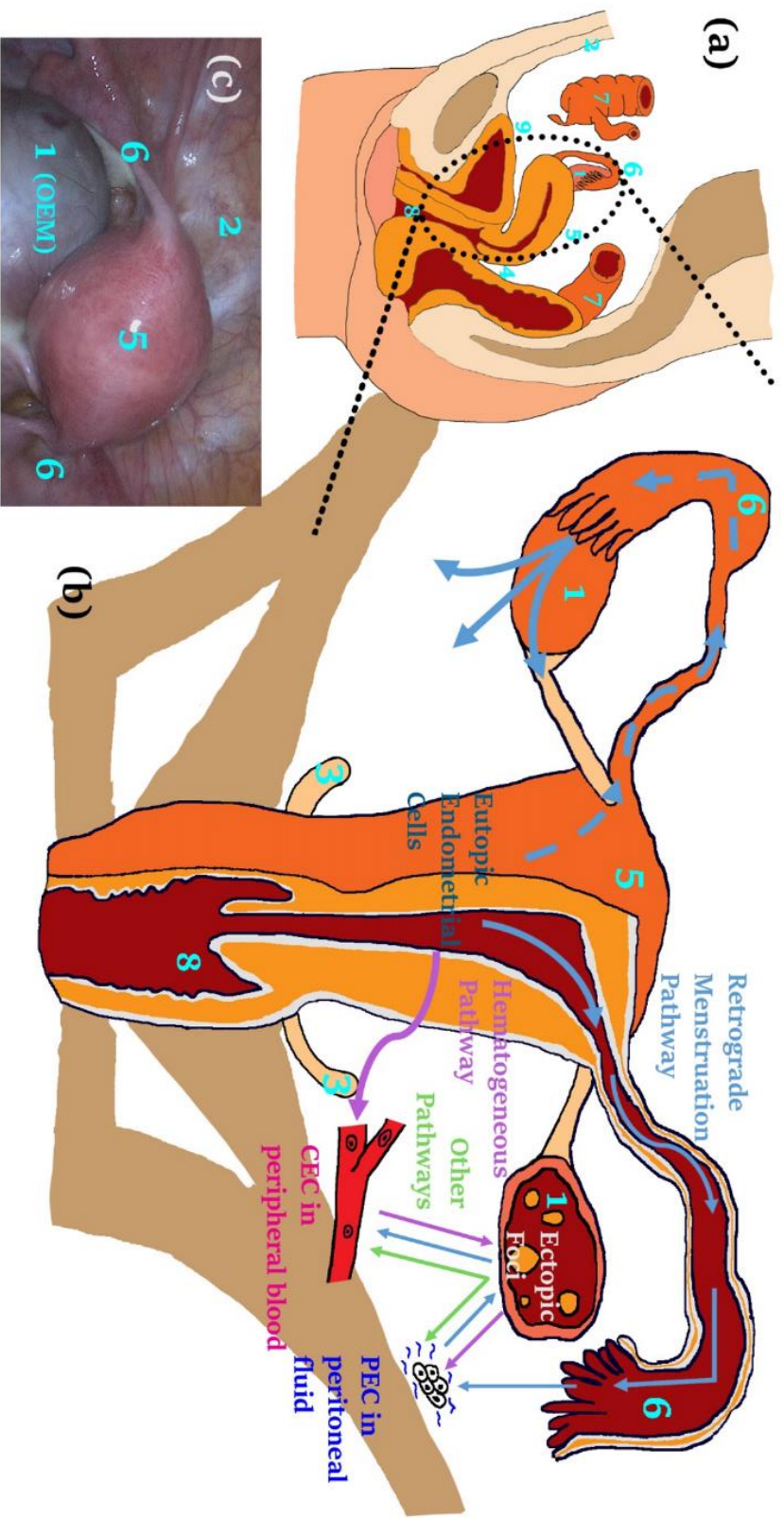


Figure 3.5 Endometriosis is mostly likely to occur in abdominopelvic cavity (a – sagittal section, b – coronal section of the pelvic cavity, c – top view laparoscope image) to: 1. Ovary (in 1.c an OEM chocolate cyst is visible in the ovary), 2. Peritoneum, 3. Uterosacral ligament, 4. Douglas pouch, 5. Surface of uterus, 6. Fallopian tube, 7. Colorectum, 8. Uterine cervix, vagina, vulva, 9. Bladder and ureteral. Current pathogenesis theories of endometriosis is illustrated in d with their explanation to the pathogenesis pathway of eutopic endometrium, CECs, PECs and ectopic foci: Retrograde menstruation theory attributes the foci to PECs in retrograde menstruation; hematogenous theory attributes the foci to CECs in peripheral blood; other theories, such as Müllerianosis theory and coelomic metaplasia theory, conclude the occurrence of endometriosis to *in situ* factors instead of from eutopic endometrium.

In a previous report, Circulating Endometrial Cells (CECs) have been discovered in the peripheral blood of EM patients with 20% detection rate, while Peritoneal Endometrial Cells (PECs) have been discovered in all patients^[107]. Its low efficiency disables it from predicting the occurrence of EM. Our CTC assay has been applied on EM and other gynecology patients to detect CECs and PECs. The results indicate that CECs is potential a EM biomarker and can provide insights to the pathogenesis of EM.

3.3.2 Detection of CEC/PECs in Endometriosis Patients

The following EM research is a collaboration work with Peking University People's Hospital. Blood samples are collected from cephalic veins of three cohorts of participants, EM patients, and two control groups are patients with other gynecology diseases that receive laparoscopy treatment and healthy volunteers. Peritoneal wash (PW), which represents the cellular content of ascites, is obtained by washing the pelvic cavity with 500 mL sterile normal saline solution using a laparoscopic needle and manual aspiration using a syringe after pre-medication and anesthesia administration. It is collected from EM patients and patients with other gynecology diseases that receive laparoscopy treatment.

CEC/PECs are identified with a combined identification strategy illustrated in Figure 3.6. A cell that has proper shape and DAPI staining, with CD45 negative, Pan-CK or EpCAM or Vimentin positive, and Estrogen Receptor (ER) or Progesterone Receptor (PR) positive, is identified as an endometrial cell. Data of participants are summarized in Table 3.5. Typical CECs and PECs identified in Capture Chips and recovered from Recovery Chips are shown in Table 3.6.

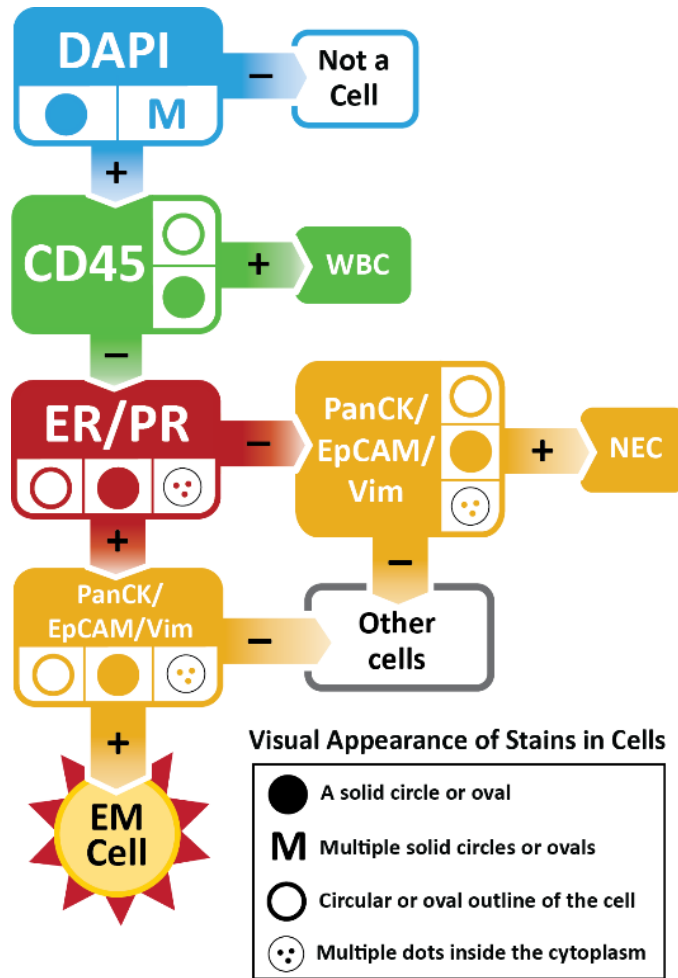
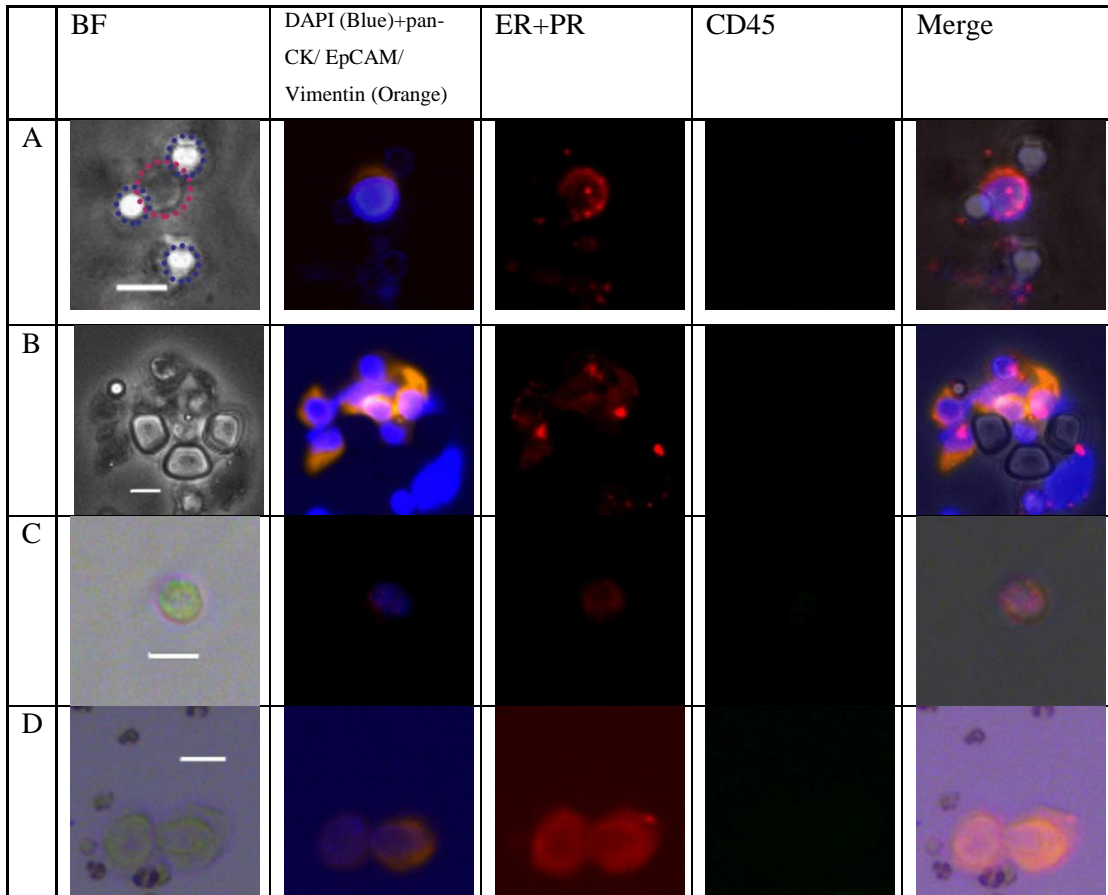


Figure 3.6 Flowchart applied to identify CEC/PECs. Circles in each decision box show typical positive phenomenon of corresponding stain: solid staining, multiple solid stains, circle outliner, or dots inside cytoplasm.

Table 3.5 Participant data.

Group	Case Number	Age	Positive Case Number	Detection Rate
EM	7	24-45	5	71.4%
Other Diseases	8	28-60	2	25%
Healthy	8	25-40	1	12.5%

Table 3.6 Captured CECs in peripheral blood (a) and PECs (b) in PW of EM patients. The red circle in (a) highlights the cell captured while the blue circles highlight the pillars of the microfluidic chip. Recovered CECs from peripheral blood (c) and PECs from PW (d) of EM patients. Bar = 10 μ m.



3.3.3 CEC – a Potential Biomarker for Endometriosis Diagnosis

Biomarker for diagnosis is regarded as one important issue in EM clinics. Currently, the diagnosis of EM relies on invasive laparoscope, while the screening of EM relies on the experience of imagological doctor, as none of the biomarkers discovered yields satisfactory results. In this section, the potential of CEC detectability in our rapid assay to become a reliable screening and differential diagnosis is discussed.

Correlation analysis shows significant difference of detectability among EM patients, patients of other gynecology diseases and healthy control (Figure 3.7, $p=0.044$). It

shows the promising prospect of CEC as a biomarker for the diagnosis of EM. Our results suggest two aspects of applications:

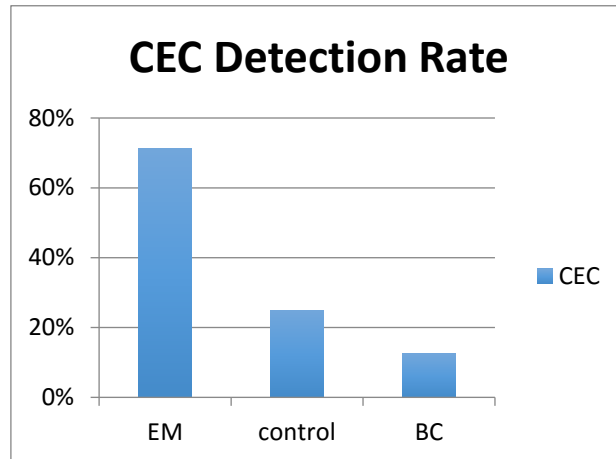


Figure 3.7 Detection rate of CECs in EM patients, other gynecology disease patients (control) and healthy volunteers (BC).

1. Screening of EM: Detectability of CEC varies significantly between EM patients and healthy volunteers (Figure 3.8, $p=0.02$) in correlation analysis. It suggests the potential application of CEC as a tool for EM screening. The sensitivity of the screening is 71.4%, and the specificity is 87.5%.

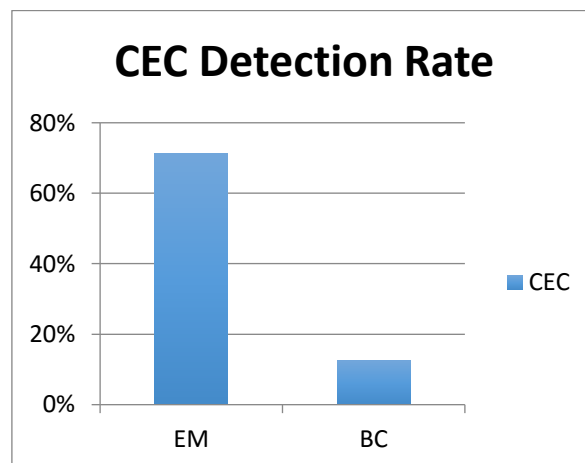


Figure 3.8 Detection rate of CECs in EM patients and healthy volunteers (BC).

2. Differential Diagnosis of EM: Detectability of CEC varies significantly between EM patients and other gynecology disease patients (Figure 3.9) in correlation analysis. It suggests the potential application of CEC as a tool for distinguish EM patients in gynecology disease patients. The sensitivity of the differential diagnosis is 71.4%, and the specificity is 75%.

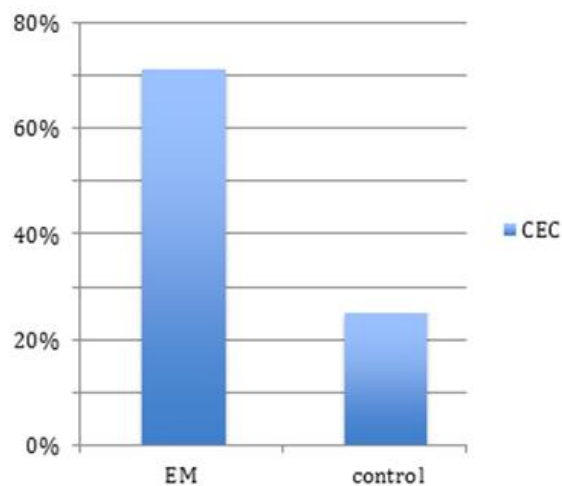


Figure 3.9 Detection rate of CECs in EM patients and other gynecology disease patients (control).

Serum CA125 level of all EM patients and other gynecology disease patients has also been tested for comparison. Rise in CA125 level has been reported in EM patients. Due to the lack of recognized biomarker with good sensitivity and specificity, CA125 is widely applied in the auxiliary diagnosis of EM, with its Upper Limit of Normal (ULN) of 35 U/ml for ovarian cancer screening. Recorded results (Table 3.7) show that the CA125 abnormal rate in EM group is only 42.9% (3/7), and in other gynecology disease group reaches 37.5% (3/8) ($p=0.83$). Its specificity is 62.5%, and sensitivity merely 42.9%.

Table 3.7 Comparison of CEC detection rate and CA125 abnormal rate

Group	Count (n)	CEC		CA125	
		Positive Cases	Detection Rate	Abnormal Cases	Abnormal Rate
EM	7	5	71.4%	3	42.9%
Control	8	2	25%	3	37.5%
Specificity		75%		62.5%	
Sensitivity		71.4%		42.9%	

Contingency table and Chi-square test on the detection of CEC and CA125 abnormality shows that they are not significantly dependent (Figure 3.10, contingency coefficient = 0.213, $p=0.398$). To evaluate the value of CEC as a biomarker for EM differential diagnosis, an ROC curve refer to “other gynecology diseases” (Figure 3.11) is plotted. The Area Under the Curve (AUC) of CEC is 0.732, which exceeds the AUC of CA125 (0.527) and joint decision of CEC and CA125 (0.705).

The pie chart (Figure 3.12) of all participants shows that all right lower quadrant participants are EM patients, and most of the rest EM patients positions at the right higher quadrant. Majority of control group participants appear on the left quadrants. In conclusion, CEC and CA125 tests should be conducted on patients with pelvic mass shown by ultrasound. When CEC is detected and CA125 level is abnormal, special attention should be paid to the possibility of EM occurrence; the detection of CEC indicates high risk of EM and its negative results indicates low risk of EM.

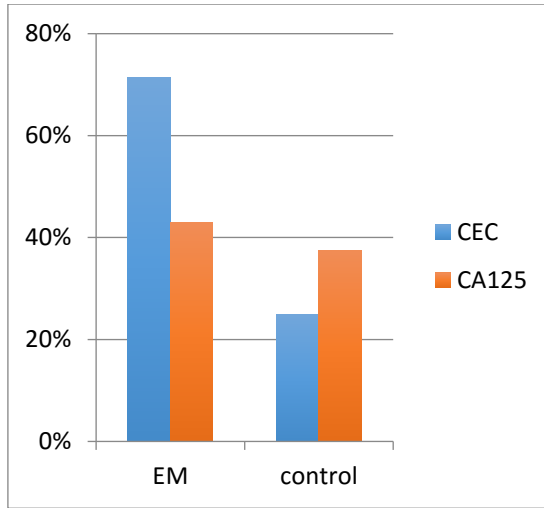


Figure 3.10 Detection rate of CEC and abnormal rate of serum CA125 level in EM patients and other gynecology disease patients.

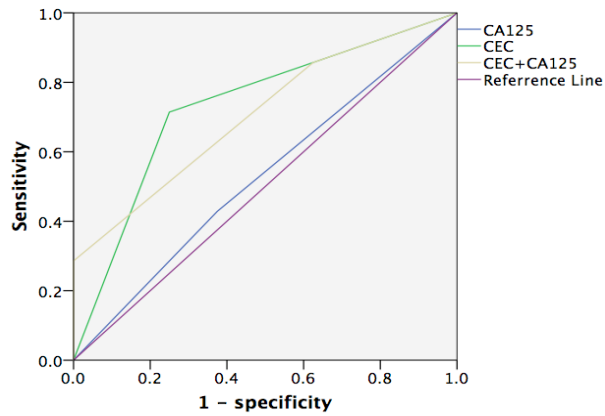


Figure 3.11 ROC curve of CEC detectability, CA125 level and joint test.

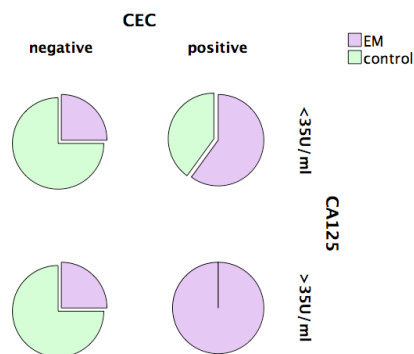


Figure 3.12 Pie chart of CEC detectability and CA125 abnormality.

3.3.4 The Role of CEC/PECs in Endometriosis Pathogenesis and Clinical Management

Through cellular and molecular analysis on recovered CEC/PECs, we can identify the source of CEC/PECs, their relationship with the status and characteristics of EM, and its role in the pathogenesis and development of EM.

PECs are almost omnipresent in samples from all participants in the research (100% in EM patient group and 80% in other gynecology disease patient group, PW is not accessible in healthy control group), while CECs have been detected in 71.4% of EM patients and 18.8% of other participants. The results (for PEC, the significance of difference is $p = 0.40$; for CEC, the significance of difference is $p = 0.04$) provide support to Retrograde Menstruation Theory through revelation of the presence of endometrial cells in abdominopelvic cavity, which can be ascribed to retrograde menstruation. The source of CECs remains unknown – whether they are hematogeneous metastasis of eutopic endometrium, or invasion of ectopic foci aroused by retrograde menstruation or induction/metaplasia. An evolutionary tree of CEC/PECs and eutopic/ ectopic endometrial tissues can be established to fully understand the relationship between them, and to reveal the pathogenesis of EM. There are trillions of cells in human body, which are genomic homological and reproduce with high genomic fidelity. However, mutations inevitably occur to genomes. Human genome consists of billions of base pairs, which mutates at a rate as low as tens to hundreds of billionth. The offspring of a cell will carry the same mutation as their ancestor, therefore the more mutations shared by two cells, the closer they are in the evolutionary tree. Through the establishment of the evolutionary tree, different metastasis sites in cancer patient have been sorted in accordance to their occurrence sequence. The revelation of occurrence

sequence of CEC/PECs and eutopic/ ectopic endometrium will evidently reveal the pathogenesis of EM.

On the other hand, CECs/PECs, just like CTCs in cancer, have the potential to be biomarker for the precise medicine of endometriosis. Existing biomarkers which are mostly molecules like glycoproteins, cytokines, non-coding RNA ^[103], can only reflect the impact of the disease on certain molecular pathway of the patient. CEC/PECs as intact cells, bear comprehensive information including genome, transcriptome, proteins, which reflect the overall condition of the disease as well as its impact on patient. The compositional, invasion and metastasis characteristic of CEC/PECs ^[108, 109] may suggest the clinicopathological type of endometriosis (OEM, PEM, DIE or OtEM); the mutations in genome and transcriptome of PEC/CEC could help to predict and detect recurrence as well as malignant transformation of EM after surgery and during the follow up of patients. Mutations in PTEN, CTNNB1 (β -catenin), KRAS, ARID1A has been linked with Endometriosis Associated Ovarian Carcinomas (EAOC) ^[110]. Moreover, PEC/CECs, considering their role in the pathogenesis pathway, provide an important target to stop the formation and metastasis of endometriosis. We can screen certain glycoproteins and surface markers in PEC/CECs, which have closer connection with pathogenesis pathway, to serve as precise target of EM treatment. For instance, VEGF is a well-studied endometriosis biomarker, and cediranib, a potent VEGFR inhibitor has been reported to cause regression of endometriotic lesions in rat model^[111].

CHAPTER FOUR

CTC-DIALYSIS ANIMAL MODEL ON RATS

Over 90% of cancer fatality is attributed to cancer metastasis and if cancer cells in a cancer patient can be removed ^[16], the patient has a very chance of prolonged survivability. In this chapter, the basic ideas of CTC-dialysis, which involves an extracorporeal circulation screening of CTCs are explored and demonstrated via a series of pioneering but limited animal model experiments on rats. The results obtained are highly preliminary and limited in scope, and they should not be taken to imply that CTC-dialysis works on cancer patients. CTC-dialysis for cancer patients is currently unavailable and we are not aware of anyone having demonstrated it on a human or even an animal. The process is conceptually similar to hemodialysis for chronic kidney patients but different in terms of the contaminant removed and the working principles involved in the removal. In CTC-dialysis, CTCs are removed from peripheral blood via a size-based microfluidic chip compared to hemodialysis that involves the removal of body wastes in peripheral blood via membrane osmosis.

4.1 Concept and Prototype of CTC-Dialysis

CTCs are widely recognized as being responsible for the hematogeneous spread of cancer ^[17]. Hence, the intuitive thinking is that the removal of CTCs in peripheral blood helps to inhibit cancer metastasis and thereby, could possibly prolong the life of a cancer patient. A conceptual setup of a CTC-dialysis system is sketched in Figure 4.1. To setup this extracorporeal circuit in a rat, we performed a laparotomy on its abdomen

with an access port dissected in a blood vessel so that the peripheral blood can be diverted to flow out of the body and into an attached microfluidic chip (for CTC removal) before it is returned back to the rat's circulation via a second access port in a blood vessel. Several devices are hooked up to the system and they include: a small pump to ensure a continuous blood flow throughout the experiment, a heparin pump for anti-coagulation injection, several units to monitor the status condition of the blood and animal, a CTC analyzer to examine the captured tumor cells, a deaerator to remove air bubbles and a blood tonic injection pump.

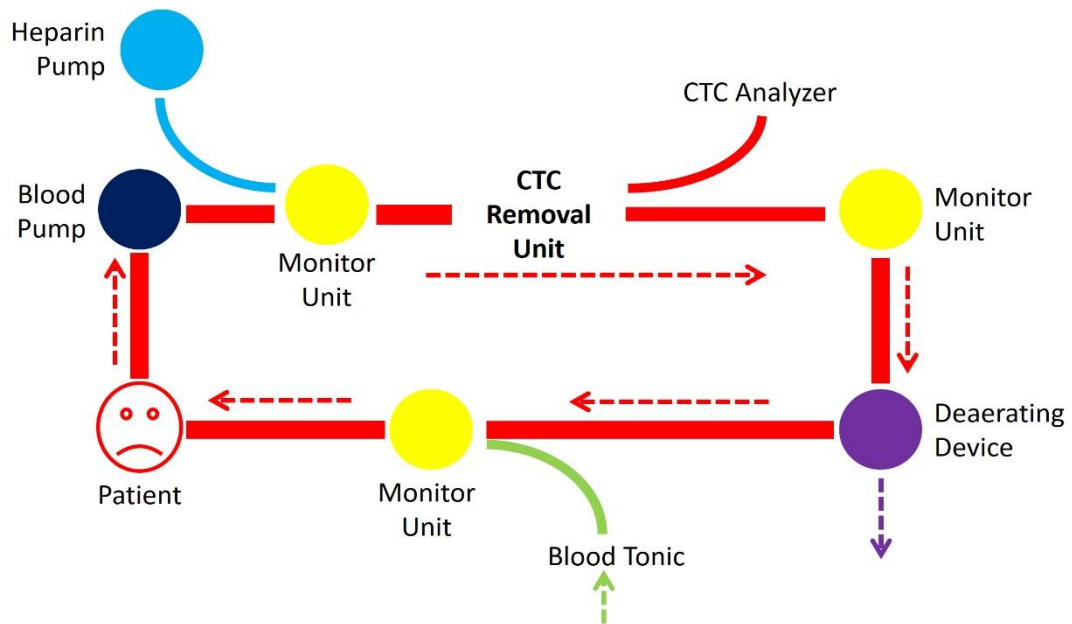


Figure 4.1 The prototype of CTC-dialysis system.

4.2 Development of the CTC-Dialysis Protocol

To perform a CTC-dialysis, we have developed a set of protocol to ensure the procedure is properly and ethically carried out with minimal damage to the rat.

1. Physical damage to blood vessels, including bleeding should be kept to a minimum. Connecting the extracorporeal circuit to the rat's circulation system for an extended period of time creates a prolonged disruption to the normal flow routine of the blood and this together with damage to blood vessels increase the risk of the life-threatening thrombosis and blood coagulation problems ^[112].

2. The duration of surgery should be kept to a minimum and ligatures should be carried out cleanly and if there are issues, they should be addressed immediately. This is to minimize the detrimental effects of the surgery on the animal.

3. Animals should be handled properly and ethically in accordance to institutional and national guidelines. This includes proper anesthesia before and during surgery, anti-infection and analgesia after surgery and proper disposal at the end of experiment.

Below are the major challenges encountered during the surgery.

1. Blood vessels in rats are tiny and fragile and thus, very difficult to handle. Further, veins, which the vessels used for our chip connection are highly ductile and this makes them especially difficult to suture a puncture. By comparison, elastic blood vessels are easier to handle.

2. The balance between anti-coagulation and bleeding can get tricky. Coagulation must be avoided to eliminate the risk of post-surgery thrombosis. On the other hand, bleeding should be prevented when blood vessels are sutured. Hence, it is a challenge to maintain

a proper balance between anti-coagulation and coagulation during and after surgery when anti-coagulant drug is administered.

3. It is most important to maintain an appropriate flow throughput in the system as the blood from the rat is diverted into the extracorporeal circulation before returning back to the rat again. The critical flow bottleneck is at the chip level and if the system throughput is much higher than the rated flow speed of the chip, the capture efficiency will be affected. On the other hand, if the flow throughout is too low, blood will backup inside the rat and be forced to flow elsewhere in the rat's circulatory system, allowing the tumor cells to bypass and escape the chip.

To get an idea of “an appropriate flow speed”, we look at the hemodialysis system for humans. Typically, the system filters whole body blood at a rate around 3 complete circulations per hour ^[113], which translates to 18 L/hr or 18,000 mL/s, which is overwhelmingly higher than the typical *ex-vivo* CTC assay speed of between 0.5-2 mL/hr. The total volume of blood in a rodent is quite small: about 1 mL for mice and 10 mL for rats and if we adopt the hemodialysis flow criteria of “3 complete circulations per hour” for CTC dialysis in rats, the flow speed in rats should be 30 mL/hr. This speed is about 15 times higher than the rated chip speed and therefore, we expect a deterioration of the capture efficiency to about 50%, which is still acceptable. The extracorporeal flow speed of 30 mL/hr or 0.008 mL/s is also much lower than the flow of blood at the draw-point of the rat, which is defined as the point where the blood is drawn. At the draw-point, the blood speed is estimated to about 0.1 mL/s (10% of the 1 mL/s flow speed at the rat's heart), which is about 10 times the extracorporeal flow-rate and this is quite acceptable.

Finally, to kick-start the filtering process, we inject into the system an amount of PBS equivalent to 5% of the total volume of blood in a rodent.

4. In a cancerous animal, the time window to maximize the effectiveness of CTC-dialysis is unknown and this reduces the expected effectiveness of CTC-dialysis.

4.2.1 Selection of the Hematogeneous Metastatic Animal Model

The optimum site for CTC-dialysis depends on the position of primary tumor. Ideally, it should be placed between the primary tumor and expected location of the metastatic tumor. For instance, to filter CTCs from a pancreatic tumor, blood from the hepatic portal vein is tapped as it flows to the metastatic tumor in the liver^[114] and thus, the proposed CTC-dialysis site should be somewhere along the portal vein. In our animal experiments, an optimum location the CTC-dialysis site and the time window can be determined only after we have constructed the hematogeneous metastatic animal model. Figure 4.2 depicts three hematogeneous metastatic animal models together with the optimum location of the CTC-dialysis sites marked by the “stop” sign.

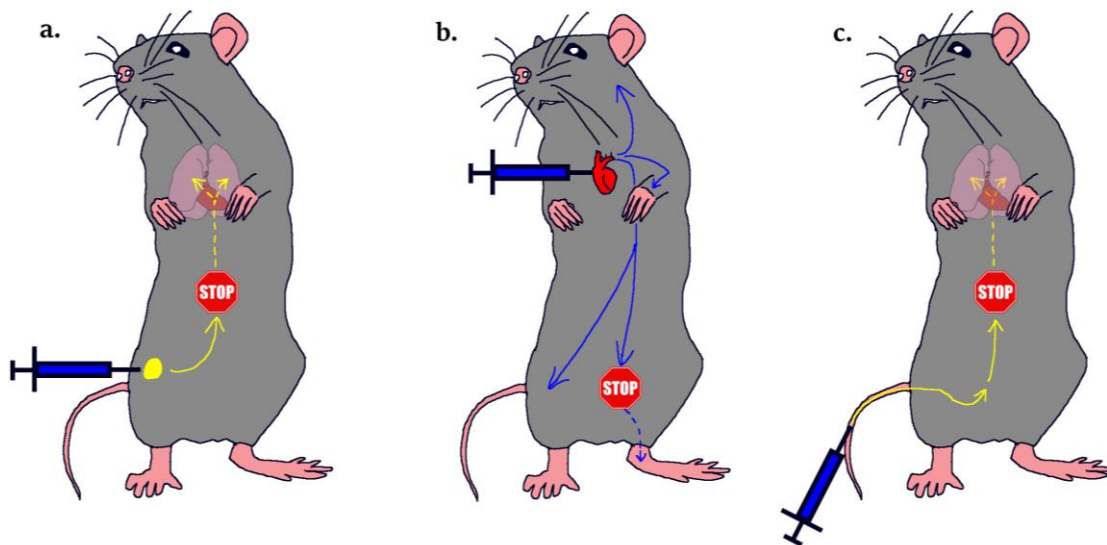


Figure 4.2 Hematogeneous metastatic animal models and potential CTC-dialysis sites marked by the “stop” sign for a) spontaneous metastatic model, b) left heart injection model, and c) tail vein injection model.

The hematogeneous metastatic animal model closest to real-life metastasis is the spontaneous metastatic model (Figure 4.2.a). The primary tumor can either be spontaneously grown or planted via an orthotopic/subcutaneous injection. Although the primary tumor will spread to other organs, hematogeneous metastasis will occur mostly in the lungs as they serve to filter-out the CTCs in the pulmonary circulation. To stop CTCs from reaching the lungs, which is directly in the downstream path of the right heart, the CTC-dialysis needs to be performed before the blood enters the right atrium. For most tumors in the abdominal cavity, post-cava is a suitable place for the CTC-dialysis placement as it collects most of the blood from inferior veins and is sufficiently large and strong for our experimentation. However, as the temporal distribution of CTC seeding is unknown, the time window for CTC-dialysis cannot be determined.

Another hematogeneous metastatic animal model is left heart injection model (Figure 4.2.b), in which the metastatic tumor cells are injected into the left ventricle under the guidance of B-ultrasound to allow the CTCs to spread throughout the body via arteries. These tumor cells often metastasize in the capitulum. The time window to find CTCs in blood begins immediately upon injection. However, the actual CTC-dialysis site is difficult to determine since the tumor cells have spread all over the entire body.

The model we have chosen for our CTC-dialysis animal experiments is the tail vein injection model (Figure 4.2.c), where labelled tumor cells ^[115] are injected into the tail vein to allow them to spread via the post cava into the lungs. In the tail vein injection model, the CTC-dialysis site and the time window are both obvious: the tumor cells spread from the post cava immediately upon injection.

4.2.2 Microsurgery to Divert the Rat's Blood through the Extracorporeal Circuit

Next, we discussed in details the microsurgery and the procedures for the CTC-dialysis and they are based on the tail vein injection model. The characteristic diameter of the post cava of a rat is approximately 3 mm, and the outer diameter of the flexible tubing for insertion into the rat's vein is 0.6 mm. Thus, a microsurgery is required to connect the extracorporeal circulation for CTC-dialysis with the rat's systemic circulation. There are 2 ports in the connection: the distal end port for drawing the blood from the rat and the proximal end port for returning the blood back to the rat. Considering the complex requirements of the system, as well as, the severe challenges confronting the life of the animal, the expected survival rate of rats undergoing the microsurgery was very low in our maiden attempts and this can be attributed to the tight post cava to the abdominal aorta attachment, which is very difficult and dangerous to split. To improve the success rate and to enhance the ease of the surgery, alternative sites for the microsurgery were explored and used. They are labelled in Figures 4.3.a and 4.3.b.

The alternative sites are located on branches of the post cava. The traditional distal and proximal insertion ports for the extracorporeal circulation is on the main post cava (Figure 4.3.c) but this approach creates too much risk to the animal. A better alternative is to install the distal and proximal insertion ports on 2 branches of the post cava (Figure 4.3.d). Other alternative veins have also been used with low risks to the animal as they are attached to the abdominal wall and not to an artery. The various recommended sites for the extracorporeal circulation hookup are summarized in Table 4.1.

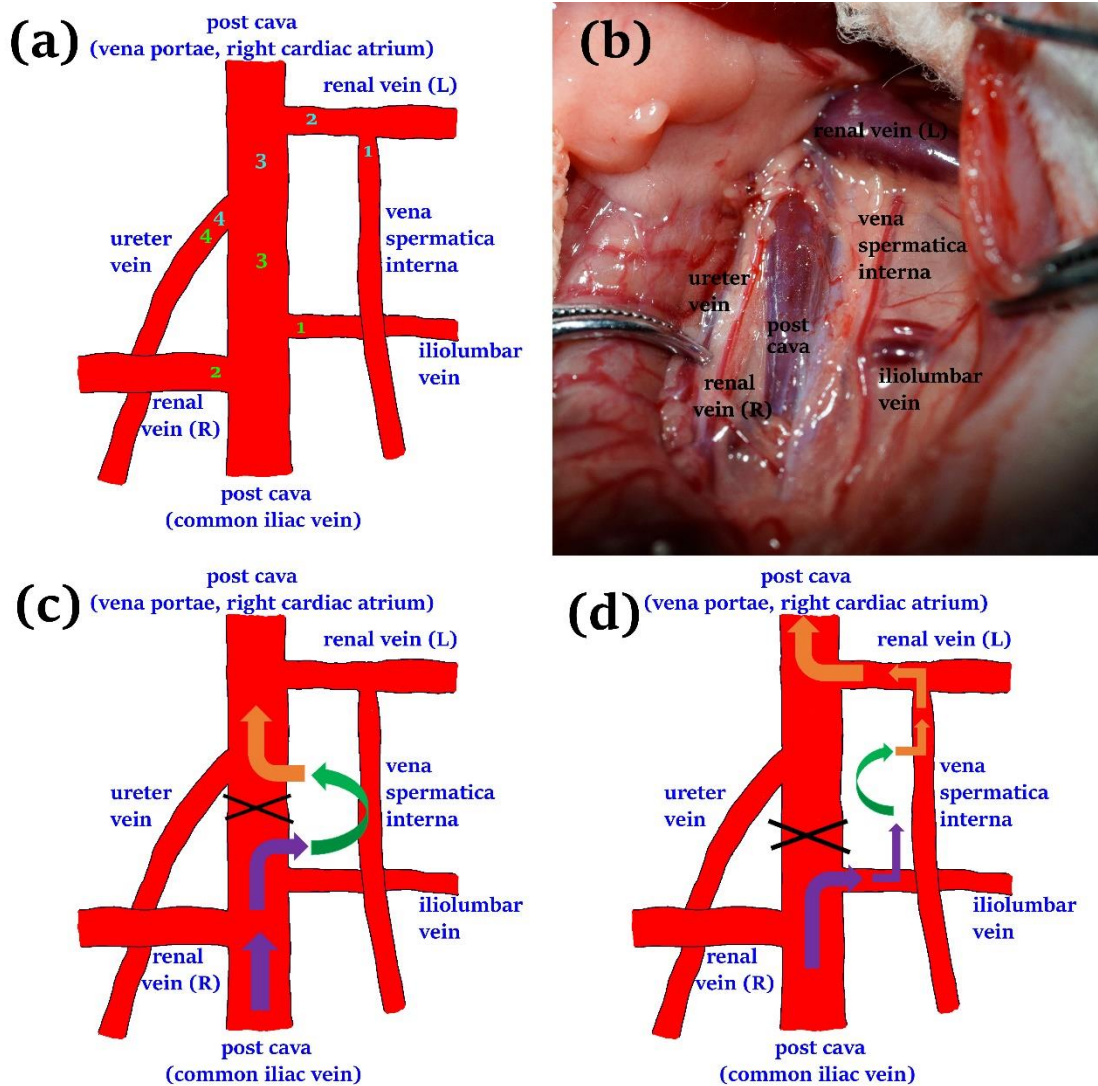


Figure 4.3 Post cava sites for the CTC-dialysis system hookup. The numbers in a) refer to the recommended priority for the distal extraction and proximal infusion ports. The approximate positions of these veins (which differ from rat-to-rat) are shown in b). Two alternative post cava locations for the placement of the extraction and infusion ports are sketched as Site 1 in (c) and Site 2 in (d).

Table 4.1 Extracorporeal circulation connection port recommendations.

Distal port (extraction of blood)	Proximal port (infusion of blood)
1. Vena spermatica interna	1. Iliolumbar vein
2. Left renal vein	2. Right renal vein
3. Post cava	3. Post cava
4. Ureter vein	4. Ureter vein

The fragility and ductility of a vein are 2 important considerations when inserting a tubing and suturing after the insertion. Veins that are thin and inelastic are highly vulnerable to tears when stretched and any improper handling may lead to a rupture, scratch and extension.

The microsurgery presented here uses a “wound-constraint” approach to avoid unnecessary and excessive damage to a vein. A circular loop is seamed on a vein to define the connection port for tubing (Figure 4.4) and this approach seems to eliminate any tear and also, minimize the extension of the vein. During the CTC-dialysis process, the loose thread can be tightened to immobilize the tubing, thus avoiding creating a scratch on the vein. Immediate fastening and knotting of the thread after tubing removal helps to close the wound with minimal bleeding and coagulation. This innovative approach contributes greatly to the survival rate of the animal after surgery.

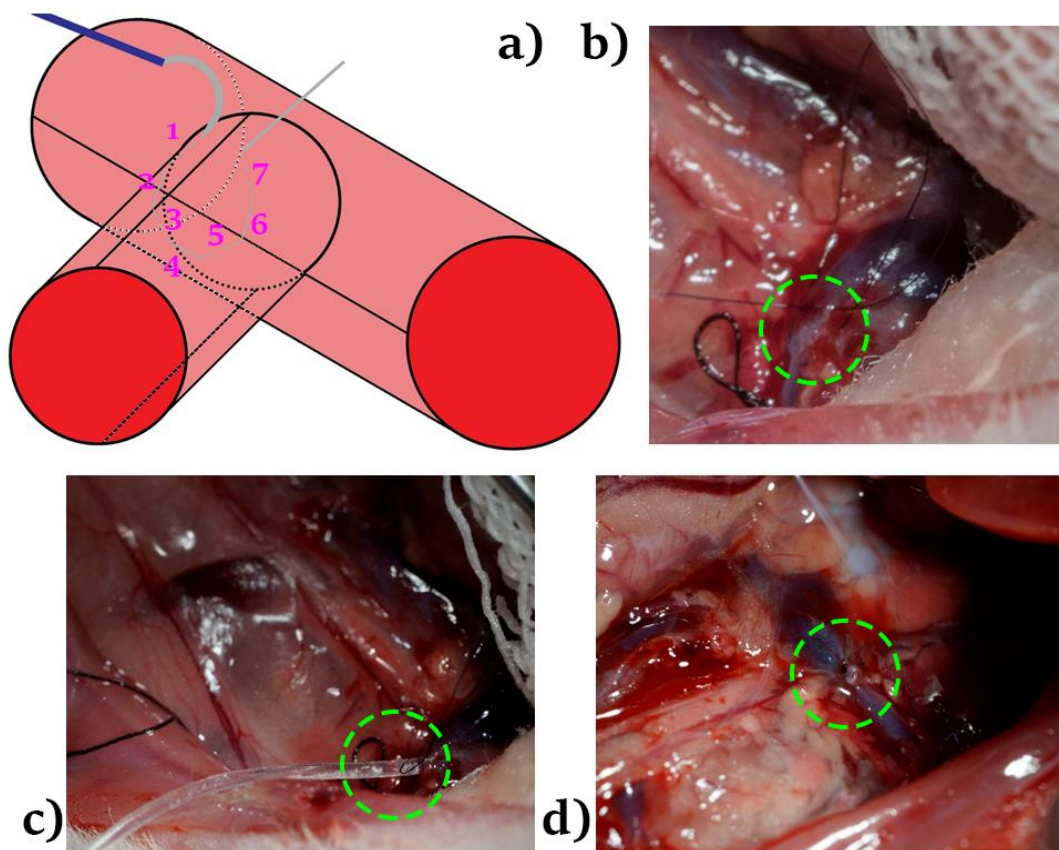


Figure 4.4 Illustration of the microsurgery: a) 7 stitches to define a pocket for tubing installation; b) circle highlights the pre-defined pocket; c) circle highlights the tightened thread to fix the tubing, on its left is the thread to ligature the distal end of the vein; d) knotted thread closes the wound immediately after the removal of the tubing.

4.2.3 Circulation Pump System

Hemodialysis system for human is driven by a peristaltic pump, which engages at least 1 mL of blood in its pump line. Using this type of pump to engage the extracorporeal circulation of a rat is possible but for a mouse, it is not feasible as the animal possesses a very low blood volume. A micro plunger pump, which engages around 100 μL of blood can reduce the extracorporeal engagement of the blood and therefore, can potentially drive a mouse's extracorporeal circulation system. The system is shown in Figure 4.5.

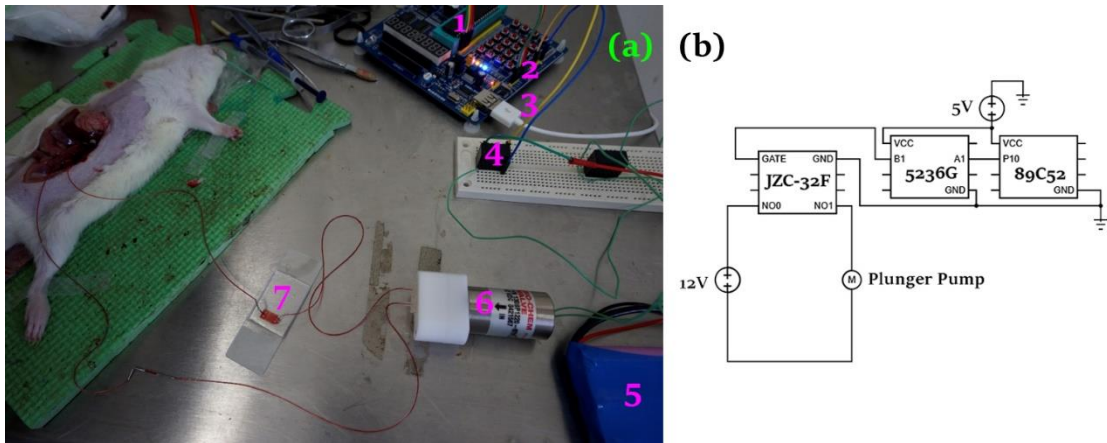


Figure 4.5 Circulation pump system based on plunger pump. Devices in b) are labelled in a): 1. 89C52 MCU, 2. 5236G switch, 3. 5V input, 4. JZC-32F electromagnetic relay, 5. 12V battery, 6. Plunger pump and 7. Microfluidic chip.

The plunger pump is driven by a square wave, which consists of a 350 ms stable 12V high level and an adjustable (at least 150 ms) 0V low level. Due to the large resistance ($\sim 10^2 \Omega$) of the pump, a normal signal generator cannot generate the current. In the system depicted in Figure 4.5.a, the power is supplied by a 12 V battery and is controlled by a JZC-32F high-voltage relay. The square wave is generated by a programmable 89C52 Micro-Control Unit (MCU), transmitted by a 5236G switch chip for the MCU cannot afford the current of the relay (Figure 4.5.b). The program for the

MCU provides a 99.9% temporal resolution accuracy and verified by the compiled assembly language.

4.2.4 Protocol of the experiment

The detailed protocol of the tail-vein injection rat model for hematogeneous metastasis is listed step-by-step in Appendix B. The flow chart of the procedures is illustrated in Figure 4.6. The experiment need to be carried out by two researchers with license for animal experiment. One of them shall focus on the treatment and surgery of the animal, while the others prepare and manipulate the microfluidic system. Before and after the surgery, the animal shall be kept in accordance to the animal welfare and ethic requirement, as well as the IRB-approved protocol of the experiment.

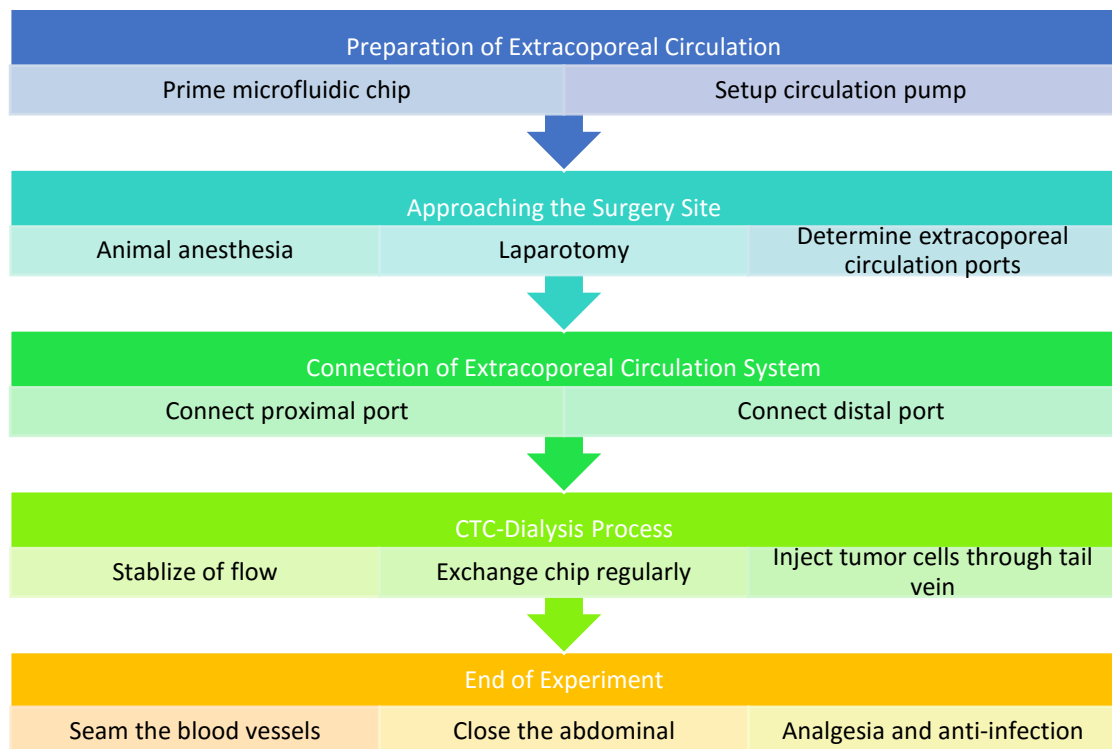


Figure 4.6 Flow chart for the procedures of the CTC-dialysis experiment.

4.2.5 Restrictions of the System

The CTC-dialysis prototype has the following restrictions in addition to those of the *ex vivo* CTC assay described in *Chapter Two*.

1. To facilitate the extracorporeal circulation, a peristaltic or plunger pump is used to drive the flow, which sends discrete pulses into the flow. Compared to the CTC assay that is driven by a syringe pump, the stability is sacrificed for the need of continuous drive of flow. Consequently, the efficiency of the assay decreases. A check valve at the proximal port helps to stabilize the flow by eliminating backflow into the microfluidic chip, which may dislodge captured tumor cells from the chip. The flow condition is still not as smooth and stable as that in an *ex vivo* CTC assay.

2. Commercial hemodialysis systems, which are installed on the veins of arms and legs, can be applied to a patient on a day-by-day basis for many years. However, due to the inevitable damage to the animal, the surgery for CTC-dialysis cannot be repeated. As a result, the application of the system is limited on rodent models.

3. When the tumor cells are injected into the tail vein, instantaneous peak pressure drives a lot of cells into collateral circulations. As a result, those cells cannot be removed and the efficiency of the system is limited.

4. Although hematogeneous metastatic models of rats have been reported, results vary with different sources of animal, as well as, tumor cells. The effort to induce tumor growth in nude rats through tail vein injection is not successful, thus a comprehensive

investigation on the effect of CTC-dialysis is unavailable and will be further carried out in the future.

4.3 Effects of the CTC-Dialysis System

Due to the restrictions on the system, full investigation on the effect of CTC-dialysis system has not been concluded. However, preliminary results show that the system 1) can remove CTCs out of the circulation, 2) has a minimum influence on the animal. This chapter concludes with some potential applications of the system in cancer research.

4.3.1 Capture of Seeded Tumor Cells

To distinguish seeded tumor cells from WBCs in peripheral blood, a metastatic breast cancer cell line that expresses the mKate fluorescent protein, MBA-MD-231S-mKate is seeded into the tail vein of the animal model. Table 4.2 shows some mKate positive tumor cells in the microfluidic chip installed in the CTC-dialysis system discovered in the chips installed (a) immediately, and (b) 10 minutes, after tail vein injection.

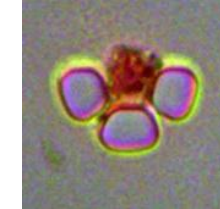
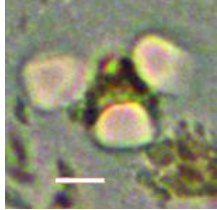
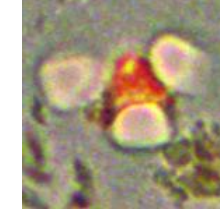
	BF Bar = 10µm	mKate	Merge
1			
2			

Table 4.2 Tail-vein-seeded tumor cells captured in CTC-assay.

4.3.2 Minimal Effects on the Operated Rat

The CTC-dialysis protocol with alternative connection ports and predefined “pocket” for connection has significantly increased the survival rate of rats undergoing the experiment. One-week post-surgery survival rate increased from around 50% to 86% (6 out of 7 rats) with the application of the protocol. The fatality is caused by anesthesia failure. It means surgery fatality has been eliminated, provided that the surgery is properly handled.

To further investigate the influence of the experiment on the animal, B-Ultrasound image (Figure 4.7) of the relevant blood vessels (post cava and left renal vein) are taken

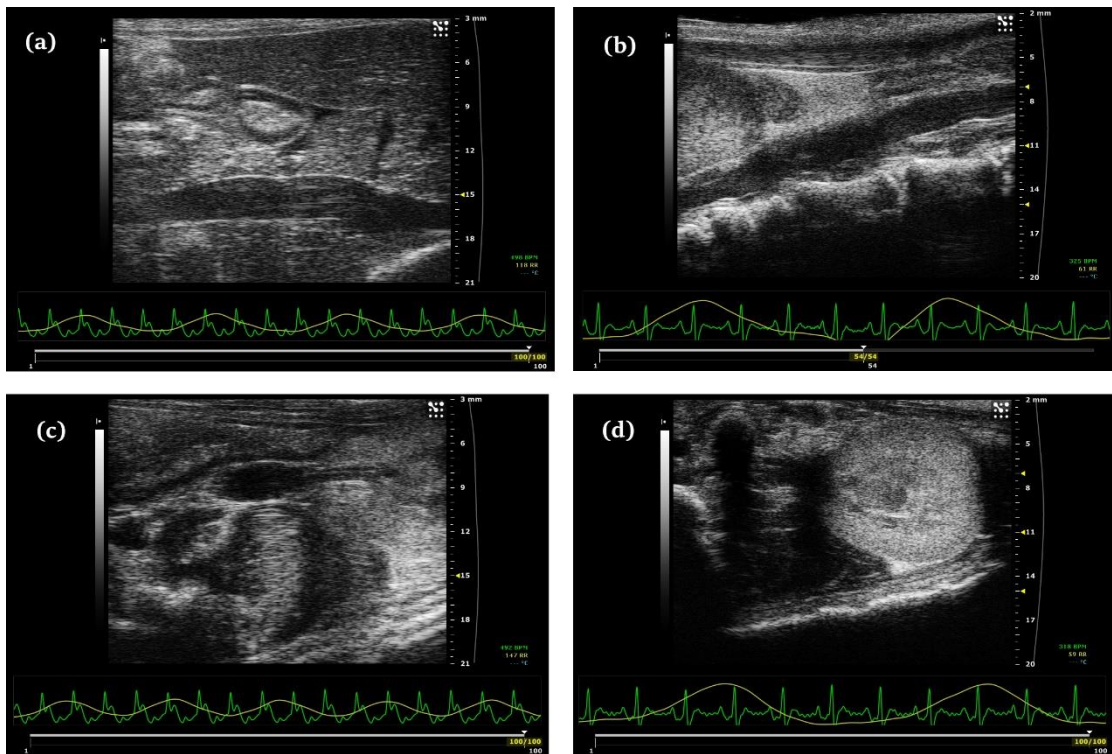


Figure 4.7 B-Ultrasound images of post cava a) before experiment and b) one week after experiment shows no notable change; images of left renal vein c) before experiment and d) one week after experiment shows slight expansion of the vein. The heart rate difference is brought about by different anesthesia methods applied: injection anesthesia is applied before experiment and gas anesthesia is applied after experiment.

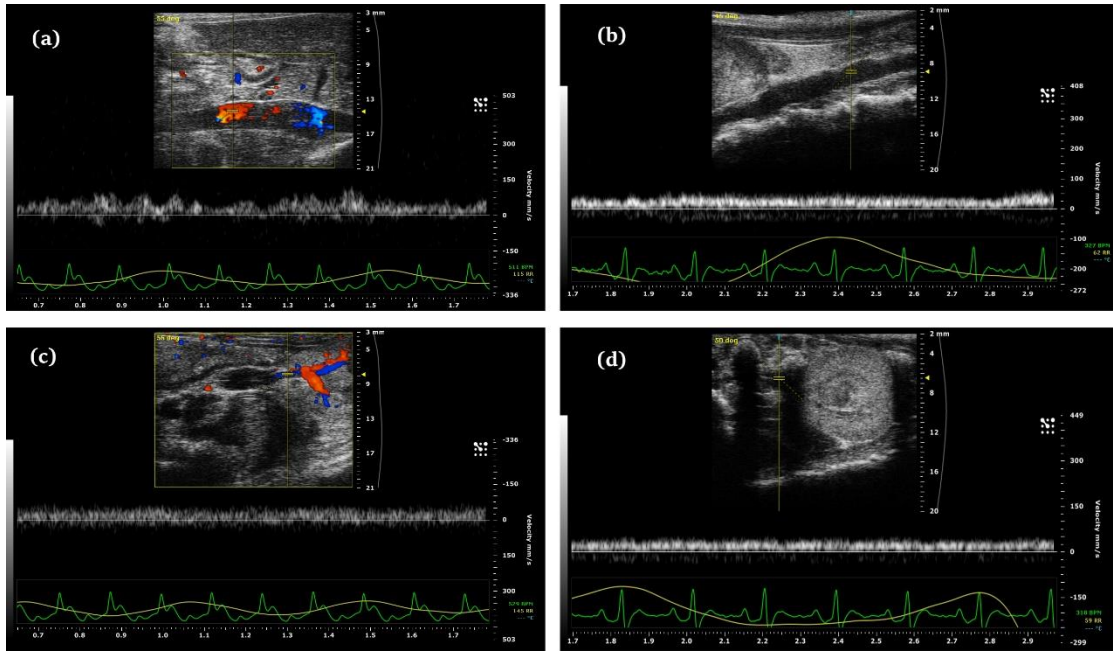


Figure 4.8 Doppler-Ultrasound measurement of flowrate in post cava a) before experiment and b) one week after experiment, and in left renal vein c) before experiment and d) one week after experiment show similar flow condition. The heart rate difference is brought about by different anesthesia methods applied: injection anesthesia is applied before experiment and gas anesthesia is applied after experiment.

and the flow rate of the vessels is analyzed with Doppler Ultrasound images (Figure 4.8). In conclusion, post cava has not been affected by the experiment. Left renal vein has been slightly expanded, which is probably caused by the ligature during CTC-dialysis. Nevertheless, the blood flow in the left renal vein is still normal.

4.3.3 Potential Applications of the System

The proposed application of the system is to reduce downstream tumor burden for the purpose of inhibiting cancer metastasis. Tumor burden and metastatic tumor development can be measured with Fluorescence Reflectance Images (FRI) imaging technology. The effects of CTC-dialysis system need to be verified by a control experiment illustrated in Table 4.3. The system can also be applied in cancer metastasis research, as it is a tool to capture and recover (after the chip is retrieved from the system) CTCs from an animal without sacrificing it.

Furthermore, the system provides a real-time tool to enumerate and characterize CTCs, as discussed in Chapter Three. The time window can be spanned over certain treatment of interest, like resection of primary tumor, injection of certain drugs, or application of certain therapy, and real-time feedback of CTCs can be obtained in the system to reflect the effect of the treatment on CTCs.

To facilitate specific research with the CTC-dialysis system, the experiment plan, including and not limited to cancerous animal model, extracorporeal circulation connection ports, CTC-dialysis time window shall be dependent on specific application.

Table 4.3 Expected control experiment for the verification of the effect of CTC-dialysis on cancer metastasis.

Type of Experiment	Seeding of Tumor Cells	Surgery	CTC-Assay	Comment
<u>BC1</u> Blank Control 1	Yes	No	No	Cancerous animal without any treatment.
<u>BC2</u> Blank Control 2	No	Yes	Yes	Non-cancerous animal undergoing CTC-Dialysis. This group of animals show the influence of the system on the survival and health of the animals.
<u>ME</u> Mock Experiment	Yes	Yes	No	Cancerous animal treated by the surgery without CTC removal. The contrast between MS and BC1 reflects the influence of the surgery on animal.
<u>CD</u> CTC-Dialysis	Yes	Yes	Yes	Cancerous animal treated by CTC-Dialysis. The contrast between CD and MS shows the effect of CTC removal, and the contrast between CD and BC1 shows the effect of CTC-dialysis on animal, which is a combination of hazard due to the surgery and benefit from CTC removal.

CHAPTER FIVE

SUMMARY AND PROSPECTS FOR FUTURE WORK

This dissertation describes 2 major research in developing engineering methodologies for harvesting cancer cells in body fluids. In the first part, it reports on a size-based microfluidic assay for the capture and recovery of CTCs and DTCs. Spiked blood using cell-line cancer cells are used to assess the efficiency and purity of the microfluidic chip designed with this physical biomarker. A systematic series of immunofluorescence staining procedure is then employed to accurately identify the captured/recovered cells as either a CTC, DTC, BGC or a non-cell. Clinical cases from several well-known cancer types are used to demonstrate the harvesting of heterogeneous and intact tumor cells and to highlight the accuracy and usefulness of the approach. Detailed procedures for stable and reliable microfluidic assays of cancer cells are given in the thesis report.

Our liquid biopsy approach is applied to three cancer types to study its potential as a diagnostic and research tool: the enumeration of CTCs in the progression assessment of pancreatic cancer(PC), the characterization of CTCs in the mitochondrial autophagy study of non-small cell lung cancer and identification of CECs as a screening and differential diagnostic tool for endometriosis.

CTCs captured in peripheral blood of PC and non-PC patients shows that CTC enumeration is a significant indicator of the PC staging. CTCs captured in blood taken from the pulmonary vein show signs of autophagy occurrence, which suggests that those cells are undergoing putative mitophagy and the impact of autophagic dysfunction on cellular oxidative stress. CECs harvested in peripheral blood of endometriosis patients, other gynecologic patients and healthy volunteers show that CEC detectability can be a potential biomarker for the screening and diagnosis of the disease. CECs recovered in the peripheral blood and PECs recovered in the peritoneal fluid are crucial media for the pathogenesis and clinical management of endometriosis.

In the second part, it presents a series of novel CTC-dialysis experiments using a rat animal model. The development of the procedure to significantly enhance the survival rate of an operated rat by imposing a minimal infliction on the animal is discussed and presented in details. The research showed the potential of using a microfluidic chip to screen out CTCs in peripheral blood via an extracorporeal circuit to meliorate the survival rates of cancer patients. Much more work needs to be done here in order to properly confirm the preliminary findings of our *CTC-dialysis* research.

The work reported here clearly demonstrates the promising prospects of microfluidic assays in basic and clinical research in medicine, whether the approach is employed as a diagnostic tool for cancer detection and treatment or as an intervening device for CTC dialysis. Further cancer research on single-cell molecular analysis of CTCs and DTCs, development of accurate and reliable biomarkers for tumor cells harvested in bladder, ovarian and lung cancers, the transition mechanism of CTCs in pancreas cancer, pathogenesis of endometriosis, etc. are ongoing within our group and it is hope that will shed new and better insights into the deadly disease.

APPENDIX A

PROTOCOL: SIZE-BASED MICROFLUIDIC ASSAY FOR CTC/DTC CAPTURE AND RECOVERY

A.1 Materials

A.1.1 Reagents

- Polydimethylsiloxane [PDMS], Sylgard 184 silicon elastomer kit (Dow Corning, Ellsworth Adhesives, cat. no, 184 Sil Elas kit, 0.5 kg)
- Sterile PBS, 1× (Wisent, cat. no. 311-010-CL)
- Bovine serum albumin [BSA] (Wisent, cat. no. 800-095-EG)
- Ficoll-Paque PLUS (GE Healthcare Life Sciences)
- Red blood cell [RBC] lysis buffer (Beyotime, cat. no. C3702)
- Peripheral blood (see REAGENT SETUP) **! CAUTION** Handle blood with care to prevent infections. **! CAUTION** Blood from patients must be obtained in compliance with the institutional and national guidelines. **▲ CRITICAL** The maximum time to processing is 4 hours, above which blood coagulation may ensue. Place the blood samples at room temperature if the time to processing is less than 1 hour. Place them in wet ice or refrigerator if otherwise.
- Peritoneal wash (see REAGENT SETUP) **! CAUTION** Handle peritoneal wash with care to prevent infections. **! CAUTION** Peritoneal wash from patients must be obtained in compliance with the institutional and national guidelines.
- Ethylenediaminetetraacetic acid [EDTA] (Xilong Chemical)
- Pluronic F-127 (Sigma-aldrich, cat. no. 101208568)

- Paraformaldehyde [PFA] (for cell fixation; Sinopharm Chemical Reagent, cat. no. 80096692) **! CAUTION** This chemical is a potential carcinogen and can be very hazardous in case of skin contact.
- Triton X-100 (for cell permeabilization; Sigma-Aldrich, cat. no. T9284)
- Appropriate antibodies (see REAGENT SETUP)
- 4',6-diamidino-2-phenylindole [DAPI] (Life Technologies)

A.1.2 Equipments

- Silicon master (for chip fabrication) printed by CapitalBio, Beijing, China.
- Petri dish, 15-cm diameter (for containing silicon master)
- Double-sided tape
- Weighing scale
- Graduated transfer pipette (for transferring PDMS prepolymer and its crosslinker, and mixing them)
- Disposable paper cup
- Vacuum dessicator (for removing air bubbles in PDMS mixture)
- Oven (for curing PDMS mixture and reinforcing bond between PDMS pieces and glass slides)
- Penknife (for removing cured PDMS from master and cutting it into pieces)
- Biopsy puncher with a plunger system, 0.75-mm diameter (for creating access ports on chips; Sigma-Aldrich, Harris Uni-Core)
- Microscope slides, 25 mm × 75 mm × 1 mm (Citoglas Labware Manufacturing, cat. no. IA5105)
- Scotch tape (for removing dust particles on PDMS pieces and glass slides; 3M, Scotch Magic Tape, cat. no. 810)

- Oxygen plasma cleaner (for cleaning PDMS pieces and glass slides; Ming Heng, PDC-MG)
- Forceps
- Inverted routine microscope (Leica Microsystems, DM IL LED)
- Tygon tubing, internal diameter (A.d.) 0.020 in, outer diameter (o.d.) 0.060 in (Cole-Parmer, cat. no. AAD02103-CP)
- Precision syringe tips (Nordson EFD, cat. no. 7018272)
- Metal connectors
- Stopcocks with Luer connection, 1-way male lock (Cole-Parmer, cat. no. 30600-05)
- Sterile disposable syringes, 5 mL and 10 mL (as recovery buffer and waste vessels; Jiangsu Zhiyu Medical Instrument)
- Syringe barrel, 5 mL (see EQUIPMENT SETUP)
- Cell culture dish, 35-mm diameter (as cell receptacle; Corning, cat. no. 430165)
- Custom-made holder
- Syringe pump (Longer Pump, TS-1B/W0109-1B)
- Cell strainer, 300 mesh
- Low speed tabletop centrifuge (Beijing Era Beili Centrifuge, DT5-2)
- Centrifuge tubes, 15 mL and 50 mL (Corning)
- Microcentrifuge tubes, 0.2 mL, 0.5 mL and 1.5 mL (Axygen Scientific)
- Computer installed with LAS Core V4.4, Leica Microsystems microscope imaging software and AutoCAD software.

A.1.3 Reagent Setup

Peripheral blood A minimum of 2 mL peripheral blood should be collected before pre-medication and anesthesia administration using purple EDTA Vacutainer tubes.

The first draw of blood should be discarded. Gently invert the purple Vacutainer tubes 8-10 times after blood draw. Place them in a collection rack in an upright position.

Peritoneal wash Peritoneal wash should be collected by wash the pelvic cavity with 500 mL sterile normal saline solution using a laparoscopic needle and manual aspiration using a syringe. The peritoneal wash is collected after pre-medication and anesthesia administration.

Primary antibody mixture Mix the required primary antibodies (conjugated and unconjugated) in 5 % (w/v) BSA solution. We use unconjugated estrogen receptor [ER] antibody (1:100; Abcam), unconjugated progesterone receptor [PR] antibody (1:200; Abcam), Phycoerythrin [PE]-conjugated Vimentin [Vim] antibody (1:100; Abcam), PE-conjugated pan-cytokeratin [pan-CK] antibody (1:20; Abcam) and PE-conjugated epithelial cell adhesion molecule [EpCAM] antibody (1:100; Abcam) for identifying endometrial cells. We use Alexa Fluor [AF]488-conjugated CD45 antibody (1:100; Invitrogen) for identifying leukocytes. We also add DAPI for nuclear staining. ▲ **CRITICAL** Avoid light exposure at all times to prevent bleaching of fluorophores.

Secondary antibody mixture Mix the required secondary antibodies in 5 % (w/v) BSA solution. We use AF647 donkey anti-rabbit to bind with ER and PR antibodies (1:200; Abcam). ▲ **CRITICAL** Avoid light exposure at all times to prevent bleaching of fluorophores.

A.1.4 Equipment Setup

Syringe barrel We use 5-mL syringe barrels as the buffer reservoir and the sample reservoir. They can be made from disposable 5-mL syringes by simply removing the beveled syringe needles and plungers.

A.2 Procedure

A.2.1 Chip design and mold preparation

- **TIMING** 10-17 d

1| Draw the microfluidic design in the AutoCAD software. It is possible for the mold to have several design duplicates of the same microfluidic chip in order to increase production of the chip.

2| Submit the design in AutoCAD file format to a vendor for mask printing and photolithography to fabricate a silicon wafer to act as the master for Capture Chip and Recovery Chip (we work with CapitalBio, Beijing, China). The vendor usually completes the master in 10-15 business days.

3| Place the master into a 15-cm-diameter Petri dish and secure it in the middle with a double-sided tape.

■ **PAUSE POINT** This master is reusable for extended periods and it should be covered with a lid.

A.2.2 Chip fabrication

- **TIMING** 6-7 h

4| Mix PDMS prepolymer with its crosslinker at 9:1 weight ratio in a disposable paper cup. The total mass of the PDMS should be 80 g.

5| Degas the PDMS mixture in the vacuum desiccator for ~30 min to remove air bubbles.

▲ **CRITICAL STEP** Beware of overflow when degassing.

6| Pour the bubble-free mixture into the wafer-containing Petri dish.

7| Repeat Step 5 to further remove any remaining air bubbles.

▲ **CRITICAL STEP** Leaving air bubbles in the PDMS mixture prior to curing may result in defects in the microfluidic chip.

8| Cure the mixture in the oven at 60 °C for 4 h.

9| Cut and peel the cured PDMS away from the silicon wafer master. Cut and trim the PDMS into several duplicate pieces.

▲ **CRITICAL STEP** Ensure that the silicon wafer is not scratched or damaged during cutting.

■ **PAUSE POINT** The PDMS pieces can be kept in a dust-free environment for prolonged periods of time.

10| Punch holes at designated access ports on the PDMS pieces using a 0.75-mm-diameter puncher to create inlet and outlet access ports. Punch three holes for Capture Chip whereas four holes for Recovery Chip.

11| Clean both sides of the PDMS pieces and microscope slides using Scotch tape to remove dirt. Make sure that the tape is entirely in contact with the surfaces of the PDMS pieces and microscope slides.

▲ **CRITICAL STEP** Gently adhere the tape onto the surfaces of the PDMS pieces to avoid damaging the lithographed features. Check for any visible dirt on the surfaces of PDMS pieces and microscope slides as it may affect bonding of PDMS pieces to the microscope slides.

12| Insert the microscope slides and the PDMS pieces with features facing up in the oxygen plasma cleaner. Plasma-treat the PDMS pieces and the microscope slides using the parameters as described in the table below.

Table A.1 Parameters for plasma treatment

Parameter	Value
Cleaner model	Ming Heng PDC-MG
Chamber dimension	165 × 210 (Ø × L) mm
RF frequency	13.56 MHz
Operating voltage	550-650 V
Operating pressure	90 Pa
End point	100 %
Time	1 min 20 s
Air flow rate	0.5 L/min
Ambient temperature	22 °C
Ambient humidity	22-45%

13| Bond the plasma-treated PDMS surfaces to the plasma-treated glass slide surfaces.

Gently tap the PDMS pieces with a pair of forceps to ensure features on the PDMS are well bonded with the microscope slides.

▲ CRITICAL STEP Do not press the PDMS pieces hardly onto the microscope slides to prevent microposts from collapsing.

14| Bake the bonded PDMS devices in the oven at 60 °C for 20 min to reinforce the bonding. Allow the devices to cool for 3-4 min.

Box 1 | Ficoll Density Centrifugation • TIMING 30-60 min

As an alternative to Step 32(A)(i) of the PROCEDURE, both blood plasma and red blood cells can be removed, as demonstrated below.

Additional materials required for Ficoll density centrifugation

Ficoll-Paque PLUS (GE Healthcare Life Sciences)

Ficoll density centrifugation

▲ **CRITICAL** Ficoll-Paque PLUS (Ficoll) and blood sample should remain at room temperature (15 – 25°C) for optimum results.

1. Dilute the blood sample with equal volume of 1× PBS buffer.
2. Add 1 mL of Ficoll per 1 mL of the diluted blood sample to a 15-mL centrifuge tube.
3. Layer the diluted blood sample on top of Ficoll carefully.

▲ **CRITICAL STEP** Do not mix the diluted blood sample with Ficoll.

4. Centrifuge at 400 *g* for 30-40 min, room temperature.
5. Remove the upper plasma layer without interrupting the buffy coat. Mononuclear cells, endometrial cells and small amount of platelets reside in the buffy coat.
6. Aspirate the buffy coat without interrupting the Ficoll layer.

? TROUBLESHOOTING

Box 2 | RBC Lysis • TIMING 15-20 min

As an alternative to Step 32 (A)(i) of the PROCEDURE, both blood plasma and RBCs can be removed, as demonstrated below.

Additional materials required for red blood cell lysis

RBC lysis buffer (Beyotime)

Lysis of Whole Blood RBCs

▲ **CRITICAL** The RBC lysis buffer and blood sample should remain at room temperature (15 – 25°C) for optimum results.

1. Add 10 mL of RBC lysis buffer per 1 mL of blood sample.
2. Gently vortex the mixture. Incubate for 10 min at 4°C.
3. Mix with 20-30 mL of 1× PBS buffer.
4. Centrifuge at 500 *g* for 5 min, room temperature. Remove the supernatant.
5. Repeat Steps 1 to 4 if RBCs are not lysed completely.

? TROUBLESHOOTING

15| Examine the PDMS devices under a microscope and look out for collapsed microposts. The PDMS devices are now functional chips.

■ **PAUSE POINT** The chips can be kept in a dust-free environment and used when necessary.

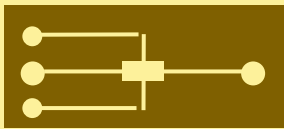
? TROUBLESHOOTING

A.2.3 Chip assembly

● **TIMING 10-15 min**

▲ **CRITICAL** See **Table A.2** for necessary items needed to assemble Capture Chip and Recovery Chip.

Table A.2 | Items needed per piece of Capture Chip and Recovery Chip.

Items	Capture Chip	Recovery Chip
		
Tygon tubing (A.d. 0.5 mm, o.d. 1.5 mm, length ~10 cm)	3	4
Precision syringe tip	3	4
Metal connector	3	4
Stopcock	3	4
Syringe barrel, 5-mL (see Equipment Setup)	2	1
Syringe, 10-mL	1	1
Syringe, 5-mL	0	1
Cell culture dish, 35-mm diameter	0	1

16| Attach a metal connector and a precision syringe tip to both ends of each of the tubings. Subsequently attach a stopcock to each of the precision syringe tips (**FigA.1b**).

17| Insert the metal connectors of all tubings into every inlets and outlets on the chip (**FigA.1.3c** for Recovery Chip).

18| Remove the beveled syringe needle from a 10-mL syringe. For Capture Chip, load the syringe with buffer solution (1× PBS with 1% (w/v) BSA and 8 mM EDTA). For Recovery Chip, load the syringe with 1% (w/v) Pluronic solution.

Recovery Chip only

19| Remove the beveled syringe needle from a 5-mL syringe. Load the syringe with 2-3 mL of 1% (w/v) Pluronic solution.

20| Connect the loaded 10-mL syringe to the waste outlet tubing. This acts as the waste reservoir.

21| Connect a 5-mL syringe barrel to the sample inlet tubing. This acts as the sample reservoir.

Capture Chip only

22| Connect another 5-mL syringe barrel to the buffer inlet tubing. This acts as the buffer reservoir.

Recovery Chip only

23| Connect the loaded 5-mL syringe to the recovery inlet tubing. This acts as the recovery buffer reservoir.

24| Place a 35-mm-diameter cell culture dish underneath the stopcock of recovery outlet tubing. This acts as the cell receptacle.

25| Hold the sample reservoir in an upright position using a custom-made holder.

The overall setup is presented in **FigA.1a**.

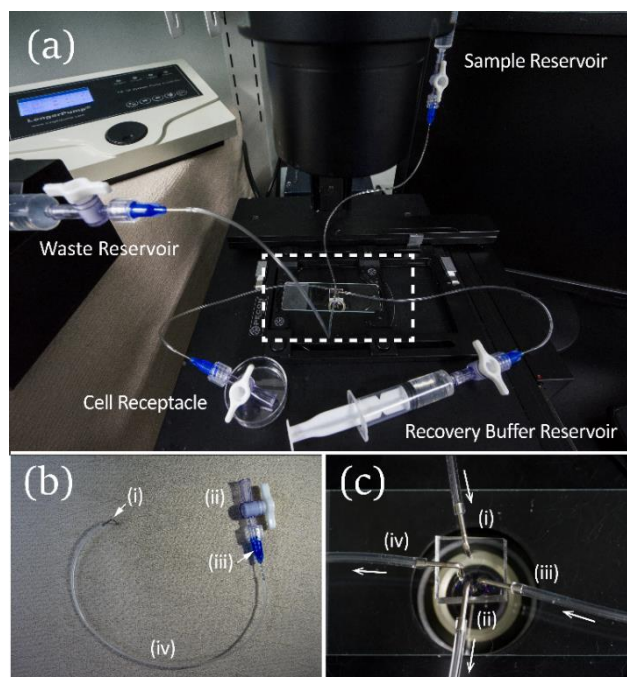


Figure A.1 Illustration of the experimental setup of Recovery Chip. (a) An overview, (b) a close-up view on the connection between (i) metal connector, (ii) stopcock, (iii) precision syringe tip and (iv) Tygon tubing, and (c) a close-up view on the connection of each tubing to (i) the sample inlet port, (ii) the waste outlet port, (iii) the recovery buffer inlet port and (iv) the cell outlet port. The access ports are punched using a 0.75-mm-diameter puncher. Arrows indicate the direction of flow.

Capture Chip only

26| Hold the buffer reservoir in an upright position using the custom-made holder.

A.2.5 Chip priming

● **TIMING 10-20 min**

27| Turn on all the stopcocks (**Fig. A.2a** for Recovery Chip).

28| Remove air bubbles from the microfluidic system by pushing the plunger of the loaded 10-mL syringe.

29| Inspect the presence of bubbles in the microfluidic chip using the microscope under bright-field mode. Inspect the tubings for visible bubbles too.

▲ **CRITICAL STEP** Leaving bubbles in the microfluidic system impairs experimental results. If bubbles cannot be removed, the microfluidic chip should be replaced with a new one.

? **TROUBLESHOOTING**

30| Watch as the solution fills any of the reservoirs. Turn off any one of the stopcocks, except the stopcock of the waste outlet tubing, once a droplet has emerged from the bottom of any of the reservoirs (**Fig. A.2b** for Recovery Chip).

31| Mount the syringe on the syringe pump. Set the syringe pump as described in the table below and run the system for ~5 min to stabilize the flow.

Table A.3 Syringe pump parameters

Parameter	Value
Syringe pump model	Longer Pump TS-1B/W0109-1B
Working mode	Withdraw
Flow rate	500 μ L/h
Internal diameter of syringe	14.40 mm

■ **PAUSE POINT** After the flow is stabilized, the syringe pump can be paused.

? **TROUBLESHOOTING**

A.2.6 Sample preparation

- **TIMING 10-20 min**

32| Sample preparation should be performed using option A for peripheral blood samples or option B for peritoneal wash samples.

(A) Peripheral blood	(B) Peritoneal wash
<p>(i) Centrifuge at 500 g for 5 min, room temperature. Remove the supernatant (plasma).</p>	<p>(i) Centrifuge at 500 g for 5 min, room temperature. Remove the supernatant.</p>
<p>▲ CRITICAL As an alternative to removing only the plasma, RBCs can also be removed by Ficoll density centrifugation (see Box 1) or RBC lysis (see Box 2).</p>	<p>(ii) Resuspend the pellet in ~20 mL of 1× PBS buffer.</p>
	<p>(iii) Centrifuge at 500 g for 5 min, room temperature. Remove the supernatant.</p>
	<p>(iv) Resuspend the pellet in ~20 mL of 1× PBS buffer.</p>
	<p>(v) Filter the cell suspension through a cell strainer (300 mesh).</p>

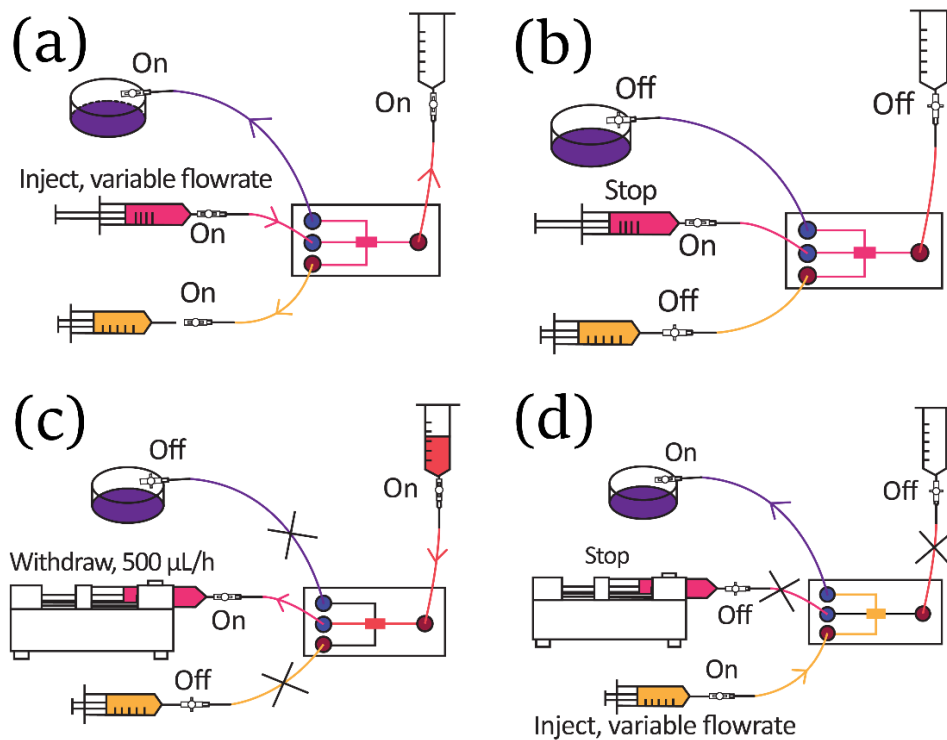


Figure A.2 | Illustration of chip priming, sample processing and cell recovery in Recovery Chip. (a) During chip priming, (b) at the end of chip priming (c) during sample processing and (d) during cell recovery. Opening and closing of stopcocks are indicated by “On/Off”. Each tubing is colored so that red tubing is the sample inlet tubing, pink tubing is the waste outlet tubing, yellow tubing is the recovery buffer tubing while purple tubing is the cell outlet tubing. Inlet ports are red while outlet ports are blue. Arrows indicate the direction of flow.

A.2.7 Pre-capture immunofluorescence staining

● **TIMING 2-4 h¹**

▲ **CRITICAL** Steps 40-45 should be performed in a dark room to prevent bleaching of fluorophores.

33| Fix the cells in 1 mL of 4% (w/v) PFA per 1 mL of the sample prepared in Step 32 for 30 min at room temperature.

[1] This section applies to Recovery Chip only

- 34|** Centrifuge the mixture at 700 *g* for 5 min, room temperature. Remove the supernatant.
- 35|** Resuspend the cells in 1-2 mL of 1× PBS buffer to wash the cells. Centrifuge the mixture at 700 *g* for 5 min, room temperature. Remove the supernatant.
- 36|** Resuspend the cells in 500 μL of 0.1% (v/v) Triton X-100 to permeabilize the cells for 10 min at room temperature.
- 37|** Add 1-2 mL of 1× PBS buffer to wash the permeabilized cells. Centrifuge the mixture at 700 *g* for 5 min, room temperature. Remove the supernatant.
- 38|** Resuspend the cells in 500 μL of 5% (w/v) BSA to saturate free protein-binding sites for 30 min at room temperature.
- 39|** Centrifuge the mixture at 700 *g* for 5 min, room temperature. Remove the supernatant.
- 40|** Add 200 μL of the prepared primary antibody mixture (see Reagent Setup) to stain the cells. Incubate the cells for 1 h at room temperature.
- 41|** Add 1-2 mL of 1× PBS buffer to wash the stained cells. Centrifuge the mixture at 700 *g* for 5 min, room temperature. Remove the supernatant.
- **PAUSE POINT** Stained cells can be stored under dark conditions at 4 °C for up to 2 days until further processing.
- If secondary antibodies are used**
- 42|** Resuspend the cells in 500 μL of 5% (w/v) BSA to saturate free protein-binding sites introduced by primary antibodies. Incubate the cell suspension for 30 min at room temperature.
- 43|** Centrifuge the mixture at 700 *g* for 5 min, room temperature. Remove the supernatant.
- 44|** Add 200 μL of the prepared secondary antibody mixture (see Reagent Setup) to stain the cells. Incubate the cells for 1 h at room temperature.

45| Add 1-2 mL of 1× PBS buffer to wash the stained cells. Centrifuge the mixture at 700 g for 5 min, room temperature. Remove the supernatant.

■ **PAUSE POINT** Stained cells can be stored under dark conditions at 4 °C for up to 2 days until further processing.

A.2.8 Sample processing

● **TIMING 3-5 h**

▲ **CRITICAL** For Recovery Chip, Steps 46-51 should be performed under dark condition to prevent bleaching of fluorophores.

Recovery Chip only

46| Resuspend the peripheral blood or the peritoneal wash cell pellet in 200 µL of Pluronic solution. Load the cell suspension into the sample reservoir.

Capture Chip only

47| Load 1 mL of peripheral blood or 200 µL of peritoneal wash into the sample reservoir.

48| Add equal amount of buffer solution (for Capture Chip) or Pluronic solution (for Recovery Chip) to the sample reservoir to dilute the sample.

49| Run the sample by turning on the stopcock of the sample inlet tubing (**Fig. A.4c** for Recovery Chip) and restarting the syringe pump.

▲ **CRITICAL STEP** Cells in peripheral blood or in peritoneal wash may clump at the bottom of the sample reservoir over time. Be sure to mix the sample regularly by pipetting in and out.

▲ **CRITICAL STEP** The processing must be allowed to run until completion without any pauses in between or any changes in the settings of the pump.

? TROUBLESHOOTING

50| When the sample in the sample reservoir is almost finished, add 500 μL of buffer solution (for Capture Cell) or Pluronic solution (for Recovery Cell) to flush any remaining cells.

51| Turn off the stopcock of the sample inlet tubing when the solution in the sample reservoir almost runs dry.

A.2.9 Post-capture immunofluorescence staining

● **TIMING 3-5 h¹**

▲ **CRITICAL** Steps 58-68 should be performed in a dark room to prevent bleaching of fluorophores.

▲ **CRITICAL** For each of Steps 53-59 and Steps 64-66, proceed to the subsequent step only when the buffer reservoir almost runs dry to minimize mixing of solutions.

52| Turn on the stopcock of the buffer inlet tubing.

▲ **CRITICAL STEP** Pre-staining solutions should be added to the buffer reservoir hereinafter.

53| Add 200 μL of 4% (w/v) PFA to fix the cells for 20 min at room temperature.

54| Add 200 μL of 1 \times PBS buffer to wash the fixed cells.

55| Add 200 μL of 0.1% (v/v) Triton X-100 to permeabilize the cells for 20 min at room temperature.

56| Add 200 μL of 1 \times PBS buffer to wash the permeabilized cells.

57| Add 200 μL of 5% (w/v) BSA to saturate free protein-binding sites for 20 min at room temperature.

[1] This section applies to Capture Chip only.

58| Add 100 μL of the prepared primary antibody mixture (see Reagent Setup) to stain the cells.

59| Add 200 μL of $1\times$ PBS buffer to allow the antibody mixture to flow thoroughly through the chip.

60| Stop the syringe pump and turn off the stopcocks of the buffer inlet tubing and the waste outlet tubing.

61| Incubate the cells under dark conditions for 1 h at room temperature.

■ **PAUSE POINT** Stained cells can be stored under dark conditions at $4\text{ }^{\circ}\text{C}$ for up to 2 days until further imaging. Make sure all stopcocks are turned off.

If secondary antibodies are used

62| Turn on the stopcocks of the buffer inlet tubing and the waste outlet tubing.

63| Start the syringe pump using the same settings as in Step 31.

64| Add 200 μL of 5% (w/v) BSA to saturate free protein-binding sites introduced by primary antibodies for 20 min at room temperature.

65| Add 100 μL of the prepared secondary antibody mixture (see Reagent Setup) to stain the cells.

66| Add 200 μL of $1\times$ PBS buffer to allow the antibody mixture to flow thoroughly through the chip.

67| Stop the syringe pump and turn off the stopcocks of the buffer inlet tubing and the waste outlet tubing.

68| Incubate the cells for 1 h at room temperature.

■ **PAUSE POINT** Stained cells can be stored under dark conditions at $4\text{ }^{\circ}\text{C}$ for up to 2 days until further imaging. Make sure all stopcocks are turned off.

A.2.10 Recovery of captured cells

- **TIMING variable**¹

- ▲ **CRITICAL** Steps 69-71 should be performed in a dark room to prevent bleaching of fluorophores.

69| Turn on the stopcocks of the recovery buffer inlet tubing and the recovered cell outlet tubing. Turn off the stopcocks of the waste outlet tubing and the sample inlet tubing (**Fig. A.4d**).

70| Push the plunger of the recovery buffer reservoir to inject Pluronic solution manually into the Recovery Chip.

71| Collect the captured cells using the cell receptacle.

A.2.11 Imaging of stained cells

- **TIMING variable**

- ▲ **CRITICAL** Perform Step 72 in a dark room to prevent bleaching of fluorophores.

72| Obtain images of cells under an inverted microscope at 40× magnification. We use Leica inverted microscope (emission filters dependent on fluorescent dyes applied).

A.2.12 Data Interpretation

- **TIMING variable**

73| Compare the corresponding image sets taken in Step 72. Follow the tumor cell identification strategy described in *Section 2.3* to identify the putative tumor cells.

? TROUBLESHOOTING

A.2.13 Troubleshooting

[1] This section applies to Recovery Chip only.

Table A.4 Troubleshooting table.

Step	Problem	Possible reason	Solution
15	Collapsed microposts	PDMS pieces are pressed onto the microscope slides.	Replace with a new chip
		Aging of the master mold	Fabricate a new master mold
29	Air bubbles are trapped in the microfluidic system	Bubbles in buffer solution	Push the plunger harder or flick the tubing to remove bubbles. Replace the chip with a new one if bubbles retain
31	Air bubbles are trapped in the microfluidic system	Bubbles in buffer solution	Increase the flow rate of the buffer solution or replace the chip with a new one
	PDMS debris are trapped in the chip	PDMS debris dislodged from the puncher tip during the punching process or debris created when inserting metal connectors into the access ports	Increase the flow rate of the buffer solution or replace the chip with a new one
49	Clogging in the chip	Blood coagulation or large clusters trapped between microposts	Replace the chip with a new one
72	False positives	Expired antibodies	Use fresh antibodies
		Inadequate blocking	Increase BSA concentration
		Incorrect antibody concentration	Reduce the antibody concentration
Box 1	Contamination of RBCs in the buffy coat	Increase in height of the blood sample in the centrifuge tube due to larger blood volume	Use a centrifuge tube of larger diameter
	Low yield of endometrial cells	Clumping of endometrial cells due to aggregation of RBCs at high temperatures (37°C). Longer time of separation due to low temperatures (4°C).	Heat/Cool Ficoll-Paque PLUS to reach room temperature (15-25°C) for optimum results
Box 2	Inefficient RBC lysis	Expired RBC lysis buffer	Use fresh RBC lysis buffer

A.2.14 Timing

The timing information for each of the sections for both Capture Chip and

Recovery Chip can be found in **Table A.5**.

Table A.5 Timing information section by section for Capture Chip and Recovery Chip.

Step No.	Section	Timing	Capture Chip	Recovery Chip
1-3	Chip design and mold preparation	10-17 d	✓	✓
4-15	Chip fabrication	6-7 h	✓	✓
16-26	Chip assembly	10-15 min	✓	✓
27-31	Chip priming	10-20 min	✓	✓
32	Sample preparation	10-20 min	✓	✓
33-45	Pre-capture immunofluorescence staining	2-4 h		✓
46-51	Sample processing	3-5 h	✓	✓
52-68	Post-capture immunofluorescence staining	3-5 h	✓	
69-71	Recovery of captured cells	Variable		✓
72	Imaging of stained cells	Variable	✓	✓
73	Data interpretation	Variable	✓	✓
Box 1	Ficoll density centrifugation	30-60 min	✓	✓
Box 2	RBC lysis	15-20 min	✓	✓

APPENDIX B

PROTOCOL: CTC-DIALYSIS ANIMAL MODEL ON A RAT

B.1 Materials

B.1.1 Reagents

- Normal saline solution
- Heparin, 50 U/mL in normal saline solution
- Erythromycin paste
- Chloral hydrate, 4%
- Rubbing alcohol
- Tumor cell suspension, 4T1-fLUC and MBA-MD-231S-mkate cell-lines, 200 μ L

B.1.2 Equipments

- Microfluidic chips (Capture Chips)
- Silicon tubing,
- Peristaltic pump
- Micro plunger pump
- Metal connectors
- Precision syringe tips (Nordson EFD, cat. no. 7018272)
- Microfilters, 0.22 μ m
- One-way valve
- Sterile disposable syringes, 1 mL and 5 mL (Jiangsu Zhiyu Medical Instrument)

- Fine scissors, straight and curved
- Fine forceps, straight and curved
- Surgical needle holder
- Surgical sutures, 4-0 and 8-0
- Surgical clamps,
- Scissors
- Forceps
- Sterile gauzes
- Sterile cotton wools
- Sterile cotton buds
- Straight razor

B.1.3 Medicine (subjected to approved use)

- Anesthesia
- Analgesic
- Antibiotic

B.2 Procedure

B.2.1 Preparation of tubing pipelines

1. Dilate one end of a piece of thin silicon tubing (ID = 0.3mm, OD = 0.64mm, length ~ 5 cm) with the help of a pair of surgical forceps. Insert a metal connector into the opening. Remove the surgical forceps once the metal connector has been properly attached to the silicon tubing.
2. Remove the beveled syringe tip from a 1-mL syringe. Load the syringe with 2 mL of saline solution supplemented with heparin (50 U/mL).

3. Attach a microfilter to the loaded syringe.
4. Attach a precision syringe tip to the microfilter.
5. Attach one end of a piece of thick silicon tubing (ID = 0.5 mm, OD = 1.5 mm, length ~1 cm) to the precision syringe tip. Attach the other end to the metal connector of the thin silicon tubing.
6. Flush the whole tubing pipeline with heparin-supplemented saline solution by pushing the plunger of the loaded syringe. Ensure there is no air bubbles.
7. Repeat Steps 1-6 for another set of tubing pipeline.

B.2.2 Preparation of pumps

8. Two types of pumps are used, namely peristaltic pump and micro plunger pump.

Their preparations are as follows:

A. Peristaltic pump

- i. Connect one end of another piece of thick silicon tubing (length ~ 2cm) to a precision tip needle. Plug the precision syringe tip into one end of the pump tube. Plug the upstream connector of the check valve into the other end. Join the downstream check valve connector with a 10-cm long thick silicon tubing via a precision tip needle. Join the other end of the silicon tubing with a plain needle.
- ii. Remove the beveled syringe tip from a 5-mL syringe. Fully load the syringe with saline solution supplemented with heparin (50 U/mL).
- iii. Attach a microfilter to the loaded syringe.
- iv. Attach a precision syringe tip to the microfilter.
- v. Connect the precision syringe tip to the thick tubing in Step 8AA.

- vi. Flush the whole tubing pipeline with heparin-supplemented saline solution by pushing the plunger of the loaded syringe. Ensure there is no air bubbles.
- vii. Install the tubing pipeline onto a peristaltic pump.

B. Micro plunger pump

- i. Connect a 4"-thread connector to one end of a 10-cm long thick silicon tubing.
- ii. Remove the beveled syringe tip from a 5-mL syringe. Fully load the syringe with saline solution supplemented with heparin (50 U/mL).
- iii. Attach a microfilter to the loaded syringe.
- iv. Attach a precision syringe tip to the microfilter.
- v. Connect the precision syringe tip to the thick tubing prepared in Step 8BA.
- vi. Connect another 4"-thread connector to another piece of 10-cm long thick silicon tubing.
- vii. Plug the rinse system prepared in step ii) into the free end of thick tubing prepared in vi). Rinse the tubing. Join the thread end of the vi) assembly with the inlet of the plunger pump. Start the micro plunger pump, at the same time push the syringe connected to the system, rinse the whole system until the syringe is nearly empty and the system is free of bubbles.

B.2.3 Preparation of animals

9. Hold a rat gently in a supine position and inject suitable dose of chloral hydrate intraperitoneally to anesthetize the rat.
10. Place the anesthetized rat into its cage in a prone position to prevent asphyxia.

11. When the rat has lost their consciousness, thoroughly shave the abdominal fur using a straight razor.
12. Place a heating pad heated to 37 °C on the operating board. Place the rat on the heating pad in a supine position. Fix its four limbs on the operating board. Fix its head using a rubber band held between its tongue and palate to prevent asphyxia.
13. Aseptically prepare the shaved areas by alcohol wipes.

B.2.4 Surgery

14. Using a pair of scissors, perform longitudinal skin incisions to the shaved areas along the abdominal midline starting at the upper section of the bladder all the way to lower section of the costal margin.
15. Using a pair of scissors, perform longitudinal muscle incisions to the shaved areas along the abdominal midline starting at the upper section of the bladder all the way to lower section of the costal margin.
16. Place a piece of saline-soaked gauze on the left side of the abdomen. Take out the gastric and the intestines and put them on the gauze. Cover these organs with another piece of saline-soaked gauze to keep it hydrated. Always keep the gauze soaked in saline solution throughout the surgery.
17. Divide the mesangium to expose the post cava, the abdominal aorta (AA), the left renal vein (LRV) and the iliac vein (IV).
18. Identify where the blood vessels branch out, carefully dividing IVC from AA, and LRV and IV from the abdominal wall when necessary.
19. Locate the tubing connection port that satisfies following criteria:
 - a. The surgery should take place on a section of blood vessel that does not have any branches, on both front and back side, and with a diameter larger than 0.7 mm.

- b. The distal port (for extraction of blood) and proximal port (for infusion of blood) are recommended in ascending order:

Table B.1 Recommended ports for extraction and infusion of blood:

Distal port (extraction of blood)	Proximal port (infusion of blood)
1. Vena spermatica interna	1. Iliolumbar vein
2. Left renal vein	2. Right renal vein
3. Post cava	3. Post cava
4. Ureter vein	4. Ureter vein

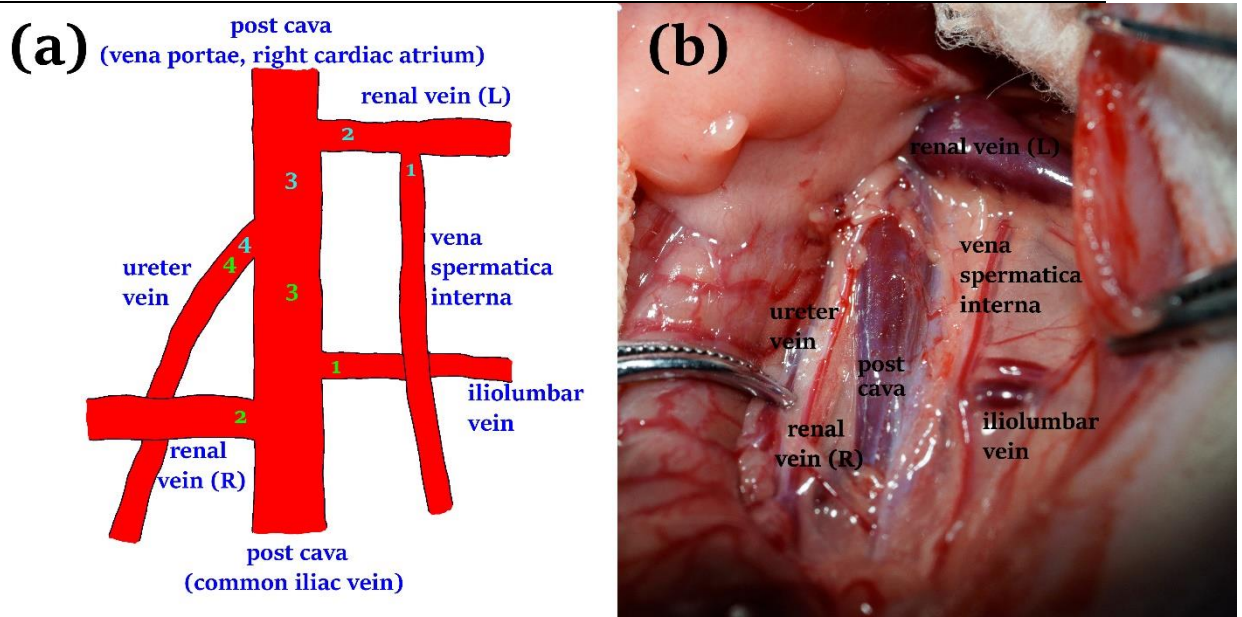


Figure B.1 Recommended ports for extraction and infusion of blood in a) schematic and b) actual view of the post cava.

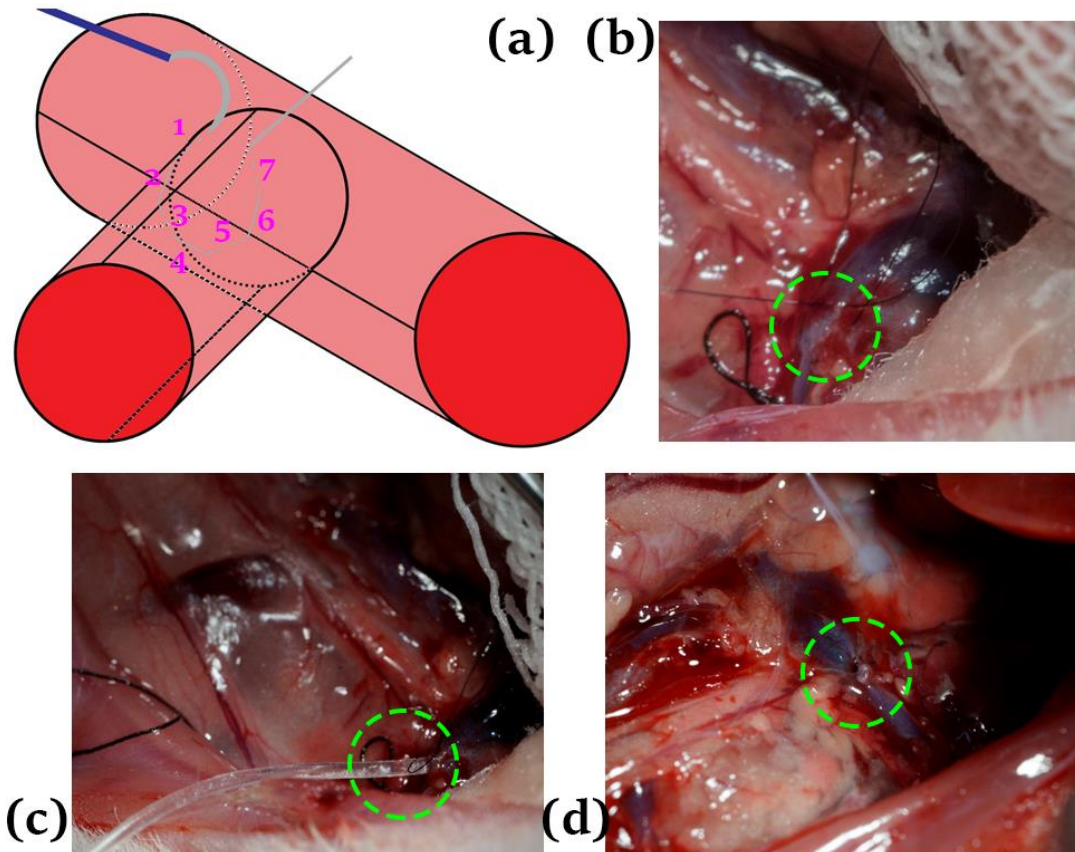


Figure B.2 Illustration of the microsurgery: a) 7 stitches to define a pocket for tubing installation; b) circle highlights the pre-defined pocket; c) circle highlights the tightened thread to fix the tubing, on its left is the thread to ligature the distal end of the vein; d) knotted thread closes the wound immediately after the removal of the tubing.

B.2.5 Tubings fixation

20. Seam 5 or 7 stitches around the connection port chosen in Step 19 as in Figure B.2.a-b. The two ends of the thread should remain free. If the vein bleeds during seaming, press the bleeding point to stop it.
21. Separate the vein with any attachment with abdominal wall or abdominal artery, traverse a 5-cm thread underneath, and ligature the vein with a single slipknot.

22. Cut a hole on the vein inside the circle seamed in Step 20. Expose the hole by lifting the thread and insert the designated tubing along the direction of the vein for a depth of around 5 mm. Slipknot the free thread to stabilize the tubing as in Figure B.2.c.
23. If the distal port is on the post cava, release the ligature on it.
24. Push and pull the syringe connected to the tubing to check whether the blood can be extracted and infused smoothly. If there is a leakage, tighten the slipknot. Adjust the connection between the vein and the tubing, its direction and depth if there is any leakages or blockages.
25. Repeat Step 20 – 24 to plug in the second tubing.

B.2.6 Dialysis

26. Disconnect the syringe on the distal tubing and connect the tubing to the upstream needle of circulation pump. Disconnect the syringe on the proximal tubing and connect the tubing to the downstream needle of circulation pump.
27. If the post cava is still unimpeded, clamp it with a vessel clamp.
28. Start the circulation pump to allow blood to flow through the system.
29. Replace the old Capture Chip with a new one after 5-10 minutes by:
 - a. Stopping the circulation pump.
 - b. Disconnecting the old chip and the needle on its Outlet Port, connect the needle to the Outlet Port of the new chip.
 - c. Disconnecting the old chip and the needle on its Inlet Port, clear the blood on the needle and connect to the Inlet Port of the new chip.
 - d. Restarting the circulation pump.
30. This step is to be done only in tail vein injection model.
 - a. Rub the skin of the tail with rubbing alcohol.

- b. Draw the cell suspension into a 1-ml syringe.
- c. Locate the tail vein, plug the needle of the syringe into the vein, gently pull the syringe, if blood is withdrawn, the needle is properly plugged into the vein.
- d. Push the plunger of the syringe to inject the cell suspension into the vein.
- e. If the cell suspension leaks out or aggregates under skin, it means that the injection has failed and needs to restart from Step 30b.

31. Repeat Step 29 for 2-3 times. Collect all chips for imaging.

B.2.7 Closure of surgical wounds

- 32. Release the vessel clamp on the post cava.
- 33. Clamp the two tubings with vessel clamps. Remove the circulation pump and chip.
- 34. Loosen one of the slipknots made in Step 22. Remove the tubing. Tighten the thread and hard knot as in Figure B.2.d.
- 35. Loosen the ligature of corresponding vein if it still applies.
- 36. Repeat Step 34-35 to close the other connection port.
- 37. Put back all organs to their original place removed from the abdominal in step 16 gently.
- 38. Seam the abdominal wall and muscle.
- 39. Seam the skin.
- 40. Apply anti-infection and analgesia in accordance to approved therapy.
- 41. Put the rat back to its cage in a prone position to avoid asphyxia.

B.2.8 Imaging and Data Analysis

42. Take images of the chips under an inverted fluorescent microscope with ~200x magnification. Bright field images and DsRed image (for mKate fluorescence) should be taken. The captured tumor cells can be identified in the image by the Red fluorescent signal.

REFERENCES

- [1] Chen, W., et al., Cancer statistics in China, 2015. *CA: A Cancer Journal for Clinicians*, 2016. 66(2): p. 115-132.
- [2] Murray, C.J., et al., Disability-adjusted life years (DALYs) for 291 diseases and injuries in 21 regions, 1990–2010: a systematic analysis for the Global Burden of Disease Study 2010. *The lancet*, 2013. 380(9859): p. 2197-2223.
- [3] Soerjomataram, A., et al., Global burden of cancer in 2008: a systematic analysis of disability-adjusted life-years in 12 world regions. *The Lancet*, 2012. 380(9856): p. 1840-1850.
- [4] Hoshino, K., et al., Microchip-based immunomagnetic detection of circulating tumor cells. *Lab on a Chip*, 2011. 11(20): p. 3449-3457.
- [5] Yoon, H.J., et al., Sensitive capture of circulating tumour cells by functionalized graphene oxide nanosheets. *Nature nanotechnology*, 2013. 8(10): p. 735-741.
- [6] Ji, J.-L., et al., Detection of Circulating Tumor Cells Using a Novel Immunomagnetic Bead Method in Lung Cancer Patients. *Journal of Clinical Laboratory Analysis*, 2016: p. n/a-n/a.
- [7] Murray, C.J. and A.D. Lopez, Evidence-based health policy--lessons from the Global Burden of Disease Study. *Science*, 1996. 274(5288): p. 740.
- [8] Yu, M., et al., Circulating tumor cells: approaches to isolation and characterization. *The Journal of Cell Biology*, 2011. 192(3): p. 373-382.
- [9] Organization, W.H., National cancer control programmes: policies and managerial guidelines. 2002.
- [10] Antolovic, D., et al., Heterogeneous detection of circulating tumor cells in patients with colorectal cancer by immunomagnetic enrichment using different EpCAM-specific antibodies. *BMC Biotechnology*, 2010. 10(1): p. 1-8.
- [11] Rubin, R., Precision medicine: The future or simply politics? *JAMA*, 2015. 313(11): p. 1089-1091.

- [12] Alix-Panabières, C. and K. Pantel, Circulating tumor cells: liquid biopsy of cancer. *Clinical chemistry*, 2013. 59(1): p. 110-118.
- [13] Crowley, E., et al., Liquid biopsy: monitoring cancer-genetics in the blood. *Nature reviews Clinical oncology*, 2013. 10(8): p. 472-484.
- [14] Zhou, J., A. Huang, and X.-R. Yang, Liquid Biopsy and its Potential for Management of Hepatocellular Carcinoma. *Journal of Gastrointestinal Cancer*, 2016: p. 1-11.
- [15] Pantel, K. and C. Alix-Panabières, Real-time Liquid Biopsy in Cancer Patients: Fact or Fiction? *Cancer Research*, 2013. 73(21): p. 6384-6388.
- [16] Mehlen, P. and A. Puisieux, Metastasis: a question of life or death. *Nat Rev Cancer*, 2006. 6(6): p. 449-458.
- [17] Gupta, G.P. and J. Massagué, Cancer Metastasis: Building a Framework. *Cell*, 2006. 127(4): p. 679-695.
- [18] van der Toom, E.E., J.E. Verdone, and K.J. Pienta, Disseminated tumor cells and dormancy in prostate cancer metastasis. *Current Opinion in Biotechnology*, 2016. 40: p. 9-15.
- [19] Alix-Panabières, C., K. Bartkowiak, and K. Pantel, Functional studies on circulating and disseminated tumor cells in carcinoma patients. *Molecular Oncology*, 2016. 10(3): p. 443-449.
- [20] Hardingham, J.E., et al., Detection of circulating tumor cells in colorectal cancer by immunobead-PCR is a sensitive prognostic marker for relapse of disease. *Molecular Medicine*, 1995. 1(7): p. 789-794.
- [21] Plaks, V., C.D. Koopman, and Z. Werb, Cancer. Circulating tumor cells. *Science*, 2013. 341(6151): p. 1186-8.
- [22] Paterlini-Brechot, P. and N.L. Benali, Circulating tumor cells (CTC) detection: clinical impact and future directions. *Cancer Lett*, 2007. 253.
- [23] Ni, X., et al., Reproducible copy number variation patterns among single circulating tumor cells of lung cancer patients. *Proc Natl Acad Sci U S A*, 2013. 110(52): p. 21083-8.
- [24] Ramskold, D., et al., Full-length mRNA-Seq from single-cell levels of RNA and individual

- circulating tumor cells. *Nat Biotechnol*, 2012. 30(8): p. 777-82.
- [25] Zhang, X., et al., Single-Cell Sequencing for Precise Cancer Research: Progress and Prospects. *Cancer Research*, 2016.
- [26] Powell, A.A., et al., Single Cell Profiling of Circulating Tumor Cells: Transcriptional Heterogeneity and Diversity from Breast Cancer Cell Lines. *PLoS ONE*, 2012. 7(5): p. e33788.
- [27] Miyamoto, D.T., et al., RNA-Seq of single prostate CTCs implicates noncanonical Wnt signaling in antiandrogen resistance. *Science*, 2015. 349(6254): p. 1351-1356.
- [28] Heitzer, E., et al., Complex tumor genomes inferred from single circulating tumor cells by array-CGH and next-generation sequencing. *Cancer research*, 2013. 73(10): p. 2965-2975.
- [29] Lohr, J.G., et al., Whole exome sequencing of circulating tumor cells provides a window into metastatic prostate cancer. *Nature biotechnology*, 2014. 32(5): p. 479-484.
- [30] Maheswaran, S., et al., Detection of mutations in EGFR in circulating lung-cancer cells. *New England Journal of Medicine*, 2008. 359(4): p. 366-377.
- [31] Sundaresan, T.K., et al., Detection of T790M, the acquired resistance EGFR mutation, by tumor biopsy versus noninvasive blood-based analyses. *Clinical Cancer Research*, 2015.
- [32] Mocellin, S., et al., Circulating tumor cells: the 'leukemic phase' of solid cancers. *Trends in molecular medicine*, 2006. 12(3): p. 130-139.
- [33] Ali, W., et al., Differentiating Metastatic and Non-metastatic Tumor Cells from their Translocation Profile through Solid-state Micropores. *Langmuir*, 2016.
- [34] Zhang, C., et al., Tumor heterogeneity and circulating tumor cells. *Cancer Letters*, 2016. 374(2): p. 216-223.
- [35] Wang, S., et al., Highly efficient capture of circulating tumor cells by using nanostructured silicon substrates with integrated chaotic micromixers. *Angewandte Chemie International Edition*, 2011. 50(13): p. 3084-3088.
- [36] Cristofanilli, M., et al., Circulating tumor cells, disease progression, and survival in metastatic breast cancer. *New England Journal of Medicine*, 2004. 351(8): p. 781-791.

- [37] Hyun, K.-A., et al., Epithelial-to-mesenchymal transition leads to loss of EpCAM and different physical properties in circulating tumor cells from metastatic breast cancer. 2016. 2016.
- [38] Yang, L., et al., Optimization of an enrichment process for circulating tumor cells from the blood of head and neck cancer patients through depletion of normal cells. *Biotechnology and bioengineering*, 2009. 102(2): p. 521-534.
- [39] Dieguez, L., et al., Efficient microfluidic negative enrichment of circulating tumor cells in blood using roughened PDMS. *Analyst*, 2015. 140(10): p. 3565-3572.
- [40] Sieuwerts, A.M., et al., Anti-Epithelial Cell Adhesion Molecule Antibodies and the Detection of Circulating Normal-Like Breast Tumor Cells. *Journal of the National Cancer Institute*, 2009. 101(1): p. 61-66.
- [41] Nagrath, S., et al., Isolation of rare circulating tumour cells in cancer patients by microchip technology. *Nature*, 2007. 450(7173): p. 1235-1239.
- [42] Tang, M., et al., A chip assisted immunomagnetic separation system for the efficient capture and in situ identification of circulating tumor cells. *Lab on a Chip*, 2016. 16(7): p. 1214-1223.
- [43] Kirby, B.J., et al., Functional Characterization of Circulating Tumor Cells with a Prostate-Cancer-Specific Microfluidic Device. *PLoS ONE*, 2012. 7(4): p. e35976.
- [44] Gleghorn, J.P., et al., Capture of circulating tumor cells from whole blood of prostate cancer patients using geometrically enhanced differential immunocapture (GEDI) and a prostate-specific antibody. *Lab Chip*, 2010. 10(1): p. 27-9.
- [45] Friedlander, T.W., et al., Detection and characterization of invasive circulating tumor cells derived from men with metastatic castration-resistant prostate cancer. *International Journal of Cancer*, 2014. 134(10): p. 2284-2293.
- [46] Moon, H.-S., et al., Continuous separation of breast cancer cells from blood samples using multi-orifice flow fractionation (MOFF) and dielectrophoresis (DEP). *Lab on a Chip*, 2011. 11(6): p. 1118-1125.

- [47] Lee, D., et al., Numerical simulation and channel configuration design for a negative dielectrophoresis based high efficiency cell sorting platform. *Journal of Mechanical Science and Technology*, 2015. 28(11): p. 4673-4679.
- [48] Kim, S.H., et al., Highly efficient single cell arraying by integrating acoustophoretic cell pre-concentration and dielectrophoretic cell trapping. *Lab on a Chip*, 2015. 15(22): p. 4356-4363.
- [49] Sollier, E., et al., Size-selective collection of circulating tumor cells using Vortex technology. *Lab on a Chip*, 2014. 14(1): p. 63-77.
- [50] Bhagat, A.A.S., et al., Pinched flow coupled shear-modulated inertial microfluidics for high-throughput rare blood cell separation. *Lab on a Chip*, 2011. 11(11): p. 1870-1878.
- [51] Warkiani, M.E., et al., Slanted spiral microfluidics for the ultra-fast, label-free isolation of circulating tumor cells. *Lab on a Chip*, 2014. 14(1): p. 128-137.
- [52] Sarkar, A., et al., Multiplexed Affinity-Based Separation of Proteins and Cells Using Inertial Microfluidics. *Scientific Reports*, 2016. 6: p. 23589.
- [53] Desitter, A., et al., A new device for rapid isolation by size and characterization of rare circulating tumor cells. *Anticancer research*, 2011. 31(2): p. 427-441.
- [54] Magbanua, M.J.M., et al., A Novel Strategy for Detection and Enumeration of Circulating Rare Cell Populations in Metastatic Cancer Patients Using Automated Microfluidic Filtration and Multiplex Immunoassay. *PLoS ONE*, 2015. 10(10): p. e0141166.
- [55] Hosokawa, M., et al., Size-selective microcavity array for rapid and efficient detection of circulating tumor cells. *Analytical chemistry*, 2010. 82(15): p. 6629-6635.
- [56] Tan, S.J., et al., Versatile label free biochip for the detection of circulating tumor cells from peripheral blood in cancer patients. *Biosensors and Bioelectronics*, 2010. 26(4): p. 1701-1705.
- [57] Aghaamoo, M., et al., Deformability-based circulating tumor cell separation with conical-shaped microfilters: Concept, optimization, and design criteria. *Biomicrofluidics*, 2015. 9(3): p. 034106.

- [58] Zhou, Z., et al., Accurate measurement of stiffness of leukemia cells and leukocytes using an optical trap by a rate-jump method. *RSC Advances*, 2014. 4(17): p. 8453-8460.
- [59] Cross, S.E., et al., AFM-based analysis of human metastatic cancer cells. *Nanotechnology*, 2008. 19(38): p. 384003.
- [60] Suresh, S., Biomechanics and biophysics of cancer cells. *Acta Materialia*, 2007. 55(12): p. 3989-4014.
- [61] Xu, W., et al., Cell stiffness is a biomarker of the metastatic potential of ovarian cancer cells. *PloS one*, 2012. 7(10): p. e46609.
- [62] Swaminathan, V., et al., Mechanical stiffness grades metastatic potential in patient tumor cells and in cancer cell lines. *Cancer research*, 2011. 71(15): p. 5075-5080.
- [63] Cross, S.E., et al., Nanomechanical analysis of cells from cancer patients. *Nature nanotechnology*, 2007. 2(12): p. 780-783.
- [64] Downey, G.P., et al., Retention of leukocytes in capillaries: role of cell size and deformability. *Journal of Applied Physiology*, 1990. 69(5): p. 1767-1778.
- [65] Dong, C. and R. Skalak, Leukocyte deformability: finite element modeling of large viscoelastic deformation. *Journal of theoretical biology*, 1992. 158(2): p. 173-193.
- [66] Lv, P., et al., Spatially graded segregation and recovery of circulating tumor cells from peripheral blood of cancer patients. *Biomicrofluidics*, 2013. 7(3): p. 34109.
- [67] Spaeth, E.E., et al., THE INFLUENCE OF FLUID SHEAR ON THE KINETICS OF BLOOD COAGULATION REACTIONS. *ASAIO Journal*, 1973. 19(1): p. 179-187.
- [68] Shen, F., et al., Threshold response of initiation of blood coagulation by tissue factor in patterned microfluidic capillaries is controlled by shear rate. *Arterioscler Thromb Vasc Biol*, 2008. 28(11): p. 2035-41.
- [69] Zucker, M.B. and J. Borrelli, Some effects of divalent cations on the clotting mechanism and the platelets of EDTA blood. *Journal of applied physiology*, 1958. 12(3): p. 453-460.
- [70] Sadagopan, N.P., et al., Investigation of EDTA anticoagulant in plasma to improve the throughput of liquid chromatography/tandem mass spectrometric assays. *Rapid*

- Communications in Mass Spectrometry, 2003. 17(10): p. 1065-1070.
- [71] Flier, J.S., et al., Molecular and cellular biology of blood coagulation. *New England Journal of Medicine*, 1992. 326(12): p. 800-806.
- [72] Bucala, R., et al., Circulating fibrocytes define a new leukocyte subpopulation that mediates tissue repair. *Molecular medicine*, 1994. 1(1): p. 71.
- [73] Keeley, E.C., B. Mehrad, and R.M. Strieter, The role of fibrocytes in fibrotic diseases of the lungs and heart. *Fibrogenesis Tissue Repair*, 2011. 4(2): p. 858-870.
- [74] Hayes, D.F., et al., Circulating tumor cells at each follow-up time point during therapy of metastatic breast cancer patients predict progression-free and overall survival. *Clinical Cancer Research*, 2006. 12(14): p. 4218-4224.
- [75] Zhang, L., et al., Meta-Analysis of the Prognostic Value of Circulating Tumor Cells in Breast Cancer. *Clinical Cancer Research*, 2012. 18(20): p. 5701-5710.
- [76] de Bono, J.S., et al., Circulating tumor cells predict survival benefit from treatment in metastatic castration-resistant prostate cancer. *Clinical Cancer Research*, 2008. 14(19): p. 6302-6309.
- [77] Cohen, S.J., et al., Relationship of Circulating Tumor Cells to Tumor Response, Progression-Free Survival, and Overall Survival in Patients With Metastatic Colorectal Cancer. *Journal of Clinical Oncology*, 2008. 26(19): p. 3213-3221.
- [78] Hardingham, J.E., et al., Detection and Clinical Significance of Circulating Tumor Cells in Colorectal Cancer—20 Years of Progress. *Molecular Medicine*, 2015. 21(Suppl 1): p. S25-S31.
- [79] Krebs, M.G., et al., Evaluation and prognostic significance of circulating tumor cells in patients with non-small-cell lung cancer. *Journal of clinical oncology*, 2011. 29(12): p. 1556-1563.
- [80] Hiltermann, T.J.N., et al., Circulating tumor cells in small-cell lung cancer: a predictive and prognostic factor. *Annals of Oncology*, 2012. 23(11): p. 2937-2942.
- [81] Hou, J.-M., et al., Clinical Significance and Molecular Characteristics of Circulating Tumor

- Cells and Circulating Tumor Microemboli in Patients With Small-Cell Lung Cancer. *Journal of Clinical Oncology*, 2012. 30(5): p. 525-532.
- [82] Naito, T., et al., Prognostic Impact of Circulating Tumor Cells in Patients with Small Cell Lung Cancer. *Journal of Thoracic Oncology*, 2012. 7(3): p. 512-519.
- [83] Pierga, J.Y., et al., High independent prognostic and predictive value of circulating tumor cells compared with serum tumor markers in a large prospective trial in first-line chemotherapy for metastatic breast cancer patients. *Annals of Oncology*, 2012. 23(3): p. 618-624.
- [84] Schulze, K., et al., Presence of EpCAM-positive circulating tumor cells as biomarker for systemic disease strongly correlates to survival in patients with hepatocellular carcinoma. *International Journal of Cancer*, 2013. 133(9): p. 2165-2171.
- [85] Goldkorn, A., et al., Circulating tumor cell counts are prognostic of overall survival in SWOG S0421: a phase III trial of docetaxel with or without atrasentan for metastatic castration-resistant prostate cancer. *Journal of Clinical Oncology*, 2014. 32(11): p. 1136-1142.
- [86] Smerage, J.B., et al., Circulating tumor cells and response to chemotherapy in metastatic breast cancer: SWOG S0500. *Journal of Clinical Oncology*, 2014. 32(31): p. 3483-3489.
- [87] Krebs, M.G., et al., Circulating Tumor Cell Enumeration in a Phase II Trial of a Four-Drug Regimen in Advanced Colorectal Cancer. *Clinical Colorectal Cancer*, 2015. 14(2): p. 115-122.e2.
- [88] Fan, Z.H., et al., Abstract IA21: Enumeration of circulating tumor cells for studying cancer drug sensitivity. *Clinical Cancer Research*, 2015. 21(4 Supplement): p. IA21.
- [89] Torre, L.A., et al., Global cancer statistics, 2012. *CA: A Cancer Journal for Clinicians*, 2015. 65(2): p. 87-108.
- [90] Headley, M.B., et al., Visualization of immediate immune responses to pioneer metastatic cells in the lung. *Nature*, 2016. 531(7595): p. 513-517.
- [91] Deng, Y., et al., An Integrated Microfluidic Chip System for Single-Cell Secretion Profiling

- of Rare Circulating Tumor Cells. *Scientific Reports*, 2014. 4: p. 7499.
- [92] Liu, Q., Q. Liao, and Y. Zhao, Myeloid-derived suppressor cells (MDSC) facilitate distant metastasis of malignancies by shielding circulating tumor cells (CTC) from immune surveillance. *Medical Hypotheses*, 2016. 87: p. 34-39.
- [93] Pailler, E., et al., Detection of Circulating Tumor Cells Harboring a Unique ALK Rearrangement in ALK-Positive Non-Small-Cell Lung Cancer. *Journal of Clinical Oncology*, 2013. 31(18): p. 2273-2281.
- [94] Stott, S.L., et al., Isolation and characterization of circulating tumor cells from patients with localized and metastatic prostate cancer. *Science translational medicine*, 2010. 2(25): p. 25ra23-25ra23.
- [95] Pua, H.H., et al., Autophagy is essential for mitochondrial clearance in mature T lymphocytes. *The Journal of Immunology*, 2009. 182(7): p. 4046-4055.
- [96] Youle, R.J. and D.P. Narendra, Mechanisms of mitophagy. *Nat Rev Mol Cell Biol*, 2011. 12(1): p. 9-14.
- [97] Zhang, H., et al., Mitochondrial autophagy is an HIF-1-dependent adaptive metabolic response to hypoxia. *J Biol Chem*, 2008. 283(16): p. 10892-903.
- [98] Tanida, A., T. Ueno, and E. Kominami, LC3 and Autophagy. *Methods Mol Biol*, 2008. 445: p. 77-88.
- [99] Klionsky, D.J., et al., Guidelines for the use and interpretation of assays for monitoring autophagy. *Autophagy*, 2012. 8(4): p. 445-544.
- [100] Rosenfeldt, M.T. and K.M. Ryan, The multiple roles of autophagy in cancer. *Carcinogenesis*, 2011. 32(7): p. 955-963.
- [101] Li, X., et al., Targeting mitochondrial reactive oxygen species as novel therapy for inflammatory diseases and cancers. *Journal of Hematology & Oncology*, 2013. 6: p. 19-19.
- [102] Cooperative Group of Endometriosis, C.S., Guideline for the diagnosis and treatment of endometriosis. *Zhonghua fu chan ke za zhi*, 2015. 50(3): p. 161.
- [103] Fassbender, A., et al., Update on Biomarkers for the Detection of Endometriosis. *BioMed*

research international, 2015.

- [104] Schliep, K., et al., Endometriosis diagnosis and staging by operating surgeon and expert review using multiple diagnostic tools: an inter - rater agreement study. *BJOG: An International Journal of Obstetrics & Gynaecology*, 2015.
- [105] Sampson, J.A., Metastatic or embolic endometriosis, due to the menstrual dissemination of endometrial tissue into the venous circulation. *The American journal of pathology*, 1927. 3(2): p. 93.
- [106] Halme, J., et al., Retrograde menstruation in healthy women and in patients with endometriosis. *Obstetrics & Gynecology*, 1984. 64(2): p. 151-154.
- [107] Bobek, V., K. Kolostova, and E. Kucera, Circulating endometrial cells in peripheral blood. *European Journal of Obstetrics & Gynecology and Reproductive Biology*, 2014. 181: p. 267-274.
- [108] Herington, J.L., et al., Immune interactions in endometriosis. Expert review of clinical immunology, 2011. 7(5): p. 611-626.
- [109] Gaetje, R., et al., Invasiveness of endometriotic cells in vitro. *The Lancet*, 1995. 346(8988): p. 1463-1464.
- [110] Pavone, M.E. and B.M. Lyttle, Endometriosis and ovarian cancer: links, risks, and challenges faced. *International journal of women's health*, 2015. 7: p. 663.
- [111] Liu, F., et al., Vascular endothelial growth factor receptor-2 inhibitor cediranib causes regression of endometriotic lesions in a rat model. *International journal of clinical and experimental pathology*, 2015. 8(2): p. 1165.
- [112] Zhong, Chen, Expert Consensus on Basic Technique and Selection of Sutures for Vessel Suture and Anastomat (2008). *Chinese Journal of Practical Surgery*, 2008. 8: p. 814-816.
- [113] Hemodialysis, A., Clinical practice guidelines for hemodialysis adequacy, update 2006. *American journal of kidney diseases: the official journal of the National Kidney Foundation*, 2006. 48: p. S2.
- [114] Bissolati, M., et al., Portal vein-circulating tumor cells predict liver metastases in patients

with resectable pancreatic cancer. *Tumor Biology*, 2015. 36(2): p. 991-996.

- [115] Vuletic, A., et al., Establishment of an mKate2-Expressing Cell Line for Non-Invasive Real-Time Breast Cancer In Vivo Imaging. *Molecular Imaging and Biology*, 2015. 17(6): p. 811-818.